AN ABSTRACT OF THE DISSERTATION OF

Nessrine Chakchouk for the degree of Doctor of Philosophy in Electrical and Computer Engineering presented on September 7, 2012.

Title: Resource Allocation Methods for Quality-of-Service Provisioning in Heterogeneous Wireless Networks

Abstract approved: _____

Bechir Hamdaoui

The increased use of mobile wireless devices that we have recently been witnessing, such as smartphones, tablets, e-readers, and WiFi enabled devices in general, is driving an unprecedented increase in the amount of data traffic. This fast market adoption of the wireless technology along with the tremendous success of multimedia applications brought about higher capacity, connectivity, and Quality of Service (QoS) requirements that can no longer be met with traditional networking paradigms. As a result, heterogeneous wireless networks have recently emerged as a potential solution for meeting such new requirements. Hybrid wireless mesh networks and femtocell/macrocell networks are examples of these newly emerging heterogeneous networks. While mesh networks are viewed as the backbone/core network, femtocell and cellular networks are viewed as the access networks linking end-users with the backbone networks. In this dissertation, we address the problem of resource allocation in heterogeneous networks. We investi-

gate both types of networks/architectures: next-generation wireless backbone networks or simply wireless mesh networks (WMNs) and next-generation wireless access networks or simply femtocell (FC) networks. WMNs were first introduced to foster the availability of Internet services anywhere and at anytime. However, capacity limitation has been a fundamental challenge to WMNs, mainly due to the interference arising from the wireless nature of the environment as well as to the scarcity of the radio/channel resources. To overcome this problem, we propose in this dissertation an efficient scheduling scheme that reduces interference among active links via wise time and frequency assignments to the wireless mesh routers. The developed scheme is traffic aware in that it maximizes the capacity of wireless links but while accounting for their traffic loads, thus meeting the end-to-end bandwidth requirements as much as possible. In the second part of this thesis, we focus on developing power allocation techniques for FC networks. FCs have recently emerged as a key networking solution that has great potential for improving the capacity and coverage of traditional macrocell (MC) networks through high-speed indoor coverage. Their deployment, however, has given rise to new interference challenges which are mainly due to the FCs' autonomous nature and to the unreliability of the wireless medium. Driven by this fact, in the second part of this thesis, we first design a fully-distributed estimation-based power allocation scheme that aims at fairly maximizing the capacity of FC networks. Second, we propose a novel distributed stochastic power control scheme that aims at maintaining the users' minimum required QoS. Finally, we provide cross-layer performance analysis of two-tier FC networks, in which we characterize the uplink interference and study its impact on the data-link layer QoS performance in FC networks.

Resource Allocation Methods for Quality-of-Service Provisioning in Heterogeneous Wireless Networks

by

Nessrine Chakchouk

A DISSERTATION

submitted to

Oregon State University

in partial fulfillment of
the requirements for the
degree of

Doctor of Philosophy

Presented September 7, 2012
Commencement June 2013

Doctor of Philosophy dissertation of Nessrine Chakchouk presented on September 7, 2012.

APPROVED:

Major Professor, representing Electrical and Computer Engineering

---

Director of the School of Electrical Engineering and Computer Science

---

Dean of the Graduate School

I understand that my dissertation will become part of the permanent collection of Oregon State University libraries. My signature below authorizes release of my dissertation to any reader upon request.

Nessrine Chakchouk, Author

ACKNOWLEDGEMENTS

I would like to express my gratitude to all those who offered their valuable help to me throughout my PhD. First I would like to express my deep and sincere thanks to my advisor Dr. Bechir Hamdaoui for his precious support and guidance, and for his availability and valuable advice throughout my PhD program at Oregon State University. I thank my Networking group colleagues for the insightful group discussions.

I also would like to thank my qualifying and PhD committee members - Dr. Thinh Nguyen, Dr. Huaping Liu, Dr. Alan Wang, Dr. Oksana Ostroverkhova, Dr. Ben Lee and Dr. Mario Magana for their valuable feedback on my research work.

I want to thank the helpful OSU and the School of EECS staff members, particularly, Ferne Simendinger, Shannon Thompson and Renee Lyon for their availability and invaluable assistance during my Ph.D. study.

A special thought goes to all the Professors/Instructors I knew from the EECS and Statistics departments for helping me strengthen my academic and research background, for providing me with their precious advice and help whenever needed, and for ensuring a lovely learning atmosphere. I also want to thank Oregon State University for providing me with an excellent education, and a wonderful learning environment.

Last but not least, I would like to express my deepest gratitude to my parents for their continuous support and encouragements during my PhD study. I dedicate this work to my dear father Moncef for his patience, help and encouragements; to my lovely mother Samia for her affection, indefinite care, support and love; to my sweet sister Yasmine and to my lovely brother Seif Eddine.

TABLE OF CONTENTS

TABLE OF CONTENTS (Continued)

TABLE OF CONTENTS (Continued)

LIST OF FIGURES

LIST OF FIGURES (Continued)

LIST OF TABLES

LIST OF ALGORITHMS

Chapter 1: Introduction

1.1 Heterogeneous Wireless Networks

Recent advances in the wireless technology as well as those in electronics enabled the mass-production and the widespread use of wireless/mobile devices capable of supporting various types of services and applications. This rapid adoption of these wireless devices along with the tremendous success of multimedia applications brought about higher capacity, connectivity, and Quality of Service (QoS) requirements that can no longer be met with traditional networking and communications paradigms. As a result, heterogeneous wireless networks have recently emerged as a key networking solution for meeting and handling these new requirements. Wireless mesh networks and femtocell/macrocell networks are examples of such heterogeneous networks. While wireless mesh networks are viewed as the backbone/core network, femtocell and cellular networks are viewed as the access networks which link end-users with the backbone networks.

The unique characteristics of these new generation networks (their random deployment, their autonomous operation), the nature of the wireless medium (unreliable channel condition and interference), and the wireless users constraints (limited energy supply, limited transmission power, etc.) have given rise to new challenges. One important challenge, among many others, that needs to be addressed in order to have success-

ful deployment and operation of such networks lies in the design of efficient resource allocation and management methods that are suitable for these networks.

From an architectural viewpoint, heterogeneous wireless networks are composed of two types of networks: wireless backbone/multihop networks, such as wireless mesh networks, and wireless access networks, such as femtocell networks.

1.1.1 Wireless Mesh Networks

Wireless backbone/multihop networks are emerging as a promising architecture to extend the wireless coverage in a flexible and cost-effective way without relying on any wired infrastructure. They can be used for various applications, such as Internet access, emergency networks, and public safety. Typically, wireless backbone networks consist of wireless nodes that are connected to each other in a mesh/multi-hop fashion in order to provide access to an external network, such as Internet. Wireless backbone networks can be classified into two types: wireless sensor networks (WSNs) and wireless mesh networks (WMNs). The main difference between these two types is that WSNs consist of battery-powered energy-constrained sensors with limited computation and storage capacity, while WMNs have high processing and buffering capacities as well as an unlimited source of energy (since they are often plugged in an electric power source). However, WMNs suffer from a capacity limitation due to the scarcity of the radio resources as well as the prominent problem of interference. On the other hand, WMNs are often infrastructure-based networks whereas WSNs are randomly deployed in Ad Hoc fashion. In our study, we rather focus on the design of WMNs. One of the

main goals for which WMNs were designed is to foster the availability of Internet services (anywhere/anytime). Nowadays, it is also being deployed for various applications, namely:

- **Smart Grid:** Cities can install telemetry and smart grid services using mesh networks to support automated traffic control, smart parking meters, and smart utility meters. For instance, electric meters are now being deployed on residences and transfer their readings from one to another and eventually to the central office for billing without the need for human meter readers or the need to connect the meters with cables.

- **Public Safety:** Public safety agencies can rapidly and efficiently deploy resilient, high-capacity wireless mesh networks almost anywhere to improve situational awareness and support emergency communications.

- **Industrial Organizations:** WMNs are ideal to connect industrial operations and sites such as oil and gas fields, mining and construction areas, which are difficult to network because of their geography. With pervasive Wi-Fi, field workers communicate easily and have access to key applications.

- **Internet Access:** The laptops in the One Laptop per Child program use wireless mesh networking to enable students to exchange files and get on the Internet even though they lack wired or cell phone or other physical connections in their area.

- **Coverage Extension:** namely wireless coverage extension in university campuses, enterprizes, hotels, hospitals, public means of transportation, etc.

1.1.2 Femtocell Networks

Wireless access networks include the cellular evolution towards fourth generation systems (LTE, etc.) and the proliferation of high-speed cellular indoor networks, namely femtocell (FC) networks. A FC network is a low power, small-area-covering wireless cellular network consisting of one Femto Access Point (FAP) and stationary or low-mobility femto-users (FUs) deployed in an indoor environment such as a home or an office environment. Recent statistics have shown that around 50% of voice calls and 70% of data traffic originate indoor. On the other hand, traditional macro-cellular networks suffer from poor indoor coverage. Hence, FC networks have appeared as a solution to improve the macrocell (MC) network capacity and coverage at a low cost. Moreover, FCs offer very high dedicated bandwidth and excellent service experience for individual users and a new class of value-added "femtozone services" that take advantage of certain unique characteristics of FCs, such as their ability to sense presence and to allow seamless communications of mobile handsets with other multimedia devices in the home or office [22]. From global roaming to innovative applications and better QoS experience, the next generation of wireless access networks, namely FC networks, promises to enable a level of mobile data connectivity and capability that is unprecedented. However, many challenges concerning resource allocation emerge in such networks mainly due to their autonomous nature. In fact, FCs operate in the licensed spectrum owned by wireless operators and share this spectrum with the under-laying MC networks, thereby inducing significant co-channel interference that could compromise system performance if it is not addressed properly. This interference arises from

MC-to-FC, FC-to-FC, and/or FC-to- MC interactions. Dealing with this interference is a very challenging task due to the lack of coordination between FCs and MCs, and among the FCs themselves, which are not necessarily associated with the same Femto-operator. Moreover, unlike traditional cellular networks, there is no centralized entity or common base station to perform resource allocation for different FCs deployed in the same geographic area. Therefore, it is important that efficient resource allocation methods tailored to the FC requirements be designed and developed in order to enable successful deployment of FC networks.

1.2 Resource Allocation for Heterogeneous Wireless Networks

The main goal of this dissertation is to develop efficient resource allocation and management methods for these next-generation wireless networks that can satisfy QoS requirements and can ensure fairness among users. The resources that we consider in our work are temporal resources (time slots), radio resources (wireless channels/subcarriers), and power resources. Radio resources are inherently scarce, since all users must communicate using a common electromagnetic spectrum. This is the case for example of the ISM band where there are multiple co-channel networks (WiFi, WiMax, etc.), and the licensed cellular bands, which are shared by multiple-tier co-located cellular networks (such as two-tier FC/MC networks). On the other hand, wireless users are becoming increasingly sophisticated, and are demanding services with a wide range of QoS requirements, designed for various applications including voice, data, and multimedia applications. Consequently, highly efficient and robust resource allocation schemes are

essential for the success of heterogeneous wireless networks. In addition to the scarcity problem, the design of such schemes is very challenging due to some properties inherent to the wireless propagation environment and the self-organizing and autonomous nature of some of these networks. A wireless network is typically associated with a dynamically changing radio environment (such as the channel gains and user locations), and changing energy consumption and traffic requirements.

In this thesis, we consider resource allocation problems in two distinct types of wireless networks: (a) centrally controlled wireless networks, where a central network controller controls and allocates the radio resources (i.e., WMNs), and (b) distributively controlled wireless networks (i.e., FC networks), where the resource allocation decisions are distributed/local to the wireless users. To perform this task, we adopted different methodologies ranging from optimization programming to adaptive control depending on the network constraints. Moreover, some of our proposed schemes rely on graphical abstract models and structures, others on physical/system level analysis or a combination of both depending on the desired design objective.

Next, we briefly describe the incentive behind using each of these approaches: centralized vs. distributed. For instance, in the case of WMNs, a centralized approach is more attractive thanks to the presence of a centralized entity that monitors the network functioning and possesses global knowledge of the network parameters, such as network topology, nodes' schedules, resource usage, traffic requirements, etc. In addition to its feasibility, a main asset of this approach is that it allows the computation of the optimal solution via some optimization programming tools. However, this comes at the cost of higher complexity, especially for large networks (with thousands of nodes).

For FC networks, however, centralized solutions are not possible, due to the lack of a central entity/agent that coordinates their operation. For this reason, distributed schemes are necessary for this type of networks. The problem of resource allocation is even very challenging for these emerging spectrum-sharing two-tier FC networks since it requires not only distributed but also non-cooperative solutions, where a given FC is not allowed to coordinate with either other FCs or the underlaying MC.

1.3 Thesis Organization and Contributions

1.3.1 Research Contributions

This dissertation makes four important contributions to the study and design of resource allocation in next-generation wireless networks. We briefly elaborate on these contributions in this section.

- First, we design a new scheduling scheme that improves multi-radio multi-channel (MR-MC) WMNs throughput and session satisfaction ratios by (i) eliminating interference among active links, (ii) taking into account the spatial traffic distribution during the channel assignment process, (iii) allowing the use of multiple channels per link, and (iv) privileging links with lower session satisfaction ratios.

- Second, we direct our attention to the problem of FC capacity improvement via adaptive power allocation to FUs. To this end, we propose a new distributed non-cooperative uplink (UL) power allocation scheme for FC networks that aims at fairly maximizing the capacity of FUs while ensuring symbiosis between the

FCs and the underlying MC, and among FCs themselves. Each time slot, each FU decides its transmission power value based on the evolution of its signal to interference ratio (SIR), and the predicted value of the interference at its FAP.

- Third, we develop a new distributed QoS-aware UL power control (PC) scheme for both FUs and MUs that aims at maintaining the minimum required SIR for a maximum number of cellular users (CUs). In addition to the fact that our scheme does not require any type of coordination (neither inter-tier nor intra-tier), it is based on the use of ordinary differential equations (ODEs) to solve the power allocation problem, which is a new contribution in itself. On the other hand, we provide a theoretical analysis of our proposed scheme. Our analysis shows that our proposed set of ODEs admits a unique solution. We also derive sufficient conditions for the stability of the solution at the equilibrium point. Analytical and simulation results encourage the implementation and adoption of our scheme in existing FC/MC systems.

- Finally, we derive a statistical characterization of the UL physical interference, SIR, and outage probability in FC networks, and study its impact on data link level performance metrics, namely the packet delay, data loss rate and the maximum achievable FU throughput for constant bit rate (CBR) type of traffic. Our analysis establishes key cross-layer relationships that can be used for designing efficient resource utilization techniques for FC networks, such as interference-aware power control, QoS-aware call admission control, etc.

1.3.2 Thesis Organization

This dissertation is organized into six chapters. Chapter 1 provides a system overview of the studied network, its architecture, applications, and the challenges that arise in the design of resource allocation schemes in such networks. It also highlights our contributions achieved in this area of research. Chapter 2 proposes an interference-free traffic-aware scheduling algorithm for MR-MC WMNs. This scheme aims at fairly maximizing the capacity of MR-MC WMNs and is formulated using binary integer programming. In chapter 3 and chapter 4, we propose two distributed non-cooperative power allocation schemes for two-tier FC networks with two different perspectives. In chapter 3 we design an estimation-based power allocation scheme that aims at fairly maximizing the capacity of FC networks, whereas in chapter 4, we propose a novel stochastic power control scheme that aims at maintaining the minimum required QoS for both MUs and FUs. Chapter 5 presents a cross-layer UL performance analysis for power-controlled two-tier FC networks. In this chapter, we characterize the UL physical interference in FC networks and study its impact on the data-link layer QoS performances, namely the delay, data loss rate, and effective throughput of CBR traffic. Finally, in chapter 6, we summarize the main contributions of the work presented in this thesis, present some of its limitations, and suggest new horizons for future research works and directions.

Chapter 2: Scheduling in Multi-Radio Multi-Channel WMNs

In this chapter, we address the problem of capacity/bandwidth improvement in wireless mesh networks (WMNs) that are capable of multiple channel access and equipped with multiple radio interfaces. Therefore, we propose an interference-free joint time and frequency scheduling scheme for wireless mesh routers. Our scheme is interference and traffic aware in that it increases the overall achievable throughput of the network by eliminating interference between the wireless mesh routers, and maximizes the satisfaction ratios of all active sessions by accounting for the sessions' data rate requirements. Simulation-based results show that our proposed scheme outperforms the Tabu-based scheduling scheme, and yields good tradeoffs between the achievable throughput of the network and the satisfaction ratios of the sessions.

2.1 Introduction

WMNs are a new networking paradigm that can be deployed as a wireless backbone network [9], aiming at extending the coverage of wireless access networks, such as femtocell networks, via wireless multi-hop connections. In this architecture, the fixed wireless mesh routers, which form a wireless backbone collect the traffic generated by the client nodes and relay it to other networks, such as Internet, cellular networks, Wi-Fi, WiMAX, etc. Nowadays, due to their low cost and ease of deployment and

maintenance, WMNs are appealing to several applications, such as enterprise backbone networks, last mile broadband Internet access, high speed metropolitan area networks, building automation, remote monitoring and control, etc., and hence, they are foreseeable as one of the potential networking solutions to the bandwidth scarcity problem [3]. Unlike the case of ad hoc networks, energy consumption and mobility do not usually present a challenge to WMNs. Capacity limitation, however, presents a fundamental challenge to WMNs due mainly to the interference arising from the wireless nature of the environment as well as the scarcity of the radio/channel resources. The interference arising from the use of one single wireless channel in a multihop environment limits the number of data communications that can occur simultaneously in a given neighborhood, thereby decreasing overall network throughput. One emerging solution to this interference problem is to enable routers with multi-radio, multi-channel (MR-MC) access. For example, multi-channel access can be made possible through the use of the multiple non-overlapping channels that are provided by IEEE 802.11 and/or IEEE 802.16 standards. Although the promises of MR-MC networks are apparent, there still requires sophisticated scheduling algorithms that can effectively assign these available channels and radios to various links. The apparent promises of MR-MC access networks have created significant research interests, resulting in numerous works ranging from capacity characterization [52, 55, 80] to performance optimization techniques and scheduling and channel assignment algorithms design [8, 10, 21, 65, 71]. In this chapter, we propose a new joint channel/radio assignment and time scheduling algorithm for MR-MC access capable WMNs that improves the overall achievable network throughput while accounting for data traffic requirements. The proposed scheduling scheme, referred to

as TAIFS (Traffic-Aware, Interference-Free Scheduling), eliminates interference among the active links via a wise combination of time and frequency domains. In addition, it is traffic aware; i.e., given a set of active paths and active link loads, TAIFS distributes the time and channel resources among the active links in a way that maximizes the capacity of these links with respect to their traffic loads, thus making them meet the end-to-end bandwidth requirements as much as possible and consequently enhancing the overall achievable network throughput. We compare our proposed scheme with the Tabu-search scheme [71], a recently proposed scheduling scheme also for MR-MC networks, and show the importance of considering data traffic rate requirements as well as channel switching capabilities in the scheduling design. Our proposed scheduling scheme uses binary integer programming (BIP) to maximize the capacity of the active links according to their traffic loads under both the protocol and physical interference models. It also exploits the radio-channel switching capability of the radio interfaces[1] in order to increase the spectral reuse, thus improving the achievable network throughput even further. Simulation results show that TAIFS outperforms Tabu Method [71] in terms of total achievable network throughput and the end-to-end flow satisfaction ratio.

2.2 Network Model

We consider a WMN modeled as a directed graph $G = (V, E)$, where V denotes the set of all the nodes (mesh routers) in the network, and E denotes the set of physical wireless links between pairs of nodes. Nodes are generated and placed randomly in a

[1]The radio switching time is shown to be decreased to approximately 80 microseconds in commercial IEEE 802.11 interfaces [11].

grid to form a WMN. We assume that all the nodes transmit with a fixed power P, and that there is a wireless link between two nodes when they are located within each other's transmission range. That is, for all $(u, v) \in V^2$, $(u, v) \in E$ when $d_{uv} \leq r$, where d_{uv} is the distance between nodes u and v, and r is node u's transmission range.

We assume that each node is equipped with m radio interfaces, and that there is a set Ω of n orthogonal channels, each of which has a capacity b (in Mbps). Moreover, we assume that all nodes (i.e., mesh routers) are stationary, and that the WMN topology is infrastructure-based with little to no topological changes. We consider a set Φ of simultaneously active sessions in the network, where each session $s_i \in \Phi$ is characterized by: Its source node $sce(i)$, its destination node $dest(i)$, its required data rate d_i, and the path P_i used to route session s_i's traffic. Given the set of sessions (i.e., source-destination pairs, their data rates and their paths), we extract the active sub-graph G' from the network graph $G = (V, E)$, where $G' = (V', E')$ is a weighted directed graph with:

- E' = $\{ e \in E : \exists s_i \in \Phi$ such that $e \in P_i\}$
- V' = $\{ v \in V : \exists e \in E'$ such that e is incident to $v\}$
- $\forall e \in E'$, the weight $w(e)$ of link e is the sum of all sessions' required data rates whose paths contain e; i.e.,

$$w(e) = \sum_{s_i \in \Phi : P_i \ni e} d_i \tag{2.1}$$

Links in the active subgraph G' are directed according to the routing direction of active

flows. It is important to mention that the focus of this chapter is on link scheduling and channel assignment algorithms rather than on routing techniques. Hence, we assume that routers use one of the existing routing algorithms for mesh networks (e.g., OLSR [1, 27]) to find optimal paths for all sessions. The proposed channel assignment and link scheduling scheme assumes that all paths are already chosen by means of the routing algorithm.

2.3 Problem Statement and Formulation

In this chapter, we propose a traffic and interference aware link-scheduling scheme that dynamically assigns channels and time slots among different active links while maximizing the achievable sessions' data rates. We assume that there exists a centralized server (e.g., a designated mesh router) in the network that has full knowledge of network topology, radio/channel resource availability, and active sessions' characteristics (i.e., source/destination, required data rate, and path). Note that because, by nature of WMNs, mesh routers can be safely assumed to be stationary (i.e., network topology does not change), and by assuming that the set of available channels and the number of radios remain unchanged over the course of sessions' durations, we argue that having a centralized scheduler/server is effective.That is, given that the topology and the number of radios remain unchanged, the scheduler/server will have to gather the sessions' information, run the proposed joint channel and time scheduling algorithm, and advertise the scheduling solutions to all mesh routers, which they will then use in their communication. This schedule is updated by the server whenever a session enters or

leaves the network, and transmitted again (via a common channel) to the different nodes in the network. In the remainder of this section, we will start by modeling and stating the different radio and interference constraints, and then define the criteria under which TAIFS performs.

2.3.1 Radio and Interference Constraints

In order to carry out a direct communication, two nodes need to be within each other's transmission range, and have at least one of their radio interfaces tuned to a common channel. A link e is said to be active if it has data traffic to carry; i.e., if it belongs to at least one of the sessions' paths. When e is active, it needs to be assigned at least one channel k. Thus, for every $(e, k) \in E' \times \Omega$, we introduce the binary variable x_e^k, and define it as:

$$x_e^k = \begin{cases} 1 & \text{if link } e \text{ is assigned channel } k \\ 0 & \text{Otherwise} \end{cases}$$

2.3.1.1 Interference Constraints

We consider two interference models: the protocol model and the cumulative model. In the protocol interference model, all links are assumed ideal, and the interference depends only on the distances separating the nodes [35, 55, 71]. In the cumulative interference model (also known as the physical interference model), the interference depends on distances, signal to interference plus noise ratio (SINR) levels, and other channel factors that affect signals' strength, such as fading and path loss [32, 35]. The interference

constraints under each of the two models are described next.

(i) The protocol Interference Model:

In our scheduling scheme, we are interested in maximizing the capacity of the active links only; i.e., the links that carry traffic loads. Given the active subgraph $G' = (V', E')$, the contention graph $C(G')$ is defined as the undirected graph whose vertex set is E' (i.e., active links), and whose edge set is all pairs $(u, v) \in E' \times E'$ such that u interferes with v or v interferes with u[2]. Fig. 2.1 shows an example of a network graph and its contention graph.

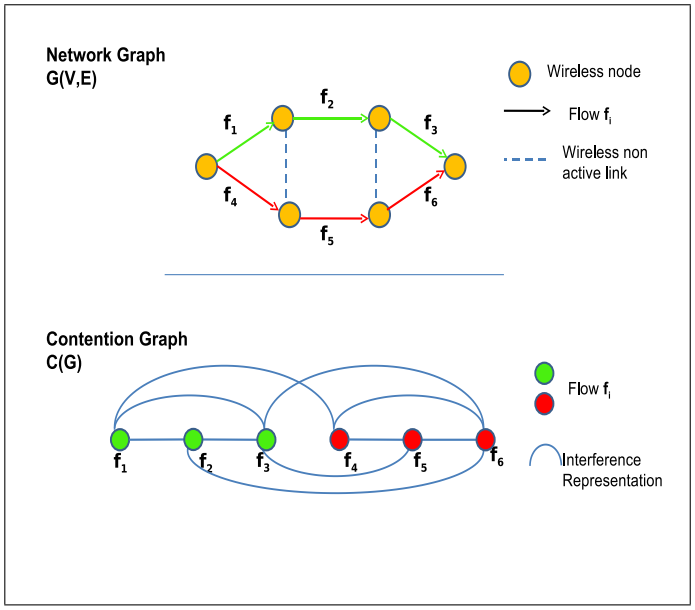

Figure 2.1: An example of network graph and its contention graph.

In this interference model [35,55,71], we assume ideal links and that the interference between nodes is mainly determined according to the distance separating them. We

[2]This contention graph model is similar to the one used in [45], and is used here to derive and formulate the different interference and radio constraints.

actually consider two types of interference constraints:

- **Interface-related Constraints**[3]: state that any two links that share at least one of their vertices can not use the same channel at the same time.

- **Pair-wise Interference Constraints**: state that in order for a transmission from node i to node j to be successful over the directed link (i, j) using channel k, the following two conditions must hold:

  1. $d_{ij} \leq r$. That is, the receiver must be within the transmitter's transmission range.

  2. $d_{lj} > r$ for every $l \in V'$ that is transmitting to any $h \in V'$ concurrently with j's reception on the same channel k. That is, the receiver j must be out of the range of interference caused by any other transmitter.

Therefore, by letting $I'(e) = \{e' \in E' :$ Transmission over e' interferes with Reception over e$\}$ one can write the interference constraints as:

$$x_e^k + x_{e'}^k \leq 1 \quad \forall (e, e') \in E' \times I'(e) \;\; \forall k \in \Omega \tag{2.2}$$

(ii) The Cumulative Interference Model:

We now formulate the interference constraints under the cumulative model. We consider the Rayleigh fading channel model, which works well in urban/no-line-of-sight (NLOS) environments [23]. Let us assume that a link e in the network transmits over channel k with power P_e^k. Let N_e denote the noise power measured at the receiver of

[3]These constraints are also adopted by the IEEE 802.11 standard.

link e. We also assume that the channel gain $G_{ee'}$ from the transmitter of link e' to the receiver of link e depends on the distance (between the transmitter and the receiver), and can be written as $G_{ee'} = K. \mid l_{ee'} \mid^{-\alpha}$, where $\alpha > 2$ is the path loss exponent, and $\mid l_{ee'} \mid$ is the distance between the transmitter of the link e' and the receiver of link e. A feasible schedule under the cumulative interference model is a set of activated links such that the minimum $SINR$ requirements are satisfied. In our case, a schedule consists of a set of links that could be active over more than one channel at the same time. Hence, the above condition should be satisfied for each link-channel pair that is active over a given time slot. To model this, we use the activation decision variables x_e^k in the $SINR$ formula (x_e^k: indicates whether a link e is active over a channel k). Thus the interference constraints can be written as:

$$SINR(e,k) \triangleq \frac{P_e^k.G_{ee}.F_e^k.x_e^k}{\sum_{e' \neq e} P_{e'}^k.G_{ee'}.F_{e'}^k.x_{e'}^k + N_e} > \beta_e.x_e^k \tag{2.3}$$

where F_e^k represents the fading coefficient of link e and channel k, and β_e is the $SINR$ threshold at the receiver of link e. In the Rayleigh fading model, we assume that for every channel k, the fading state variables, F_e^k for $e = 1, \ldots, |E'|$, are i.i.d. exponentially distributed random variables with unit mean. We also assume that the interference from other transmitters is much larger than the white Gaussian noise at the receivers, and therefore, we ignore the receiver noise in our analysis. Hence, Eq. (2.3) becomes:

$$SINR(e,k) \triangleq \frac{P_e^k.G_{ee}.F_e^k.x_e^k}{\sum_{e' \neq e} P_{e'}^k.G_{ee'}.F_{e'}^k.x_{e'}^k} > \beta_e.x_e^k \tag{2.4}$$

Note that $SINR$ here is a random variable. Therefore, for practicality reasons and since

we do not know the fading states ahead of time (i.e. before the actual transmission occurs), Eq. (2.4) is replaced by Eq. (2.5) (given hereafter), which uses the average value of $SINR$, denoted by $\overline{SINR}$ and written as:

$$\overline{SINR(e,k)} = \frac{E[P_e^k.G_{ee}.F_e^k.x_e^k]}{E[\sum_{e' \neq e} P_{e'}^k.G_{ee'}.F_{e'}^k.x_{e'}^k]}$$

Hence, the interference constraints under the cumulative interference model are:

$$\overline{SINR(e,k)} = \frac{P_e^k.G_{ee}.x_e^k}{\sum_{e' \neq e} P_{e'}^k.G_{ee'}.x_{e'}^k} > \beta'_e.x_e^k \quad \forall e \in E'; \forall k \in \Omega \tag{2.5}$$

In the particular case, where all the links use the same power level P for transmission, the cumulative interference constraints become:

$$\overline{SINR(e,k)} = \frac{G_{ee}.x_e^k}{\sum_{e' \neq e} G_{ee'}.x_{e'}^k} > \beta'_e.x_e^k \quad \forall e \in E'; \forall k \in \Omega \tag{2.6}$$

2.3.1.2 Radio Constraints

Given that every node is equipped with m radio interfaces, a node can at most communicate on m different channels at a given time. By letting $E'(i) = \{e \in E' :$ e incident to $i \in V'\}$, these radio constraints can be written as

$$\sum_{k \in \Omega} \sum_{e \in E'(i)} x_e^k \leq m \qquad \forall i \in V' \tag{2.7}$$

Similar interface constraints and interference models have already been used in the literature [32,35]. However, it is important to reiterate that in this chapter, we do not propose an interference model. The main contribution rather lies in: (i) the formulation of the scheduling problem in the case of a Rayleigh fading environment, (ii) the construction of an interference-aware frequency and time schedule, which is optimized with respect to the spatial traffic distribution (Phase I of TAIFS), and (iii) the exploitation of interface switching capability to increase the channel reuse and further improve the network throughput (Phase II of TAIFS).

2.3.2 Session Satisfaction Ratio

TAIFS increases the achievable network throughput by eliminating interference among the active links in the WMN while satisfying the data rate requirements of active sessions as much as possible; i.e., while maximizing the *satisfaction ratios* of active sessions, which are defined next. Recall that a link $e \in E'$ could be used to communicate traffic belonging to multiple different sessions, where again each session s_i is associated with a data rate requirement d_i. Hence, every link e is assigned an aggregate data demand $w(e)$ as defined by Eq. (2.1). Let $\mathbf{w} = [w(e)]_{e \in E'}$ be the vector representing all aggregate data demands on all active links. For all $e \in E'$, the total data rate that can be achieved on link e per frame (a frame is a set of time slots that repeat periodically; i.e., schedule length) is:

$$c(e) = \frac{\sum_{t=1:n_{ts}} \sum_{k \in \Omega} x_e^{k,t}}{n_{ts}} \times b \tag{2.8}$$

where b is the capacity of one channel, n_{ts} is the total number of time slots per frame, and

$$x_e^{k,t} = \begin{cases} 1 & \text{if link } e \text{ is assigned channel } k \text{ at time slot } t \\ 0 & \text{otherwise} \end{cases}$$

Under the physical interference model, the link throughput $c(e)$ can be expressed as:

$$c(e) = \frac{\sum_{t=1:n_{ts}} \sum_{k \in \Omega} x_e^{k,t}.b(e,k)}{n_{ts}}$$

where $b(e,k)$ is the channel capacity given by Shannon Formula, $b(e,k) = b.\log_2(1 + SINR(e,k))$, and $SINR(e,k)$ is the signal to interference plus noise ratio for link e over the channel k as defined by Eq. (2.3). For every $e \in E'$, we now define the per-session satisfaction ratio $\mathbf{sr}(e)$ of link e as:

$$\mathbf{sr}(e) = \frac{c(e)}{w(e)}$$

And for every session $s_i \in \Phi$, the session satisfaction ratio sr_i as:

$$sr_i = \min_{e \in P_i} \mathbf{sr}(e)$$

2.4 Traffic-Aware Interference-Free Scheduling

TAIFS operates in two main phases. The first phase performs a joint channel and time scheduling by solving a binary integer program (BIP) whose objective is to maximize the capacity of active links according to their traffic loads subject to interference and

radio constraints. The output of this phase is a set of active links, each assigned one time slot and a number of channels. The second phase is a heuristic that checks the possibilities of increasing the spectrum usage further by assigning more time slots and channels to active links whenever possible (i.e., without violating radio and interference constraints) while privileging the links with the least satisfaction ratios.

2.4.1 TAIFS Phase I: Traffic-Aware BIP-Based Scheduling

We will start by formulating our problem of traffic and interference aware channel assignment as a binary integer program (BIP). The outcome of this BIP is a subset of links that are assigned channels in a way that they can be active at the same time without interfering with each others. We present a BIP for each of the two studied interference models.

2.4.1.1 BIP Formulation for Channel Assignment

Case 1: Using the Protocol Interference Model

In this model, we assume that all links are ideal; i.e., the probability of transmission success on link e over channel k (given that both the radio and interference constraints are met) is $P_{success}(e, k) = 1$. Thus, the channel assignment program can be formulated

as:

$$\text{BIP(1):} \quad \begin{aligned} &\max_{x_e^k} \sum_{k\in\Omega}\sum_{e\in E'} w(e)\times x_e^k \\ &x_e^k + x_{e'}^k \le 1 \quad \forall k\in\Omega, \forall e\in E', \forall e'\in I'(e) \\ &\textstyle\sum_{k\in\Omega}\sum_{e\in E'(i)} x_e^k \le m \quad \forall i\in V' \\ &x_e^k \in \{0,1\} \quad \forall k\in\Omega, \forall e\in E' \end{aligned}$$

The above BIP assigns as many channels as possible to active links while giving priority to those with higher traffic loads under interference (Eq. 2.2) and radio (Eq. 2.7) constraints.

Case 2: Using the Cumulative Interference Model

We now consider the physical interference constraints introduced in the previous section, and account for the link reliability. In this model, transmitted signals are likely to attenuate and decay, thereby increasing the chances of the receiver not being able to decode its intended signal ($P_{sucess}(e,k) \neq 1$). Using Eq. (2.4), one can define the transmission failure probability for a link e using channel k as $Prob(SINR(e,k) \le \beta_e.x_e^k)$; i.e.,

$$P_{out}(e,k) = Prob(P_e^k G_{ee} F_e^k x_e^k \le \beta_e x_e^k (\sum_{e'\neq e} P_{e'}^k G_{ee'} F_{e'}^k x_{e'}^k))$$

The expression of $P_{out}(e,k)$ could be derived from the following result [48]:

Result: Suppose $z_1, z_2, , z_n$ are independent exponentially distributed random variables with means $E[z_i] = 1/\lambda_i$, Then we have:

$$Prob(z_1 \le \sum_{i=2:n} z_i) = 1 - \prod_{i=2:n} \frac{1}{1+\lambda_1/\lambda_i}$$

Now given that for every channel k, the random variables, F_e^k, $e = 1...|E'|$, are independent and exponentially distributed with $E[F_e^k] = 1, \forall k \in \Omega$, one can write

$$P_{out}(e,k) = 1 - \prod_{e' \neq e} \frac{1}{1 + (\frac{\beta_e . P_{e'}^k . G_{ee'} . x_{e'}^k}{P_e^k . G_{ee}})}$$

The probability $P_{success}(e,k)$ of transmission success of link e over channel k can be expressed as $1 - P_{out}(e,k)$. Or,

$$P_{success}(e,k) = \prod_{e' \neq e} \frac{1}{1 + \frac{\beta_e . P_{e'}^k . G_{ee'} . x_{e'}^k}{P_e^k . G_{ee}}} \tag{2.9}$$

Thus, the channel assignment per time slot optimization problem can be formulated as a MINLP:

$$\begin{aligned} \max_{x_e^k, P_e^k} \sum_{k \in \Omega} \sum_{e \in E'} w(e) \times P_{succes}(e,k) \times x_e^k \\ \overline{SINR(e,k)} = \frac{P_e^k . G_{ee} . x_e^k}{\sum_{e' \neq e} P_{e'}^k . G_{ee'} . x_{e'}^k} > \beta'_e . x_e^k \quad \forall k \in \Omega, \forall e \in E' \\ \textstyle\sum_{k \in \Omega} \sum_{e \in E'(i)} x_e^k \leq m \quad \forall i \in V' \\ P_e^k \leq P_0 \quad \forall k \in \Omega, \forall e \in E' \\ x_e^k \in \{0,1\} \quad \forall k \in \Omega, \forall e \in E' \end{aligned}$$

This optimization program is equivalent to BIP(1). It aims at maximizing link capacity by increasing the number of channels assigned to each link according to its traffic demand, while taking into account the quality of the link modeled via $P_{success}$. The first set of inequalities in this program (MINLP) corresponds to the physical interference constraints. The second set corresponds to the radio interface constraints. The third set

corresponds to the power constraints, stating that the transmission power of any link must not exceed P_0. Finally, the last set of inequalities corresponds to the channel-to-link assignment indicator variable, which can only take the value of zero or one. This new optimization program is a MINLP (Mixed Integer Non Linear Program), which aims at optimizing not only the channel-to-link assignment, but also the transmission power allocated for every active link-channel pair. Power allocation variables appear in both expressions of $P_{success}(e,k)$ and $SINR(e,k)$. When all links are assumed to transmit at the fixed power P, the probability of transmission success becomes

$$P_{success}(e,k) = \prod_{e' \neq e} \frac{1}{1 + \frac{\beta_e . G_{ee'} . x_{e'}^k}{G_{ee}}}$$

and MINLP becomes a binary integer program, termed BIP(2):

$$\begin{aligned} \max_{x_e^k} \sum_{k \in \Omega} \sum_{e \in E'} w(e) \times \prod_{e' \neq e} \frac{1}{1 + \frac{\beta_e . G_{ee'} . x_{e'}^k}{G_{ee}}} \times x_e^k \\ \overline{SINR(e,k)} = \frac{G_{ee} . x_e^k}{\sum_{e' \neq e} G_{ee'} . x_{e'}^k} > \beta'_e . x_e^k \quad \forall k \in \Omega, \forall e, e' \in E' \\ \sum_{k \in \Omega} \sum_{e \in E'(i)} x_e^k \leq m \quad \forall i \in V' \\ x_e^k \in \{0,1\} \quad \forall k \in \Omega, \forall e \in E' \end{aligned}$$

Note that we can use the same heuristic that we developed for solving the problem of joint scheduling and channel assignment under the interference protocol model to solve the above physical interference model based formulation. It suffices to solve BIP(2) in the first algorithm (that we will present in the next paragraph) instead of solving BIP(1).

2.4.1.2 TAIFS Phase I Description

Since BIP(1) and BIP(2) perform the same task, namely channel assignment, but with respect to two different interference models, we will use the "unique" notation BIP to refer to any of them. Because solutions to the BIP presented above may be such that some active links may not be assigned any channels due to resource (channels and radio interfaces) limitations, we propose to proceed iteratively in order to ensure that all active links are scheduled. In the first iteration, the set of all the active links (i.e., E') is injected as an input to BIP. After solving this BIP, there will be two disjoint sets: a set E_1 of these active links that have been assigned channels; i.e., $E_1 = \{e \in E' : \exists k \in \Omega, x_e^k = 1\}$ and a set E'_2 of all these unassigned active links; $E'_2 = E' \setminus E_1$. In the second iteration, BIP is solved again, but while considering E'_2 instead of E' as the set of active links (those active links that were not assigned any channels during the first iteration). After solving this second BIP, there will also be two disjoint sets: a set E_2 of all active links that are assigned channels during the second iteration; i.e., $E_2 = \{e \in E'_2 : \exists k \in \Omega, x_e^k = 1\}$ and a set E'_3 of all the unassigned active links; $E'_3 = E'_2 \setminus E_2$. These iterations continue until all the active links in E' are each assigned at least one channel. Once this is done, each set E_i obtained during iteration i will be assigned a time slot, during which all links in E_i are scheduled to carry traffic during that time slot. These iterations constitute the first phase of TAIFS, and are summarized in Algorithm 1. In this algorithm, **SM** represents a 3-dimensional schedule matrix, containing information about the time and channel assignment for the whole set of active links after execution of TAIFS Phase I.

Algorithm 1 TAIFS Phase I: BIP based Scheduling

Input: $G' = (V', E')$, Ω, **w**, CM: The set of constraints.
Output: n_{ts}: Number of time slots per time frame, **SM**: Time and Channel assignment matrix.
$A \leftarrow E'$
$n_{ts} \leftarrow 0$
Initialize **SM** to zero matrix
while $A \neq \emptyset$ **do**
    Solve BIP
    $S \leftarrow \{e \in A : \exists k \in \Omega, x_e^k = 1\}$
    $A \leftarrow A \setminus S$
    Update **SM** and CM
    $n_{ts} \leftarrow n_{ts} + 1$
end while

2.4.2 TAIFS Phase II: Traffic-Aware Link-Capacity Improvement

The first algorithm described above partitions the set E' of all active links into disjoint subsets, each of which consists of multiple non-interfering links that can be active concurrently during a time slot. Each of these links is assigned a number of channels that it can use during that time slot. We now propose a heuristic that aims at increasing the number of active links that can be scheduled during each of the time slots determined by Algorithm 1. Basically, the heuristic tries to further increase the data rate $c(e)$ that every link e can achieve, while prioritizing the links with the lowest satisfaction ratios. The heuristic works as follows. First, it uses the outcome of Algorithm 1 (run during TAIFS Phase I) to calculate the satisfaction ratio $\mathbf{sr}(e)$ of every active link e. Recall that the algorithm allocates one time slot and assigns a number of channels for every link e. Second, the heuristic ranks these links according to their increasing order of their satisfaction ratios. The rationale behind this ordering is to give a privilege to links that

are the farthest from satisfying their data rate requirements. Once this preparation phase is done, the heuristic picks the "neediest" link e_c among all links, and for every time slot T_j that chronologically follows the time slot T_i that has been assigned to e_c in Phase I, it computes the set of channels over which link e_c could be activated during T_j without causing any interference. Among these channels, only the channels that, once assigned to e_c, do not violate the radio constraints are then kept. We denote this set of channels by $\Gamma(e_c, T_j)$. If $\Gamma(e_c, T_j) \neq \emptyset$, channels from this set are assigned to e_c on a per channel-by-channel basis until $floor(sr(e_c)) = 1$ or until all channels in $\Gamma(e_c, T_j)$ are assigned to e_c. The steps needed to perform this check operation (i.e. check whether a link e_c can be activated in time slot T_j and determine the set of channels $\Gamma(e_c, T_j)$ it will use during that time slot, if possible) is given by Algorithm 2.

Algorithm 2 TAIFS PHASE II: **check module**

Input: e_c: candidate link, T_j: candidate time slot, $L(T_j)$: set of links active during T_j.
Output: $\Gamma(e_c, T_j)$: set of channels to be assigned to e_c in T_j.
$A \leftarrow L(T_j)$, $\Gamma(e_c, T_j) \leftarrow \Omega$, $exit = 0$
while $(A \neq \emptyset)$ and $(exit = 0)$ **do**
    Pick $l \in A$
    if (e_c interferes with l) or (l interferes with e_c) **then**
        $\Gamma(e_c, T_j) \leftarrow \Gamma(e_c, T_j) \backslash CH(l, T_j)$
        if $\Gamma(e_c, T_j) = \emptyset$ **then**
            $exit = 1$
        end if
    end if
    $A \leftarrow A \backslash \{l\}$
end while
if $\Gamma(e_c, T_j) \neq \emptyset$ **then**
    Check channels in $\Gamma(e_c, T_j)$: remove those violating radio constraints when assigned to e_c during T_j
end if

Note that in Algorithm 2, $L(T_j)$ (the set of links active in time slot T_j) and $CH(l, T_j)$ (the set of channels used by link l in time slot T_j) are deduced from the **SM** matrix. After the check module related to the activation of link e_c in slot T_j is performed, if $floor(\mathbf{sr}(e_c)) < 1$, then we move to the next time slot T_{j+1} and apply the check module for link e_c and time slot T_{j+1}. We keep performing the same operations until $floor(\mathbf{sr}(e_c)) = 1$ or until the end of the frame is reached; i.e., all the time slots that follow T_i are scanned. The steps of the whole heuristic run during TAIFS Phase II are summarized and provided in Algorithm 3.

Algorithm 3 TAIFS Phase II: Network Capacity Improvement

Input: E'_{sorted}: Array of links in E' sorted according to their capacities, T_{sorted}: Array of time slots assigned to links in E'_{sorted}, n_{ts}, **SM**: The schedule matrix, **sr**: The link satisfaction ratio vector.
Output: SM: Time and Channel assignment matrix, **sr**: The link satisfaction ratio vector.
for $counter = 1 : |E'_{sorted}|$ **do**
  $e_c \leftarrow E'_{sorted}[counter]$
  $T_i \leftarrow T_{sorted}[counter]$
  $T_j \leftarrow T_{i+1}$
  while $(T_j \leq n_{ts}) and (floor(\mathbf{sr}(e_c)) < 1)$ **do**
    $\Gamma(e_c, T_j) \leftarrow$ **check module**$(e_c, T_j, L(T_j))$
    if $\Gamma(e_c, T_j \neq \emptyset)$ **then**
      Update **SM**
      Update ($\mathbf{sr}(e_c)$
    end if
    $T_j \leftarrow T_{j+1}$
  end while
end for

Now that we have presented the two phases of our scheme in detail, we will next show how TAIFS (i) eliminates interference between wireless routers, (ii) increases

spectral reuse, and (iii) improves network throughput.

By design, TAIFS assigns channels/time slots to active links in such a way that they do not interfere with each other. In fact, in the first phase of our scheme the active links are scheduled iteratively. In each iteration, a set of links are assigned some channels over which they can be active during a given time slot while meeting the interference and radio constraints. The second phase of our scheme conserves the "interference-free" property. Indeed, in this phase, we only activate link e in some slot $T_j > T_i$ if and only if there exists some channel k such that if link e transmits in slot T_j over channel k it will not interfere with the other links which are already active in T_j, and the radio constraint is not violated by this activation. Hence, the schedule obtained after phase II is also interference-free.

On the other hand, TAIFS improves spectral reuse during both phases. In the first phase, spectral reuse is increased by assigning the same channel to multiple, non-interfering links that can be active during the same time slot. Channel reuse is further increased in the second phase. In fact, note that in the first phase, if a link e is activated in time slot T_i, $(i < n_{ts})$, e is not considered for activation in time slot T_j $(\forall j, i+1 \leq j \leq n_{ts})$. In the second phase we study the possibility of activating link e in time slots different from the time slot it has been initially assigned during phase I. Thus, in phase II, by increasing the number of slots in which a link is activated, we increase not only the link capacity, but also the channel reuse (i.e. the number of users per channel at a given time).

As far as network throughput is concerned, in our scheduling scheme, the channel-to-link assignment is performed with respect to the link's current traffic load as shown in BIP. Thus, the number of channels assigned per link is proportional to the link's traf-

fic load. As a consequence, links participating in forwarding traffic of more than one session (thus representing potential bottlenecks) are given higher priority and assigned more channels. Hence, the per session achievable throughput will be increased compared to the case where every link is assigned only one channel independently of the traffic load, as done in previous works: [5, 8, 59, 65].

In short, the proposed scheduling scheme improves the network throughput and the session satisfaction ratios by (i) eliminating interference among active links, (ii) taking into account the spatial traffic distribution during the channel assignment process, (iii) allowing the use of multiple channels per link, and (iv) privileging links with lower session satisfaction ratios.

2.5 Performance Evaluation

2.5.1 Simulated Scheme and Performance Metric

For completeness, we first begin by providing a brief overview of Tabu Method [71], and then present the performance metric used in this evaluation section.

2.5.1.1 Simulated Scheme

Tabu-Method [71]. is a centralized channel assignment algorithm also designed for MR-MC WMNs. It consists of two main phases: In the first phase, it assigns channels (or colors) to vertices in the contention graph, where each vertex corresponds to one

link in the active graph, but without taking radio interface constraints into account. It starts first from a random channel assignment, and then tries to improve this assignment iteratively by using the tabu-based search technique [38]. The goal of this phase is to minimize interference by achieving a graph vertex coloring that maximizes the number of edges that link vertices of different colors in the contention graph. Since the channel assignment obtained from the first phase may not satisfy the radio interface constraints, during the second phase, Tabu Method applies a merge procedure repeatedly to eliminate these constraint violations.

2.5.1.2 Performance Metric

The main purpose of this work is to provide a scheduling scheme for MR-MC wireless mesh networks with the main objective of increasing the active sessions' satisfaction ratios. Therefore, we use this metric as a means to evaluate and analyze the performance of the proposed scheduling scheme. The session satisfaction ratio is defined as the ratio of the session's achieved data rate to that of its required one. It is viewed as a metric of assessing how well the scheme performs from a session (i.e., user)'s viewpoint.

2.5.2 Simulation Settings and Results

2.5.2.1 Simulation Settings

We implemented both TAIFS and Tabu Method in MATLAB. We used TOMLAB (linked with MATLAB) to solve the BIPs of TAIFS Phase I. TOMLAB offers a variety of tools

to solve BIPs efficiently and reliably; the one that we used is based on the Branch and Cut algorithm [70]. We ran our simulations, analyzed them, and plotted our results also using MATLAB. In our simulations, we generated random MR-MC WMNs, each consisting of 50 mesh routers randomly deployed in a $1000m \times 1000m$ area. We also fixed the transmission range r of every node to 250m. We consider n wireless channels, and assume that every mesh router is equipped with m radio interfaces. For evaluation purposes, we varied n from 2 to 12 and m from 2 to 6. For every generated network topology, we also generate $|\Phi| = 20$ sessions by randomly selecting 20 random pairs of source/destination nodes. $MaxRate$ denotes the maximum data rate that a session can require. Session i's data rate, $i = 1, 2, \ldots, |\Phi|$, is set to $i \times MaxRate/|\Phi|$. The total traffic load is then $T_{MaxRate} = \frac{(|\Phi|+1)MaxRate}{2}$.

It is known that BIPs are NP-hard problems. However, there exists some fast operation research approaches/heuristics implemented in Tomlab/CPLEX (e.g., Branch and Cut) that can provide fast and accurate enough solutions to BIPs. For example, for the case of our simulations (a network with 50 nodes and 12 channels) the CPU time for computing the BIP based schedules is around few milliseconds. This computation time could be further decreased if computation is performed by more powerful computing machines/servers. In the following subsection, we will present the performances of our scheme in terms of satisfaction ratio improvement.

2.5.2.2 Simulation Results

First, we study the general performance behavior of our system under different aggregate network traffic demands and resource availabilities (channels and radio interfaces). Figs. 2.2 and 2.3 show the average session satisfaction ratio when both the number of channels and the number of radios are varied respectively for $MaxRate = 10Mbps$ and $MaxRate = 60Mbps$. We can see that, for both cases of $MaxRate$, the aver-

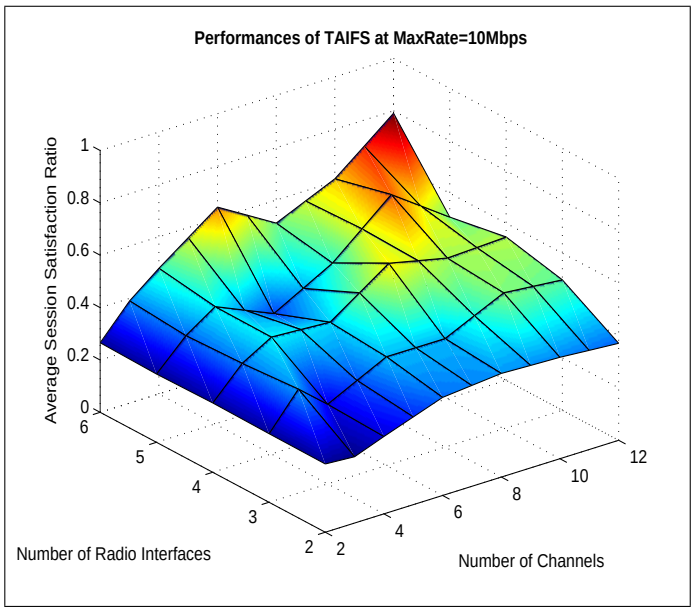

Figure 2.2: Impact of the number of channels and radios on the average satisfaction ratio for $MaxRate = 10Mbps$

age session satisfaction ratio has the same trend: It increases as the number of channels and/or radio interfaces increases. We notice that when the number of radios per node m equals 2, an increase in the number of channels has little to no impact on the achieved per session satisfaction ratio. Likewise, when the number of channels n equals 2, an increase in the number of radios slightly improves the average session satisfaction ra-

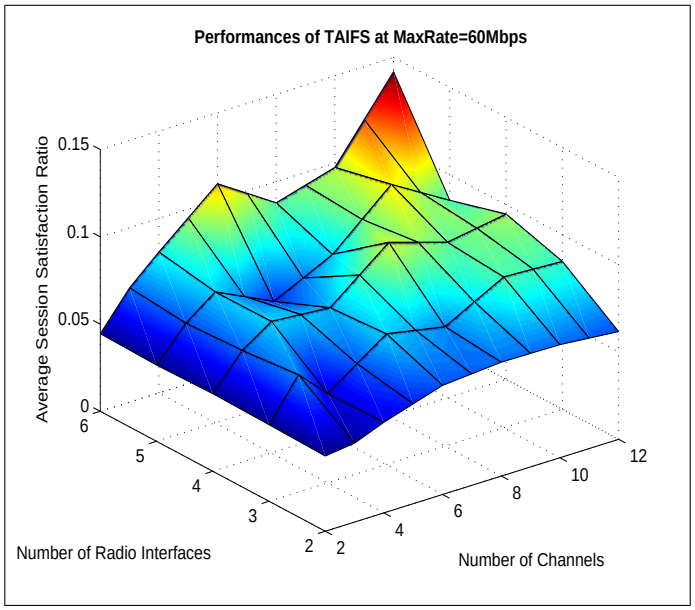

Figure 2.3: Impact of the number of channels and radios on the average satisfaction ratio for $MaxRate = 60Mbps$

tio. However, when n gets closer to 12, an increase in the number of radios incurs a significant improvement in the achieved session satisfaction ratio; this can be seen from the steep slope of the obtained curves. On the other hand, by varying $MaxRate$, we can clearly see the impact of total traffic load on the performances. For instance, when $MaxRate = 10Mbps$, the total traffic load is $T_{10} = 105Mbps$, and we can achieve up to 80% per session satisfaction ratio. While, when $MaxRate$ is increased to $60Mbps$ (i.e., total traffic load $T_{60} = 630Mbps$), we can only achieve up to 15% of the required data rate. This gives us good insights on the capacity of our network during the WMN planning phase. In other words, given a set of resources and sessions' rate requirements, we can determine the average session satisfaction ratio guaranteed by our scheduling scheme.

Second, we compare the session satisfaction ratios of TAIFS with those of Tabu Method. Since Tabu Method does not eliminate the interference completely and assigns only one channel per link, we consider that the obtained link capacity with this scheme is $c(e) \approx \frac{b}{|I'(e)|+1}$, where $I'(e)$ is the set of links that interfere with link e and are assigned the same channel as this one using the Tabu approach. Hence, what we measure for the Tabu Method is an upper bound rather than the actual achievable performance.

Figs. 2.4 and 2.5 show the average session satisfaction ratios under both schemes for

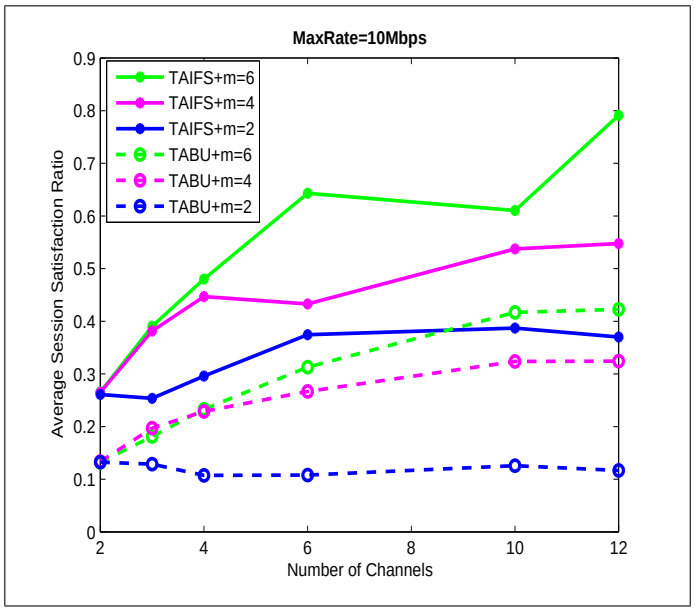

Figure 2.4: Session satisfaction ratio: $MaxRate = 10Mbps$

two different values of $MaxRate$: 10Mbps and 60Mbps. Observe that the session satisfaction ratio realized under our scheme is double the one realized under Tabu-scheme. In addition, notice that the variation of the number of radio interfaces affects the performances of our scheme; by looking at the satisfaction ratios depicted via the 3 curves shown in Fig. 2.4, we can see that when n is greater than 6 channels, adding 2 more ra-

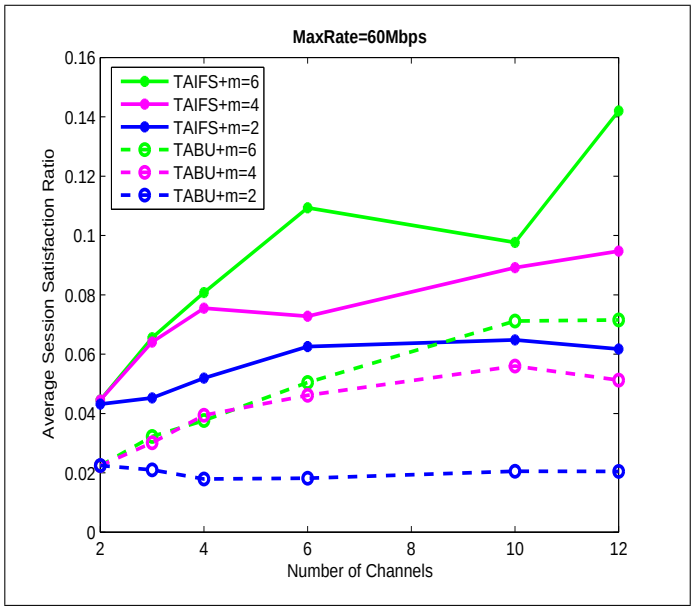

Figure 2.5: Session satisfaction ratio: $MaxRate = 60Mbps$

dio interfaces increases the satisfaction ratio level by about 20%. With Tabu Method, on the other hand, as m increases from 4 to 6, the achieved session satisfaction ratio level increases slightly and tends to stabilize around the value of 35%. Tabu Method performs even poorly when $MaxRate$ is increased to 60Mbps. In fact, Fig. 2.5 shows that when $n = 6$ and $m = 6$, our scheme performs three times better than Tabu Method. The figure also shows that for a given value of $MaxRate$, the best session satisfaction ratio realized under our scheme is around 15% versus 7% for Tabu Method. We also notice that the curve related to our scheme is still far from stabilizing at a fixed bound/value for $n = 12$.

In essence, these obtained results show that our proposed scheme, TAIFS, outperforms the TABU based scheme in terms of sessions' satisfaction ratios. Although Tabu Method minimizes the interference in the network, it does not make an efficient use of

the available resources (i.e. channels vs. time). Unlike Tabu Method, TAIFS can assign active links more than one channel per time slot. In addition, TAIFS allows links to switch across different channels during different time slots, thereby utilizing the available spectrum and radio resources more efficiently.

2.6 Summary

In this chapter, we proposed an interference-free, traffic-aware scheduling scheme for MR-MC WMNs. Our scheme uses binary integer programming to assign channels and time slots to active links while accounting for sessions' traffic loads. Results show that our scheme increases throughput and sessions' satisfaction ratios by (i) eliminating interference and (ii) taking into account the spatial traffic distribution. Simulation results also show that our proposed scheme outperforms Tabu-based scheduling scheme in terms of session satisfaction ratios.

Chapter 3: Fairness-Oriented Power Allocation in Two-Tier FC Networks

In this chapter we develop a new distributed non-cooperative uplink (UL) power allocation scheme for femto-users (FUs). Our scheme aims at fairly maximizing the throughput of FUs based on periodic estimation of the interference at the femto access points (FAPs). We compare our scheme to the optimal centralized one. Simulation results show that our scheme presents good performances in terms of throughput and fairness.

3.1 Introduction

Femtocells (FCs) operate in the licensed spectrum owned by wireless operators and share this spectrum with macrocell (MC) networks, thereby inducing significant co-channel interference that could compromise system performances if it is not taken into account. This interference arises from MC-to-FC, FC-to-FC, and/or FC-to-MC interactions. Dealing with this interference is a very challenging task due to the lack of coordination between FCs and MCs, and among the FCs themselves, which are not necessarily associated with the same Femto operator. Moreover, unlike traditional cellular networks, there is no centralized entity or common base station to perform resource allocation for different FCs deployed in the same geographic area. Therefore, traditional centralized interference mitigation and power control schemes are no longer applicable to this type of networks. Even distributed cooperative solutions are not appropriate in

this context, since FCs are independent of and often cannot communicate with one another. There have been some research works recently proposed to analyze and solve the FC interference problem in UL communications. Claussen [26] evaluated the impact of deploying FCs on existing co-channel MCs based on system level simulations. On the other hand, Shi et al. [67] developed an analytical model to study the UL capacity and coverage of UMTS FCs coexisting within the MCs. Other works proposed some resource management schemes in two-tier FC/MC networks in order to reduce the interference and improve the capacity of these networks. For instance, in [56, 64], the authors designed fractional frequency reuse (FFR) based scheduling techniques to mitigate the interference at the FCs, while in [72], a distributed hashing-based scheduling scheme is proposed for OFDMA FCs, under the assumption of FC-MC cooperation. These different spectrum management schemes might be further improved by optimizing power allocation. Therefore, some works have been recently proposed to decrease UL co-channel interference via adaptive power allocation: In [82], Yavuz et al. tried to mitigate interference via power calibration. Jo et al. [47] proposed a simple UL power control for FCs. Their scheme adjusts the transmit power of FUs in proportion to the fed-back interference level of MCs. However, they focused only on the protection of a MC's UL communication and neglected inter-FC interference. In [19], Chandrasekhar et al. characterized the maximum achievable MC signal to interference plus noise ratio (SINR), given a set of feasible FC SINRs, using the Pareto optimality criterion. They also proposed a coordinated UL power control architecture for both MCs and FCs, which requires MCs to use their proposed power control algorithm. Their work assumes cooperation and possibility of communication between FCs and underlying MCs, which

is not often the case since FCs co-located with the MC do not necessarily belong to the same cellular/wireless operator. One of the main priorities of the research community and the industry with the emergence of FCs was to ensure that the performance of the existing MC networks will not be affected by the introduction of these new entities: the FCs. Therefore, most of the related work, either focused on the protection of MC from interference originating from FCs, or coupled (femto and macro) resource management while assuming the possibility of coordination between the macro base station (MBS) and the FAPs, which is not always true. Therefore, in this chapter we direct our attention to the problem of FC capacity improvement via adaptive power allocation to FUs. To this end, we propose a new distributed non-cooperative UL power allocation scheme for FC networks in which we try to fairly maximize the capacity of FUs while ensuring $symbiosis$ between the FCs and the the underlying MC, and inter-FCs. Our scheme is completely distributed. Each time slot, each FU decides its transmission power value based on the evolution of its signal to interference ratio (SIR), and the predicted value of the interference at its associated FAP. Thus, our scheme does not require any exchange of information between FCs neither between FCs and MCs. Simulations have shown that our scheme achieves good performances in terms of throughput and fairness compared to the optimal centralized case despite the absence of information exchanges between the active FCs.

3.2 Network Model

We consider a single-carrier two-tier cellular system consisting of N_{FC} FCs (with coverage radius R_F) overlaid on one MC (with coverage radius R_M), where both of them operate over an identical carrier frequency f. Each FC consists of one FAP and N_{FU} femto-users. On the other hand, the MC consists of one macro base station (MBS_0) and N_{MU} macro users. We assume that both FCs and MC use TDMA as a channel access technique, that is, we assume that time is slotted and at every time slot only one MU is active per MC and only one FU is active per FC. We denote the currently active MU by m and the currently active FU associated with the femto access point FAP_i by FU_i. In this chapter, we consider the UL communication stream; i.e., communication from MU to MBS_0 and from FUs to FAPs. We also assume that these UL communications are synchronized [57][1]. We denote MUs' and FUs' maximum transmit powers respectively by P^m_{max} and P^f_{max}, where P^f_{max} is relatively small compared to P^m_{max}. In our network, we assume that there are no FCs in the vicinity of the macro base station, and that the maximum power used by FUs, P^f_{max}, is low enough so that UL communications at FCs will not cause harmful interference at the macro base station, MBS_0. Hence, this study focuses on and addresses the UL interference at active FAPs, created by their neighboring active MUs and FUs. The physical channel is represented by a combination of path-loss, log-normal shadowing and Rayleigh fading. The channel gain g_{ji} of user j to base station i is modeled in compliance with the ITU specifications [2], according to

[1]Once turned on and before initiating any communication, FCs get synchronized to the cellular core network using an asymmetric communication link such as xDSL thanks to an enhanced version of IEEE 1588 [57].

which at time slot t

$$g_{ji}(t) = K_j d_{ji}^{-\alpha_j}(t) S_{ji}(t) \tag{3.1}$$

where K_j is a constant factor, $d_{ji}(t)$ represents the distance from user j to base station i at time t, α_j the path loss propagation factor related to the transmission environment (we distinguish between three environments cellular, indoor, and indoor-to-outdoor), and S_{ji} represents the log-normal shadowing realization at time t with a standard deviation of $8dB$ for MUs and $4dB$ for FUs. We have superimposed the Rayleigh fading to this model by simply multiplying these channel gains by their corresponding Rayleigh fading coefficients F_{ji} in order to take into account the non-line-of-sight (NLOS) nature of the outdoor-to-outdoor/outdoor-to-indoor signal propagation. In fact, the impact of NLOS propagation conditions is significant especially in urban zones. Let $G_{ji}(t) = F_{ji}(t)g_{ji}(t)$ denote the resulting channel gain for transmission from user j to base station i at time t. Hence, given that there is only one active MU per time slot and only one active FU per FC per time slot, the signal to interference plus noise ratio (SINR) of the transmission from FU_i belonging to FC i to its FAP_i at time slot t is

$$\gamma_i(t) = \frac{g_{ii}(t)P_i(t)}{I_i(t)} \tag{3.2}$$

where $P_i(t)$ denotes the transmission power of FU_i at time t, and $I_i(t)$ (Eq. 5.14) is the interference experienced by FAP_i at time t due to the transmission of FU_j, $(j \neq i)$ of

neighboring FCs and the transmission of the simultaneously active MU m.

$$I_i(t) = \sum_{FU_j; j \neq i} G_{ji}(t) P_j(t) + \sigma_i(t) \tag{3.3}$$

where $\sigma_i(t) = G_{mi} P^m(t) + n_i$ with $P^m(t)$ denoting the transmission power of the active MU m at time t and n_i denoting the additive white Gaussian noise at FAP_i. Thus, under this physical interference model, the throughput of FU_i can be expressed as

$$Th_i = \frac{\sum_{t=1:T} C_i(t)}{T} \tag{3.4}$$

where $C_i(t) = W \log_2(1 + \gamma_i(t))$ is FU_i's Shannon capacity with W representing the channel bandwidth in Hz.

3.3 Problem Statement and Formulation

In this chapter, we aim at maximizing the capacity of FCs while accounting for some of their specificities, such as their low power operation, the lack of cooperation among the FCs, and between the FAPs and the macro BS. As mentioned before, a FAP is a small device that is installed in an indoor environment, like a home or an office, to provide access to its indoor users. Typically, FAPs are not associated with the macro cellular networks, and henceforth, they are likely to be managed and owned by different entities/operators. They are, however, expected/assumed to operate over the same wireless channel that the underlying macro cellular network uses. Therefore, there is a need for mechanisms that manage the exploitation of the common wireless channel by the FUs

so that their physical capacity in terms of achievable throughput is fairly increased. The key challenge as well as the focus of this chapter is on how FCs can effectively allocate the transmission powers of their associated FUs in spite of the lack of coordination among FCs themselves as well as between FCs and the macro cellular network, in order to maximize their throughput. The problem of uplink (UL) power allocation to FUs can be formulated as a non-linear program (NLP):

$$\begin{aligned} \max_{P_i(t)} & \sum_{i \in \Omega_t} w_i(t) \log_2(1 + \frac{g_{ii}(t)P_i(t)}{\sum_{(j \in \Omega_t, j \neq i)} G_{ji}(t)P_j(t) + \sigma_i(t)}) \\ P_i(t) & \leq P_{max}^f \quad \forall i \in \Omega_t \\ P_i(t) & \geq 0 \quad \forall i \in \Omega_t \end{aligned}$$

where $\Omega_t = \{FU_i$ active/scheduled during time slot $t\}$. We recall that in our study we assume that FCs use TDMA; that is, there is only one active FU per FC at a given time slot. This NLP should be run every time slot before the scheduled FUs start communicating. It aims at allocating power to FUs with the objective of fairly maximizing their overall achievable throughput. In fact, the objective function is expressed as the maximization of a weighted sum of the channel capacity (and consequently the throughput) of FUs. The weights $w_i(t)$ somehow translate the fairness in power allocation to simultaneously active FUs. Indeed, if an active FU $i \in \Omega_t$ has not been allocated power at time slot t (i.e. $P_i(t) = 0$) via this optimization program, its associated weight will get incremented by one for the next time slot during which it will be active. Hence, this optimization program (expressed as a maximization of a weighted sum) privileges the FUs that have higher weights (i.e., those that have been activated less frequently dur-

ing their scheduled/assigned time slots). This power allocation is subject to maximum transmission power P^f_{max} constraints, where P^f_{max} is assumed to be low enough to avoid interference with the UL communication from the active MU and the macro base station (MBS_0). Note that this NLP can be solved optimally only if there exists a centralized entity that monitors all the FAPs deployed in the MC. In fact, solving this NLP requires that each FAP possesses a global knowledge about all the other FC properties, namely their schedule, their positions, their channel gains, their transmission power, etc. However, as clearly stated in the system model, for the case of FCs, assuming and relying on a centralized approach is not realistic; i.e., it is not practical to assume the existence of a centralized entity that can gather and have such a global information. Moreover, the FCs themselves are isolated entities that are independent of one another, and therefore they are unable to communicate/cooperate with each others. With this in mind, in this chapter, we design and propose a non-cooperative power allocation scheme that allows each FAP to efficiently allocate power to its active FUs in a distributed manner; i.e., without requiring information exchange with the surrounding FAPs nor with the MBS.

3.4 Estimation Based Power Allocation

In this section, we present our scheme which consists of determining at every time slot the amount of power to be used by each active FU in order to increase its chances of getting a higher throughput. In our scheme, at every time slot, each FAP reports some interference related measurements to its active FU to help it decide the amount of transmission power it needs to use. Since FCs cannot communicate with each other,

each active FU, say FU_i, associated with FAP_i will decide the amount of power to use at time slot t by estimating the amount of interference $I_i(t)$ that will be experienced by FAP_i during the time slot t. This estimate is calculated based on the measurements provided by FAP_i and is denoted as $\widehat{I}_i(t)$.

3.4.1 General Description of Proposed Scheme

Our proposed solution consists of the following steps: At the initial time slot t_0 (i.e., the very first time slot), FU_i chooses a random value of $P_i(t)$ that satisfies the maximum power constraint, and uses it to start its communication with its associated FAP_i. At each subsequent time slot $t \neq t_0$, each active FAP_i measures the amount of interference $I_i(t)$ (given in Eq. 5.14) that it receives. This measured interference will then be used to estimate the amount of interference, $\widehat{I}_i(t+1)$, that FAP_i is expected to experience during the next time slot. FAP_i can also measure the received SINR, $\gamma_i(t)$, corresponding to FU_i's UL transmission. We assume that FAP_i is able to estimate the value of channel gain $\widehat{g}_{ii}(t)$ of its currently active FU (before it actually starts communicating) using some well-known filtering technique [39]. These measurements are important, because they will help FU_i decide the amount of power it needs to use as explained later (in our algorithm presented below). Recall that time is assumed to be slotted, where each slot consists of an UL subslot (communication from FU_i to FAP_i) and a downlink (DL) subslot (communication from FAP_i to FU_i). Hence, the measurements made by FAP_i at the UL subslot of slot t can be transmitted to FU_i during the DL of subslot t. These measurements will be used by FU_i to calculate $\widehat{I}_i(t+1)$ (the predicted value of $I_i(t+1)$)

and decide on the amount of transmission power that it will use at time slot $(t+1)$. In order to have good estimation values, we assume that each active FU is scheduled over N_{TS} contiguous time slots (where $N_{TS} > 3$).

3.4.2 Proposed Transmission Power Allocation Algorithm

Once FU_i acquires all necessary information (described in the previous paragraph) from its associated FAP_i (via the DL of time slot $(t-1)$), it decides on the amount of power it needs to use at the UL of time slot t using the following algorithm, which consists of two main tests:

Test 1: Wireless Channel Condition.

If $\widehat{g}_{ii}(t) = 0$, then FU_i decides not to transmit at time t; i.e., it sets its transmission power $P_i(t)$ to 0, because of the bad wireless propagation conditions. Otherwise, if $\widehat{g}_{ii}(t) \neq 0$, the active FU_i runs Test 2 below.

Test 2: Transmission Power Determination.

In this test, FU_i checks whether its SINR, $\gamma_i(t-1)$, achieved at the previous time slot is included in the interval $[\gamma_i^{min}, \gamma_i^{max}]$, and decides on the value of its transmission power $P_i(t)$ accordingly. Based on this value of $P_i(t)$, it decides whether to update the value of γ_i^{min} or γ_i^{max}. The detailed description of this test is presented below.

1. First Case: If $\gamma_i(t-1) < \gamma_i^{min}$, then
   - Set $P_i(t) = \frac{\widehat{I}_i(t)(1+\varepsilon(t-1))\gamma_i^{min}}{\widehat{g}_{ii}(t)}$ if this fraction does not exceed P_{max}^f. Other-

wise, set $P_i(t) = 0$.

- Set $\gamma_i^{min} = \beta\gamma_i^{min}$ if $P_i(t) = 0$, where $0 < \beta < 1$ is a chosen design parameter.

2. Second Case: If $\gamma_i(t-1) > \gamma_i^{max}$, then

   Let:

$$P_{desired}^{max} = \frac{\widehat{I}_i(t)(1+\varepsilon(t-1))\gamma_i^{max}}{\widehat{g}_{ii}(t)} \tag{3.5}$$

$$P_{desired}^{min} = \frac{\widehat{I}_i(t)(1+\varepsilon(t-1))\gamma_i^{min}}{\widehat{g}_{ii}(t)} \tag{3.6}$$

   - If $P_{desired}^{max} \leq P_{max}^f$, set $P_i(t) = P_{desired}^{max}$
   - Else if $P_{desired}^{min} \leq P_{max}^f$, set $P_i(t) = P_{desired}^{min}$
   - Else set $P_i(t) = 0$ and update $\gamma_i^{max} = \beta\gamma_i^{max}$

3. Third Case: If $\gamma_i^{min} \leq \gamma_i(t-1) \leq \gamma_i^{max}$, then

   Let:

$$P_{desired}^{max} = \frac{\widehat{I}_i(t)(1+\varepsilon(t-1))\gamma_i(t-1)}{\widehat{g}_{ii}(t)}$$

$$P_{desired}^{min} = \frac{\widehat{I}_i(t)(1+\varepsilon(t-1))\gamma_i^{min}}{\widehat{g}_{ii}(t)}$$

   - If $P_{desired}^{max} \leq P_{max}^f$, set $P_i(t) = P_{desired}^{max}$
   - Else if $P_{desired}^{min} \leq P_{max}^f$, set $P_i(t) = P_{desired}^{min}$
   - Else set $P_i(t) = 0$

In our algorithm, γ_i^{min} and γ_i^{max} are two design parameters; γ_i^{min} is greater than γ_i^{th} (the SINR threshold); γ_i^{max} is at least three times as high as γ_i^{th}; and $\varepsilon(t-1)$ is the interference estimation error, expressed as

$$\varepsilon(t-1) = \frac{|I_i(t-1) - \widehat{I}_i(t-1)|}{\max(I_i(t-1), \widehat{I}_i(t-1))}$$

Our proposed algorithm uses the weighted moving average technique to compute the estimated value of interference $\widehat{I}_i(t)$, as it gives more importance to the most recent interference measurements. In fact, we assume that the interference measured in the previous time slot is the closest to the current interference value. The rationale behind the use of γ_i^{min} and γ_i^{max} in our algorithm (Test 2) is to try to figure out the optimal $\gamma_i(t)$ (i.e., the one that would allow us to achieve optimal throughput). This is made via successive adjustments of γ_i^{min} and γ_i^{max}: Note that in our algorithm, we decrease these two parameters whenever their use would incur a zero power for FU_i. In fact, we know that the transmission power P_i of FU_i (and consequently its SINR γ_i) cannot be increased indefinitely to maximize its throughput not only because of the maximum power constraint, but also and most importantly because of the behavior of FU_i's throughput Th_i (as shown in Eq. 3.4) as a function of P_i. Indeed, as P_i increases, Th_i also increases up to a point where it reaches its maximum and after which it starts decreasing again. Here, as P_i increases, I_j (the interference experienced at FAP_j, $j \neq i$) increases and hence the power P_j of FU_j increases too to overcome this high interference (I_j). As a consequence, the interference at FAP_i (i.e., I_i) will also increase, thereby decreasing Th_i. Therefore, we decided to bound the value of γ_i and consequently that of P_i so

that Th_i is maximized without impacting the achieved throughput of other FUs that are simultaneously active with FU_i. In other words, the incentive behind our algorithm is to try to fairly maximize the throughput of the different FUs without needing to exchange information among their FAPs.

3.5 Performance Evaluation

In this section, we evaluate the performances of our proposed distributed algorithm, and compare it with the optimal centralized one presented in Section 3.3.

3.5.1 Simulation Settings and Performance Metrics

3.5.1.1 Simulation Method and Settings

We implemented both the centralized solution and our scheme in MATLAB. We ran our simulations, analyzed them, and plotted our results also using MATLAB. In our simulations, we generated a grid network with one MBS in the center surrounded by $N_{FC} = 96$ uniformly placed FAPs and $N_{MU} = 20$ randomly generated MUs. Each FC has a transmission range $R_F = 20m$ and consists of one FAP placed in the center and $N_{FU} = 3$ FUs generated randomly in its coverage area. In our simulation, we assume that the MC and the FCs operate over the same wireless channel, and that both FCs and the MC use TDMA as a channel access mechanism. For evaluation purposes, we varied the inter-FAP distance from $10m$ to $45m$ in order to vary the network coverage ratio. Unless otherwise stated the number of contiguous time slots assigned per FU, N_{TS}, is

Table 3.1: Summary of Simulation Parameters

Maximum FU Power P^f_{max}	125 mWatt
Maximum MU Power P^m_{max}	1 Watt
Femto SINR Threshold γ^{th}_i	3.2dB
Channel Bandwidth W	160Mbps
Carrier Frequency f	2.5GHz
Number of Simulation Slots	3000 Time Slots
Total number of femto-users N_{tot}	288 FUs
SINR Bounds Update Factor β	0.9

fixed to 10. The main simulation parameters are summarized in Table 3.1.

3.5.1.2 Performance Metrics

The goal of this chapter is to provide a distributed, non-cooperative scheme for power allocation with the two objectives of: (i) increasing FUs' overall achievable throughput, and (ii) maximizing fairness among them. To this end, the following two metrics are used to evaluate and analyze the performance of the proposed power allocation scheme.

Average Throughput: is the average per user achieved data rate. It is viewed as a metric of assessing how well the scheme performs from a user's point of view.

Fairness Indicator: represents an important metric for distributed, non-cooperative/selfish systems, where some resources (e.g., wireless channel) need to be shared by a set of users that all try to maximize and go after their own benefit. The idea here is to quantify and assess how fair the proposed scheme is in terms of the FUs' achieved throughput, by using the following fairness indicator [66]: $F = \frac{(\sum_{i=1:N_{tot}} Th_i)^2}{N_{tot}(\sum_{i=1:N_{tot}} Th_i^2)}$, where N_{tot} is the total number of FUs. This metric is viewed as a metric of assessing how well the scheme

performs from a network's point of view.

3.5.2 Simulation Results

3.5.2.1 Throughput Performance

Fig. 3.1 shows the per-FU average achieved throughput for various time frames (one time frame equals 30 time slots). First, note that in the long run, our scheme achieves 50% of the optimal throughput obtained via the centralized optimization program. Second, observe that both schemes, our distributed and the centralized, are stable as the average per-FU throughput does not fluctuate much; they both quickly converge to a fixed value. For the proposed distributed scheme, the convergence time is around 10 time frames (i.e. 300 time slots which is equal to 6 seconds).

Fig. 3.2 shows the per-FU average throughput as a function of the FC coverage ratio. We define the coverage ratio as the ratio of the total FC area to the total MC area. From Fig. 3.2, we can clearly see that the average throughput achieved with the centralized scheme decreases rapidly as the FC coverage ratio increases. In fact, it decreases from 158 Mbps for femto-coverage-ratio=0.08 (8%) to 110 Mbps for coverage ratio equal to 0.85 (85%). In other words, the decrease is of 623 kbps for 1% increase in the coverage ratio for throughput obtained with the centralized scheme, whereas the decrease of throughput achieved with our scheme is barely noticeable. For our scheme, the decrease ratio is of the order of 129 kbps for 1% coverage ratio increase. Hence, although our scheme does not achieve as much throughput as the centralized approach

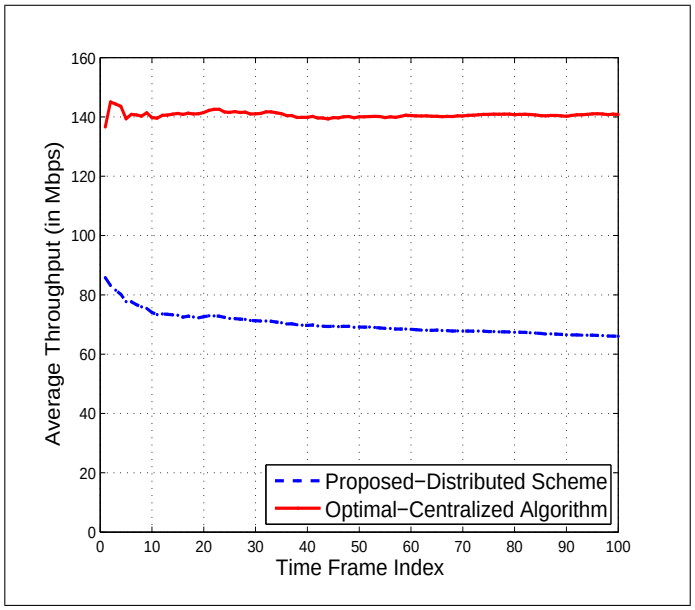

Figure 3.1: Per-FU average achievable throughput.

does, it presents better performances in terms of scalability.

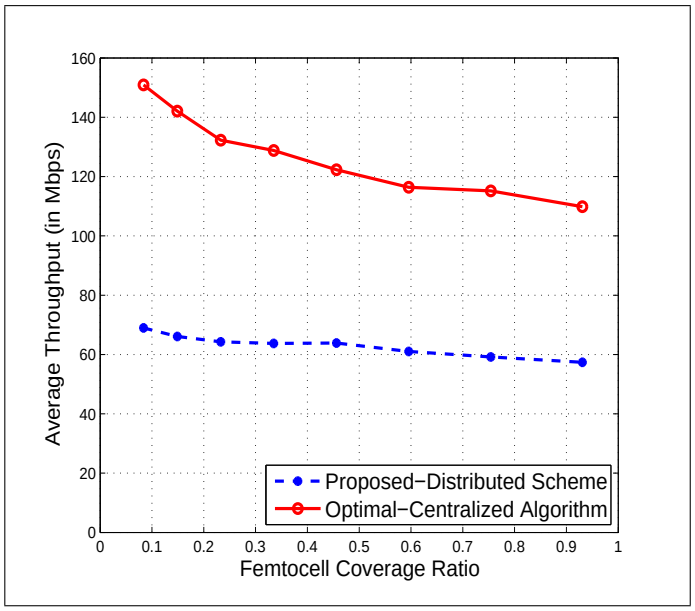

Figure 3.2: Impact of the FC Coverage Ratio on the average achieved throughput.

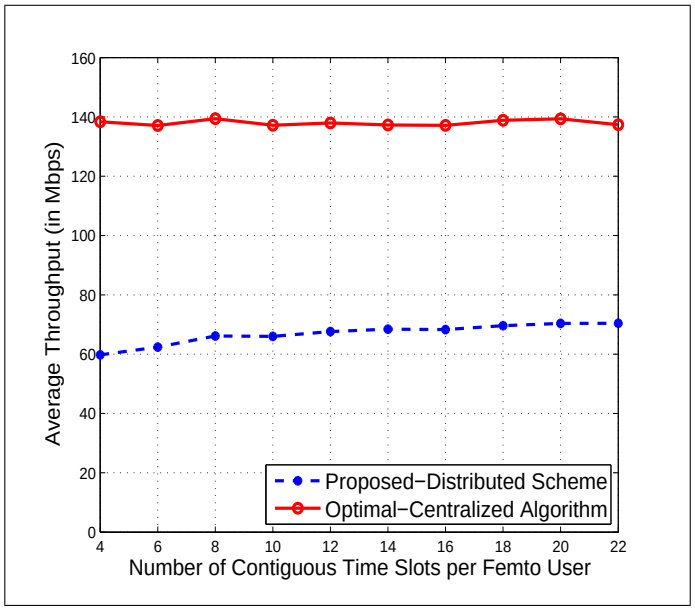

Figure 3.3: Impact of the number of per-FU Contiguous Time Slots on the average achieved throughput.

We also study and show in Fig. 3.3 the impact of varying the number of contiguous time slots assigned per FU on the average achieved throughput. Note that the average throughput obtained with our scheme increases from 60Mbps to 70Mbps as the number of contiguous slots assigned per FU increases from 4 to 22 slots. This is because the estimation error is smaller for higher assigned numbers of contiguous slots. Indeed, the more slots a FU has, the more interference measurements/samples it gets, the more accurate its interference estimates is, and consequently the better the decision of the allocated transmission power is. On the other hand, observe that the performances of the optimization program is independent of the number of contiguous slots assigned per FU, which is expected.

3.5.2.2 Fairness Performance

Fig. 3.4 shows the fairness indicator of the proposed scheme when varying the time frame index. The figure shows that our scheme achieves good fairness performances. Observe that fairness indicator reaches up about 0.65. Therefore, not only does our scheme perform in a distributed manner; i.e., each FC runs the algorithm without needing to cooperate or exchange information with the surrounding FCs, but also ensures good fairness among the FUs by allowing them to achieve approximately equal amounts of throughput. This is because each FC takes into account the presence of surrounding FCs by estimating the interference they might incur and by bounding and adjusting the SINR achieved by its associated active FU so that it would not harm the communication of surrounding FUs.

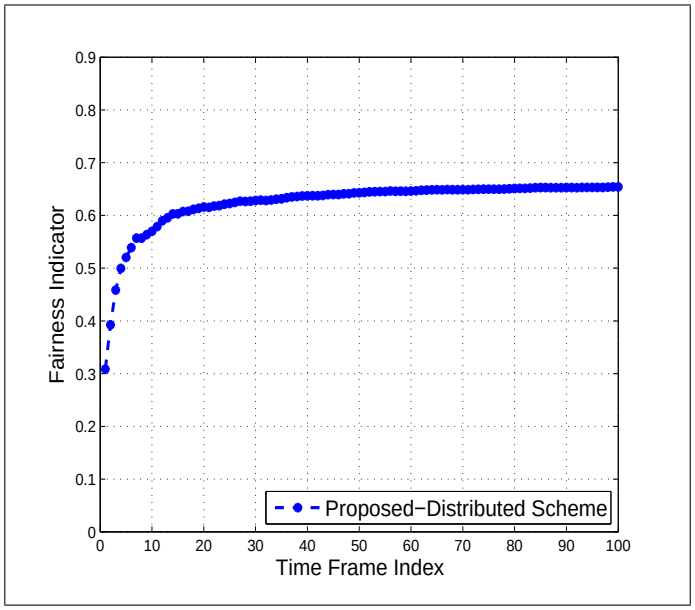

Figure 3.4: Fairness indicator as a function of time frame index.

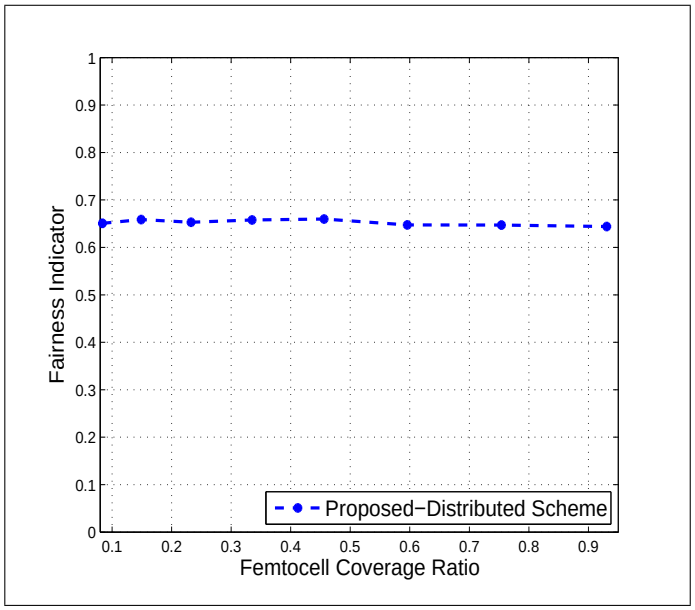

Figure 3.5: Fairness indicator as a function of the FC Coverage ratio.

In Fig. 3.5, we also show that the fairness performance of the proposed scheme is not affected by the increase of the FC coverage ratio, which further confirms its suitability to areas with high FC coverage such as the urban areas.

3.6 Summary

In this chapter, we proposed a distributed, non-cooperative uplink power allocation scheme for FC networks. Through simulation, we showed that our scheme achieves good throughput performances while ensuring fairness among all active femto-users. In addition, we showed that our proposed scheme presents good scalability property, which makes it suitable for femto-networks deployed in urban areas.

Chapter 4: QoS-Aware Power Allocation in Two-Tier Macrocell/Femtocell Networks

In this chapter, we develop a new distributed power control (PC) scheme for the uplink traffic in femtocell/macrocell networks that can be used by both femto-users (FUs) and macro-users (MUs). Our work aims at maintaining the minimum required signal to interference ratio (SIR) for as many cellular users (CUs) as possible via distributed QoS-aware stochastic power allocation. We also provide a theoretical analysis of our proposed PC scheme, and evaluate and compare its performance with existing power allocation techniques. Simulation results show that our scheme yields a significant performance improvement in terms of percentage of satisfied users when compared with these existing solutions.

4.1 Introduction

Designing efficient PC schemes is very challenging in the case of two-tier FC networks, mainly due to their autonomous nature. Therefore, it has been the focus of many recent works. Some of these works resort to game theoretical approaches to design PC schemes [19, 41, 49, 58, 61, 77, 79], some of which [19, 28, 61] use the famous Foschini-Miljanic power update formula [31]. Other works use new optimization approaches such as: predictive modeling [16,29], particle swarm optimization [43], fractional power con-

trol [14,60,78], etc. In [14,60,78], the authors use fractional power control, a new PC approach that lies between the channel inversion and the water filling policy. Their scheme aims at helping disadvantaged users by attenuating the impact of the fading factor related to their communications with their associated base stations (BSs). However, the optimization of the assignment of the PC exponents in such a scheme would necessitate a central network entity that possesses a global knowledge of the different channel gains of these CUs. Likewise, the PC scheme proposed in [53], which aims at maximizing FC capacities while maintaining a minimum SIR value at the MC, requires the existence of a central FC/MC resource managing unit/agent. Other prior works [19, 29, 77, 79], although distributed in nature, still require inter-tier/intra-tier coordination for their operation. For instance, in [29], the authors propose a new PC scheme, in which they used the predictive modeling approach (a widely used approach in industrial applications such as process plants control or production control). In their scheme, a CU needs to know its channel gain at the BSs different from the one to which it is associated, which is only possible under the condition of communication/cooperation between that CU and its surrounding BSs. On the other hand, in [19, 77, 79], the authors formulate the power allocation problem using a game-theoretic approach, where inter-tier coordination (equivalently coordination between the FC and the MC) is assumed. In fact, in [79], the primary user (PU) needs to broadcast some measurements to the secondary user (SU) in order to allow it adjust its transmission power. Likewise, in [77], the authors use a Stackelberg game-based PC, in which the SU determines its transmission power while taking into account the price decided by the PU. The implementation of their algorithm requires the knowledge of the cross channel gains (i.e that of the SU at

the PU's BS and that of the PU at the SU's BS). In our work, however, no inter-tier or intra-tier coordination is required. The cellular user (CU) only needs to communicate with its associated base station (whether MBS or FAP) to get the information required to adjust its transmission power.

From a modeling perspective, several works ([19,58,61,77,79]) addressed the problem of power allocation in two-tier networks while differentiating between two types of users: prioritized PUs and SUs (with lower priority). Indeed, in [58], the authors propose a game-based PC scheme, where the SUs are assigned bounded power to meet their SIR requirements. Their assigned power should not exceed a target power value so that the interference at the MU could not exceed a certain threshold. A similar concept has been adopted in [61], where a joint power and admission control algorithm is proposed to support the MUs with guaranteed QoS requirements, while letting the FUs only exploit the remaining network capacity. In our work, we consider a MC network overlaid with multiple FC networks where all considered active users (FUs and MUs) have a QoS constraint expressed in terms of a minimum SIR requirement that needs to be maintained. Both the FUs and the MUs are licensed users. Therefore, we do not distinguish between them in terms of resource allocation.

Finally, the authors of the game-theoretic power control schemes proposed in [19, 41,49,58,61,77,79] proved the existence of Nash equilibria (in [19,41,49,58,61]) and Stackelberg equilibria (in [77, 79]) for these games. In our work [15], we prove that our PC scheme, derived using ordinary differential equations (ODEs), admits a unique solution that we compute. We also derive sufficient conditions on the stability of our system at the equilibrium.

4.2 Network Model

We consider a single-carrier two-tier cellular system consisting of FCs overlaid on one MC, where both of them operate over an identical carrier frequency f. The MUs and the FUs are spatially distributed in the two-dimensional plane according to two independent homogeneous Poisson point processes with intensities (i.e. spatial densities) λ_{MU} and λ_{FU} respectively. In this work, we consider the uplink (UL) communication stream; i.e., communication from the MUs to the MBS and from the FUs to their corresponding FAPs. We assume that time is slotted and TDMA is used by the CUs (ie., MUs and FUs) to access the wireless channel, and that the UL communications at the FCs are synchronized with those at the MC [57][1], and consequently are mutually synchronized. We further assume that FUs residing in the same FC do not interfere with each other since they are scheduled in different TSs. Likewise, we assume that the MUs inside the MC are scheduled according to TDMA.

The wireless channel gain g_{ji} of user j to base station i is modeled in compliance with the ITU specifications [2], according to which at time slot t

$$g_{ji}(t) = d_{ji}^{-\alpha_j}(t)10^{-\frac{Y_{ji}(t)}{10}} \tag{4.1}$$

where $d_{ji}(t)$ represents the distance from user j to base station i at time t, α_j the path loss exponent related to the transmission environment (we distinguish between three environments: cellular, indoor, and indoor-to-outdoor), and $Y_{ji}(t)$ represents the normal

[1]Once turned on and before initiating any communication, FCs get synchronized to the cellular core network using an asymmetric communication link such as xDSL thanks to an enhanced version of IEEE 1588 [57].

variable associated to the log-normal shadowing realization at time t, with zero mean and standard deviation $\sigma_{MU} = 8dB$ for MUs and $\sigma_{FU} = 4dB$ for FUs. Hence, the SIR of the transmission from FU_i belonging to FC_i to its associated FAP_i at time slot t is:

$$\gamma_i(t) = \frac{g_{ii}(t)P_i(t)}{I_i(t)} \tag{4.2}$$

where $P_i(t)$ denotes the transmission power of FU_i at time t, and $I_i(t)$ is the interference experienced by FAP_i at time t due to concurrent transmissions from active neighboring FU_j $(j \neq i)$ and MU_k. $I_i(t)$ can be written as

$$I_i(t) = \sum_{FU_j; j \neq i} g_{ji}(t)P_j(t) + g_{ki}(t)P_k(t) \tag{4.3}$$

Likewise, the SIR corresponding to the transmission from MU_k to its MBS_0 is given by:

$$\gamma_0(t) = \frac{g_{k0}(t)P_k(t)}{I_0(t)} \tag{4.4}$$

where $I_0(t) = \sum_{FU_j} g_{j0}(t)P_j(t)$ is the interference at MBS_0. In our model, we assume that FUs' positions are fixed, and hence, their corresponding shadowing coefficients are considered constant across time. On the other hand, we assume that MUs are moving and their movement is described by the Random Way Point Mobility Model [13]. Hence, for any given MU, a realization of its shadowing coefficient at time $t + T$ is correlated to that at time t following Cox's model [75] and is described as follows.

$$Y_{ki}(t+T) = Y_{ki}(t)\exp\left(-\frac{v_k(t)T}{d_c}\right) + \eta_k(t) \tag{4.5}$$

where $\eta_k(t)$ is a normally-distributed random variable with zero mean and variance $\sigma_{\eta_k} = \sigma_{MU}\sqrt{1-\exp\left(-\frac{2v_k(t)T}{d_c}\right)}$, $v_k(t)$ is the speed of MU_k and $d_c = 50m$ models the large-scale fading outdoors [75]. For $d_{ki} \ll d_c$, the object is enormous relative to the inter-node separation d_{ki}. Thus, from the receivers perspective, the transmitter appears stationary, since any displacement of the transmitter over a relatively short period of time is insignificant relative to the size of the object. For $d_{ki} \gg d_c$ this same local shadowing object can be modeled as a point, and thus, the receiver sees the transmitter traveling.

4.3 Problem Statement and Proposed Solution

Consider a set of n simultaneously active FUs and one active MU whose traffic requires a minimum data rate to guarantee a desired QoS. An example of such traffic is the voice traffic which requires a data rate of about 56 to 64 kbps in order to achieve an acceptable QoS. Recall that the data rate achievable by a wireless node i could be expressed as a function of its achievable SIR, γ_i (according to Shannon capacity formula). Hence, this data rate constraint could be mapped into the following minimum SIR constraint:

$$\gamma_i(t) \geq \gamma^{th}, \forall i = 1..n+1$$

where γ^{th} is the minimum required SIR threshold. In this work, our objective is to ensure that each CU_i (i.e. any simultaneously active FUs or the MU) achieve and maintain a SIR value $\gamma_i(t)$ that is as close as possible to the target γ^{th}; i.e., $\gamma_i(t) \simeq \gamma^{th}$. The idea here is that the achieved SIR should be above the threshold in order to receive an acceptable QoS, but it is not desirable to be more than the threshold, as this would not be beneficial to these applications. This objective can be formulated with the following equation:

$$\mid \gamma_i(t) - \gamma^{th} \mid = \frac{\mid \gamma_i(t_0) - \gamma^{th} \mid}{t - t_0 + 1} \tag{4.6}$$

The physical interpretation of this equation (4.6) is that the distance between the achieved SIR and the minimum required SIR decays geometrically with rate $1/t$ as $t \rightarrow \infty$ for any active CU_i. This represents the target we want to achieve via our distributed autonomous power control scheme developed hereafter. Notice that in our problem formulation, we use a backward/reverse engineering approach. That is, starting from the desired solution (4.6), we develop a PC scheme which aims at achieving our goal of sustaining the achieved SIR $\gamma_i(t)$ in the vicinity of/at the desired γ^{th} level.

Starting from (4.6), the differential dynamic of our system can be derived as

$$\begin{aligned} \frac{\partial(\gamma_i(t) - \gamma^{th})}{\partial t} &= -sign(\gamma_i(t) - \gamma^{th}) \times \frac{\mid \gamma_i(t_0) - \gamma^{th} \mid}{(t - t_0 + 1)^2} \\ &= -(\gamma_i(t) - \gamma^{th}) \left| \frac{\gamma_i(t) - \gamma^{th}}{\gamma_i(t_0) - \gamma^{th}} \right| \end{aligned}$$

Thus, the differential dynamic of our system can be described by the following set

of ODEs:[2]

$$\dot{\gamma}_i(t) = -(\gamma_i(t) - \gamma^{th}) \left| \frac{\gamma_i(t) - \gamma^{th}}{\gamma_i(t_0) - \gamma^{th}} \right|, \forall i = 1..n+1 \tag{4.7}$$

Moreover, as mentioned in Section 4.2 the FUs' channel gains are considered constant during the power control process, since they are immobile. On the other hand, we assume that the MUs are slowly moving so that their channel gains at two consecutive time slots are almost the same $g_{ii}(t+1) \approx g_{ii}(t)$. Hence, by differentiating (4.2) with respect to time, we get:

$$\dot{\gamma}_i(t) = g_{ii} \frac{\dot{P}_i(t) I_i(t) - P_i(t) \dot{I}_i(t)}{I_i^2(t)} \tag{4.8}$$

Then, by equating (4.7) and (4.8), we get:

$$\dot{P}_i(t) = P_i(t) \frac{\dot{I}_i(t)}{I_i(t)} - \frac{I_i(t)}{g_{ii}} (\gamma_i(t) - \gamma^{th}) \left| \frac{\gamma_i(t) - \gamma^{th}}{\gamma_i(t_0) - \gamma^{th}} \right|$$

Finally, using Taylor Series Expansion of order one, it follows that

$$\begin{aligned} \frac{\dot{I}_i(t)}{I_i(t)} &= \frac{\frac{\partial I_i(t)}{\partial t}}{I_i(t)} = \frac{\partial \ln(I_i(t))}{\partial t} \\ &\simeq \ln\left(\frac{I_i(t+1)}{I_i(t)}\right) \end{aligned}$$

Moreover, we assume that $I_i(t+1) \simeq I_i(t)$. Hence, our desired transmission power

[2]Here, we use the mathematical notation $\dot{x}(t) = \frac{\partial x(t)}{\partial t}$

dynamics are described by the following set of ODEs:

$$\dot{P}_i(t) = -\frac{I_i(t)}{g_{ii}}(\gamma_i(t) - \gamma^{th}) \left| \frac{\gamma_i(t) - \gamma^{th}}{\gamma_i(t_0) - \gamma^{th}} \right| \ \forall i = 1..n+1 \ \forall t \geq t_0 \tag{4.9}$$

Based on (4.9), we deduce our desired power control rule as, $\forall i = 1..n+1 \ \forall t \geq t_0$

$$P_i(t+1) = P_i(t) - \frac{I_i(t)}{g_{ii}}(\gamma_i(t) - \gamma^{th}) \left| \frac{\gamma_i(t) - \gamma^{th}}{\gamma_i(t_0) - \gamma^{th}} \right| \tag{4.10}$$

Our proposed power control scheme given in (4.10) above can then be refined with:

1. *Power constraint:* When $P_i(t+1)$ obtained from (4.10) is negative, CU_i chooses not to transmit, and when $P_i(t+1)$ exceeds the maximum allowed power level, P_{max} (P_{max} equals P^f_{max} for the FUs and P^m_{max} for the MUs), CU_i sets its transmission power to P_{max}. Formally, $P_i(t+1) = \min(\max(0, f_i(t)), P_{max})$.

2. *Safety margin:* The value of γ^{th} is multiplied with a safety factor $\delta \geq 1$ in order to provide a safety margin. The intuition here is that targeting an SIR slightly higher than the threshold γ^{th} provides more guarantees by increasing the chances of meeting the required γ^{th}.

3. *Smoothing factor:* A smoothing factor $0 \leq \beta < 1$ is introduced to reduce the fluctuations in CU_i's transmission power evolution during the power control process/period. This is shown in (4.12) below.

To sum up all the above, the final proposed power control rule can be written as

$$P_i(t+1) = \min(\max(0, f_i(t)), P_{max}) \ \forall i = 1..n+1 \tag{4.11}$$

with

$$f_i(t) = \beta h_i(t) + (1-\beta)P_i(t) \tag{4.12}$$

where $h_i(t)$ is the function defined by

$$h_i(t) = P_i(t) - \frac{I_i(t)}{g_{ii}}(\gamma_i(t) - \delta\gamma^{th})\left|\frac{\gamma_i(t) - \delta\gamma^{th}}{\gamma_i(0) - \delta\gamma^{th}}\right| \tag{4.13}$$

Now that we have defined our PC rule, we next give a brief description of our PC algorithm used by each active CU_i. First, recall that in our system, CUs are scheduled according to TDMA so that only one FU is active per FC per TS; same thing applies for the MC. We further assume that in each time slot, when a CU becomes active, it stays so for N_{TS} contiguous TSs, during which it uses the proposed PC algorithm (Algorithm 4) for determining/allocating its power. In this algorithm, BS_i refers to the base station associated to CU_i (either FAP_i or MBS_0).

Algorithm 4 Power Control Algorithm at CU_i

1: **Initialize** t=0, Select $P_i(t)$ randomly from $[0, P_{max}]$, Send data.
2: **while** $t \leq N_{TS}$ **do**
3: Collect Previous Interference measurement from its associated BS_i
4: Compute Transmission power $P_i(t+1)$ using (4.11)
5: Send data
6: $t \leftarrow t+1$
7: **end while**

4.4 Theoretical Analysis of the Proposed Solution

Our proposed power control scheme is a stochastic process deduced from a finite set of ODEs given by (4.9). Therefore, in order to characterize its long term behavior, our analysis resorts to some control theory results. In the following, we study the existence and uniqueness of a solution to this system of ODEs and derive sufficient condition on its stability. The analysis that we provide in this section applies to the case of immobile FUs and MUs. Notice that by plugging equation (4.6) in (4.9), the system of ODEs (4.9) that defines our PC scheme is equivalent to

$$\dot{P}_i(t) = -\frac{I_i(t)(\gamma_i(t) - \gamma^{th})}{(t - t_0 + 1)g_{ii}} \ \forall i = 1..n+1 \ \ \forall t \geq t_0 \tag{4.14}$$

In this section, for the sake of analysis we will use the system of ODEs (4.14) instead of (4.9).

Theorem 1. *The system of ODEs in (4.14) admits a unique solution given by*

$$\underline{P}(t) = \exp\left(\ln\left(\frac{1}{t - t_0 + 1}\right)\boldsymbol{M}\right)\underline{P}(t_0) \tag{4.15}$$

where $\boldsymbol{M} = \boldsymbol{I} - \boldsymbol{G}$*,* $\boldsymbol{I}$ *is the identity matrix of order* $(n+1)$*, and* $\boldsymbol{G}$ *is a* $(n+1)$ *by* $(n+1)$ *matrix with zeros diagonal elements* $G_{ii} = 0$ *and non-zero off-diagonals* $G_{ij} = \frac{\gamma^{th} g_{ji}}{g_{ii}}, \forall i, j = 1, .., (n+1)$.

Proof. **Proof of Existence:** From (4.14), we have, $\forall i = 1..n+1 \ \ \forall t \geq t_0$,

$$\begin{aligned}\dot{P}_i(t) &= -\frac{I_i(t)\gamma_i(t)}{(t-t_0+1)g_{ii}} + \frac{I_i(t)\gamma^{th}}{(t-t_0+1)g_{ii}} \\ &= -\frac{P_i(t)}{(t-t_0+1)} + \frac{\gamma^{th}}{(t-t_0+1)}\sum_{j\neq i}\frac{g_{ji}}{g_{ii}}P_j(t)\end{aligned}$$

This set of ODEs could be further transformed using a matrix form as follows:

$$\underline{\dot{P}}(t) = \frac{-1}{t-t_0+1}(\mathbf{I}-\mathbf{G})\underline{P}(t) \tag{4.16}$$

where **I** is the identity matrix of order $(n+1)$, and **G** is defined in the theorem statement. Now let **A(t)** $= \frac{-1}{t-t_0+1}(\mathbf{I}-\mathbf{G})$,$\forall \underline{P}_1, \underline{P}_2 \in [0, P_{max}]^{n+1}$. We have

$$\begin{aligned}\|\mathbf{A(t)}\underline{P}_1 - \mathbf{A(t)}\underline{P}_2\| &= \|\mathbf{A(t)}(\underline{P}_1 - \underline{P}_2)\| \\ &\leq \|\mathbf{A(t)}\|_\infty \|\underline{P}_1 - \underline{P}_2\|_2 \\ &\leq \frac{\max_{i,j}\left\{|\frac{\gamma^{th}g_{ji}}{g_{ii}}|;1\right\}}{t-t_0+1}\|\underline{P}_1 - \underline{P}_2\|_2\end{aligned}$$

Let $k(t) = \frac{\max_{i,j}\left\{|\frac{\gamma^{th}g_{ji}}{g_{ii}}|;1\right\}}{t-t_0+1}$, a piecewise continuous function for all $t \geq t_0$. Therefore, $\forall \underline{P}(t_0) \in [0, P_{max}]^{n+1}$ there exists a unique solution to (4.14), defined as

$$\underline{P}(t) = \Phi\left(t, t_0, \underline{P}(t_0)\right)\underline{P}(t_0)$$

Solution Computation: Notice that **A(t)** could be written as **A(t)** $= \alpha(t)\mathbf{M}$ with $\alpha(t) = \frac{-1}{t-t_0+1}$ and $\mathbf{M} = (\mathbf{I}-\mathbf{G})$ a constant matrix. Hence, **A(s)** and $\int$ **A(s)** ds commute.

Thus,

$$\begin{aligned}\Phi\left(t, t_0, \underline{P}(t_0)\right) &= \exp\left(\int_{t_0}^{t} \mathbf{A(s)}\, ds\right) \\ &= \exp\left(\int_{t_0}^{t} \alpha(s)\, ds\mathbf{M}\right) \\ &= \exp\left(\ln\left(\frac{1}{t-t_0+1}\right)(\mathbf{I}-\mathbf{G})\right)\end{aligned}$$

□

Theorem 2. *If* $\boldsymbol{M = (I - G)}$ *is diagonalizable and has positive eigenvalues, then the equilibrium* $\underline{P}^*$ *of the system (4.14) is both stable and asymptotically stable.*

Proof. Recall that by definition, $\underline{P}^*$ is an equilibrium vector for the system (4.14) is equivalent to $\dot{\underline{P}}(t) = \underline{0}$ at $\underline{P}^*$. Given that **M** is diagonalizable and with positive eigenvalues, there exists an invertible matrix **Q** and a diagonal matrix **D** whose diagonal elements $\lambda_1, \lambda_2, .., \lambda_{n+1}$ are positive such that: $\mathbf{M = QDQ^{-1}}$. That is, $\mathbf{I - G = QDQ^{-1}}$. Hence, using Taylor series expansion, we get:

$$\begin{aligned}\exp\left(-\ln(t-t_0+1)\mathbf{M}\right) &= \sum_{n=0}^{+\infty} \frac{(-\ln(t-t_0+1)\mathbf{QDQ^{-1}})^n}{n!} \\ &= \mathbf{Q}\exp\left(-\ln(t-t_0+1)\mathbf{D}\right)\mathbf{Q^{-1}}\end{aligned}$$

Let $\underline{x}(t) = \underline{P}(t) - \underline{P}^*$. Note that $\dot{\underline{x}}(t) = \dot{\underline{P}}(t)$ and the zero vector is an equilibrium vector for $\underline{x}(t)$. Hence, studying the stability of the equilibrium vector for (4.14) or (4.16) is equivalent to studying the stability of the zero vector for the system $\dot{\underline{x}}(t) =$

$\frac{-1}{t-t_0+1}\mathbf{M}\underline{x}(t)$. We have:

$$\begin{aligned}\|\underline{x}(t)\| &= \left\|\exp\left(\ln\left(\frac{1}{t-t_0+1}\right)\mathbf{M}\right)\right\|.\|\underline{x}(t_0)\| \\ &\leq \left\|\mathbf{Q}\exp\left(-\ln(t-t_0+1)\mathbf{D}\right)\mathbf{Q^{-1}}\right\|.\|\underline{x}(t_0)\| \\ &\leq \|\mathbf{Q}\|\left\|\mathbf{Q^{-1}}\right\|\exp\left(-\ln(t-t_0+1)\min_i \lambda_i\right)\|\underline{x}(t_0)\|\end{aligned}$$

and hence, $\forall \varepsilon > 0$,

$$\|\underline{x}(t_0)\| < \frac{\varepsilon}{\|\mathbf{Q}\|\|\mathbf{Q^{-1}}\|\exp\left(-\ln\left(t-t_0+1\right)\min_i \lambda_i\right)}$$

implies that

$$\|\underline{x}(t)\| < \varepsilon \ \forall t \geq t_0$$

Hence, $\underline{x} = \underline{0}$ is a stable solution for $\dot{\underline{x}}(t) = \frac{-1}{t-t_0+1}\mathbf{M}\underline{x}(t)$. Consequently, $\underline{P}^*$ is a stable solution for (4.14). Moreover,

$$0 \leq \|\underline{x}(t)\| \leq \|\mathbf{Q}\|\left\|\mathbf{Q^{-1}}\right\|\exp\left(-\ln(t-t_0+1)\min_i \lambda_i\right)\|\underline{x}(t_0)\|$$

and $\lim_{t\to+\infty}\exp\left(-\ln(t-t_0+1)\min_i \lambda_i\right) = 0$. Hence, $\lim_{t\to+\infty}\underline{x}(t) = \underline{0}$. Thus, $\underline{x} = \underline{0}$ is also asymptotically stable, which implies that $\underline{P}^*$ is asymptotically stable for (4.14). □

Corollary 1. *The final proposed power control rule given by (4.11) has the same properties as the one given by (4.10). That is, it admits a unique solution and presents similar*

stability characteristics.

Proof. The proof follows from [81] which states that by modifying a power control function (in our case it is given in (4.10), which is derived from (4.9) or equivalently (4.14)), by using a smoothing/averaging factor and adding a maximum power constraint, the resulting new power control function, see (4.11), has the same properties as the initial one (i.e. (4.10)) in terms of solution existence and stability. □

In this work, we analyze the theoretical performances of our PC scheme only for the case of fixed MUs and FUs. These results are still valid also for the case of fixed MUs and mobile FUs (as long as they do not leave the coverage area of their associated FCs). In fact, in that case, the FUs displacements are restricted to the indoor premises, so the distance separating the FU from its associated FAP is generally less than $d_c = 50m$. Hence, using Cox's model [75], these mobile FUs' channel gains can also be considered constant across time. On the other hand, extension of these results to the case of mobile MUs is analytically complex since in that case the MUs' channel gains are no longer constant and represent a stochastic process as shown in Section 4.2. Indeed, in the case of mobile MUs, the key convergence/stability condition is [40]:

$$\lim_{t\to+\infty} \frac{1}{t} \log \|\mathbf{A}(1)\mathbf{A}(2)...\mathbf{A}(t)\| < 0$$

4.5 Performance Evaluation

We now evaluate the performance of our proposed PC scheme (referred to as Proposed-PC) and compare it with two existing PC schemes: Utility-PC [19] and Stackelberg-

PC [77]. We first start with a brief description of these two existing schemes, and then evaluate and analyze the performance gain Proposed-PC achieves in terms of the percentage of satisfied users when compared with Utility-PC and Stackelberg-PC.

4.5.1 Simulated Schemes and Performance Metric

4.5.1.1 Utility-PC Scheme [19]

Utility-based PC (hereafter referred to as Utility-PC for short) scheme, proposed by Chandrasekhar et al. [19], assumes that both the FUs and the MUs use TDMA as the multiple access method for sharing the wireless channel. Further, it also assumes that there is only one active FU per FC per TS and one active MU per TS in the underlying MC. Utility-PC's power control formula, proposed to allow the active FU_i to achieve its desired SIR threshold γ^{th}, is as follows:

$$P_i(t+1) = \min\left(\left(\frac{P_i(t)}{\gamma_i(t)}\left[\gamma^{th} + \frac{1}{a}\ln\left(\frac{ag_{ii}}{bg_{0i}}\right)\right]^+\right); P_{max}^f\right) \tag{4.17}$$

where $\left[\gamma^{th} + \frac{1}{a}\ln\left(\frac{ag_{ii}}{bg_{0i}}\right)\right]^+ = \max\left(0, \gamma^{th} + \frac{1}{a}\ln\left(\frac{ag_{ii}}{bg_{0i}}\right)\right)$, g_{0i} is the channel gain from the active MU to FAP_i, and a and b are two constants set respectively to 0.1 and 1 in order to maximize the FCs capacities. On the other hand, the formula used to update the active MU's power is nothing but the Foschini-Miljanic power update formula [31]:

$$P_k(t+1) = \min\left(\frac{P_k(t)}{\gamma_0(t)}\gamma^{th}, P_{max}^m\right) \tag{4.18}$$

where $\gamma_0(t)$ is the SIR associated with the transmission of the active MU_k to its MBS. Although this scheme is distributed, it still requires coordination between the FCs and the underlying MC.

4.5.1.2 Stackelberg-PC Scheme [77]

We also compare our PC scheme to another recently-proposed game-based power allocation scheme [77]. In what follows, this scheme is referred to as Stackelberg-PC. In Stackelberg-PC, the active FU determines its transmission power while taking into account the price decided by the active MU. The implementation of this scheme requires the knowledge of the cross channel gains acquired under the assumption of FC-MC coordination. The PC update rule used by the active MU_k is:

$$P_k(t+1) = \min\left(\frac{I_0(t)}{g_{k0}}, P_{max}^m\right) \tag{4.19}$$

On the other hand, the active FU_i updates its power as follows

$$P_i(t+1) = \min\left(\max\left(\frac{1}{\ln(2)g_{i0}\pi_i} - \frac{I_i(t)}{g_{ii}}, 0\right), P_{max}^f\right) \tag{4.20}$$

where π_i is the price associated to the transmission of FU_i calculated as follows:

$$\pi_i = \frac{1}{\ln(2)g_{i0}\left(\frac{\sigma_0 g_{ki}}{g_{k0}g_{ii}} + \frac{\sigma_i}{g_{ii}}\right)}$$

g_{k0} and g_{i0} are the channel gains of the active MU_k and FU_i at the MBS respectively, g_{ii} is the channel gain of the active FU_i at its associated FAP_i, and g_{ki} is the channel gains of the active MU_k at FAP_i.

4.5.1.3 Performance Metric

The goal of this work is to provide a distributed, non-cooperative PC scheme with the objective of maintaining the SIR achieved by each CU as close as possible to the desired level γ^{th}. Therefore, the outage percentage defined as the percentage of CUs (FUs and MUs) whose QoS constraints are not met is used as as the performance metric to evaluate the effectiveness of our proposed PC scheme.

4.5.2 Simulation Settings and Results

4.5.2.1 Simulation Settings

We consider a two-tier FC/MC network, in which the FAPs, the FUs and the MUs are scattered randomly over a $70m \times 70m$ area, with spatial densities λ_{FAP}, λ_{FU} and λ_{MU} respectively. In each FC, the FUs are scheduled in a round robbin fashion. Each active FU is allowed to transmit during N_{TS} contiguous time slots. Likewise, the MUs are scheduled according to TDMA. In our simulation, the FUs are assumed fixed across time while the MUs are moving and their mobility is modeled using the Random Way-Point model. Main simulation parameters are summarized in Table 4.1.

Table 4.1: Summary of Simulation Parameters

Maximum FU Power P^f_{max}	0.5 Watt
Maximum MU Power P^m_{max}	2 Watt
Femto SIR Threshold γ^{th}	1.8 dB
Number of Contiguous Time Slots per CU	100 Time Slots
Average number of FCs	75 FCs
Average number of FUs	294 FUs
Average number of MUs	50 MUs
PC Smoothing Factor β	0.8

4.5.2.2 Simulation Results

In our performance evaluation we focus on two main aspects: First, and most importantly, we study the outage percentage since it allows us to measure how well the proposed PC scheme performs in terms of meeting the CUs' QoS constraints. Second, we consider investigating the general behavior of the power and/or SIR obtained as a result of using our PC scheme, so as to assess the ability of our scheme vis-a-vis of stability and convergence in the case of mobile MUs (since these properties have been already studied for the case of immobile MUs in Section 4.4).

Fig. 4.1 shows that our scheme, Proposed-PC, achieves a gain of 15% and up to 20% of satisfied FUs when compared to Utility-PC and Stackelberg-PC. Recall that Proposed-PC achieves such gain without needing any coordination among other FCs nor the underlying MC (as opposed to Utility-PC and Stackelberg-PC); i.e., it is fully decentralized. Moreover, Fig. 4.2 shows that Proposed-PC achieves such performance with 3 times less average power consumption than that by its counterpart Utility-PC (0.15 Watt for our scheme vs. 0.48 Watt for the Utility-PC scheme), and almost the same power level as Stackelberg-PC. On the other hand, the slight variations in our

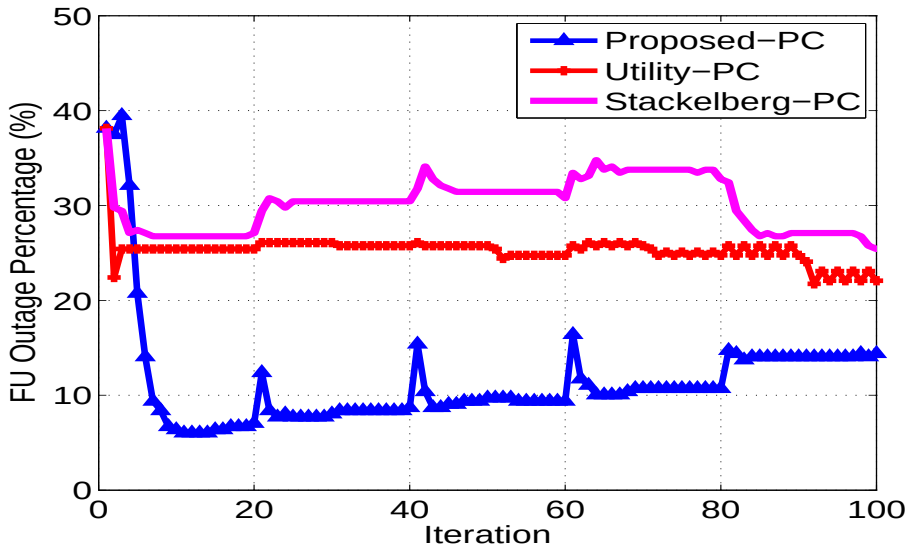

Figure 4.1: FU Outage Percentage

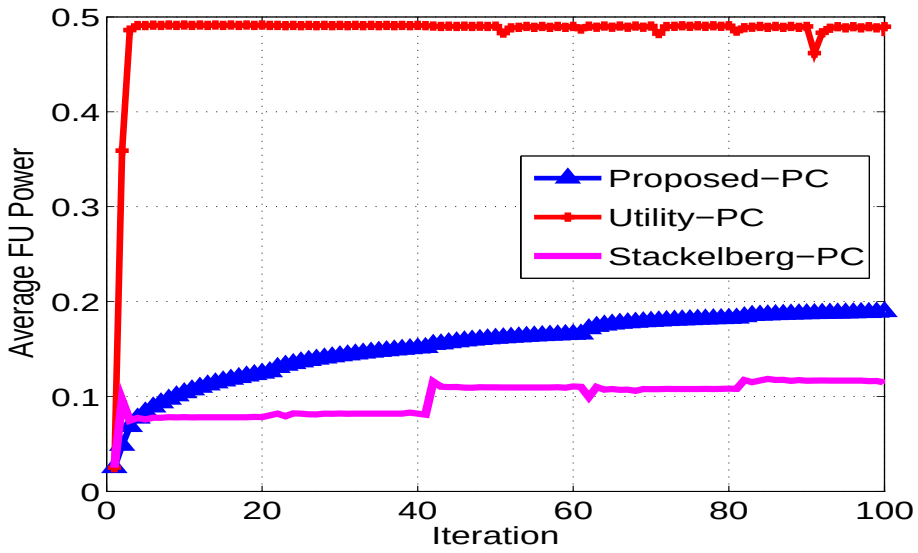

Figure 4.2: Average FU Power

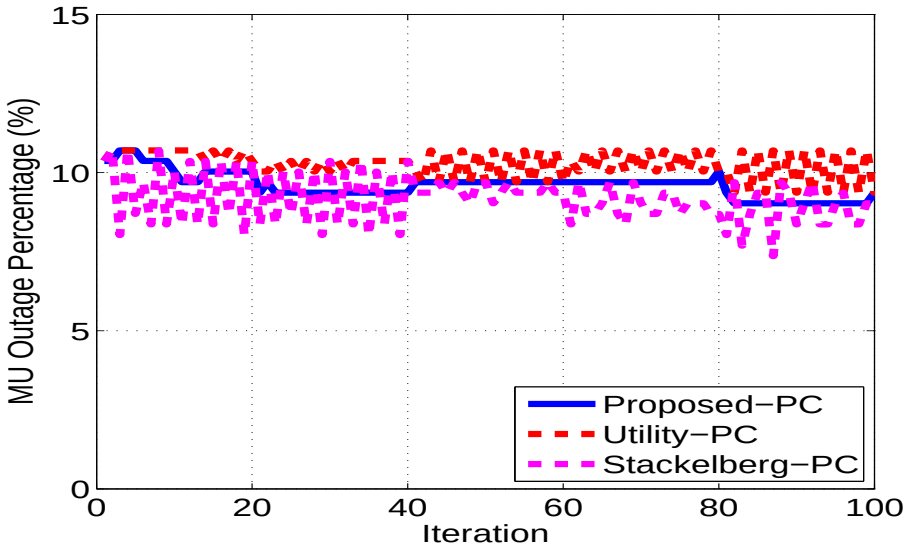

Figure 4.3: MU Outage Percentage

system behavior observed every 20 TSs (see Fig. 4.1) are due to the mobility of the MUs. In fact, in our case we assume that the coherence interval is equal to 20 TSs. Hence, the change in the MUs' shadowing factors are observed every 20 TSs.

As far as the MUs are concerned, Fig. 4.3 shows that the percentage of unsatisfied MUs is almost the same for the three PC schemes, and Stackelberg-PC slightly outperforms ours. This result is expected since Stackelberg-PC was designed with the objective of guaranteeing the QoS requirement of the MU, the game leader, which jointly determines its power allocation and the interference price charged to the active FUs. Second, we study the impact of the FC spatial density on the FU outage percentage (Fig. 4.4(a)) and the MU outage percentage (Fig. 4.4(b)). Fig. 4.4(a) shows that the FU outage rate increases as the FC spatial density increases. However, our scheme still realizes the best performance among the three schemes with a gain of about 15% of QoS-guaranteed

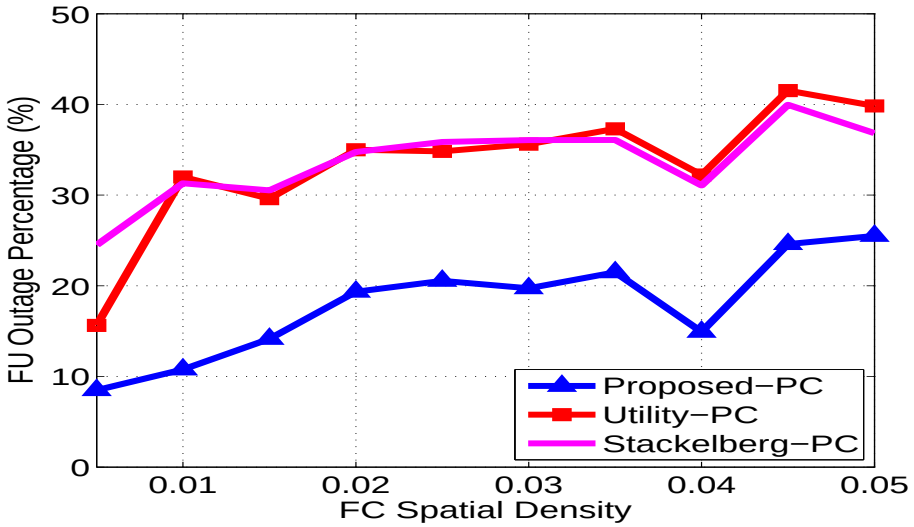

(a) FU Outage Percentage

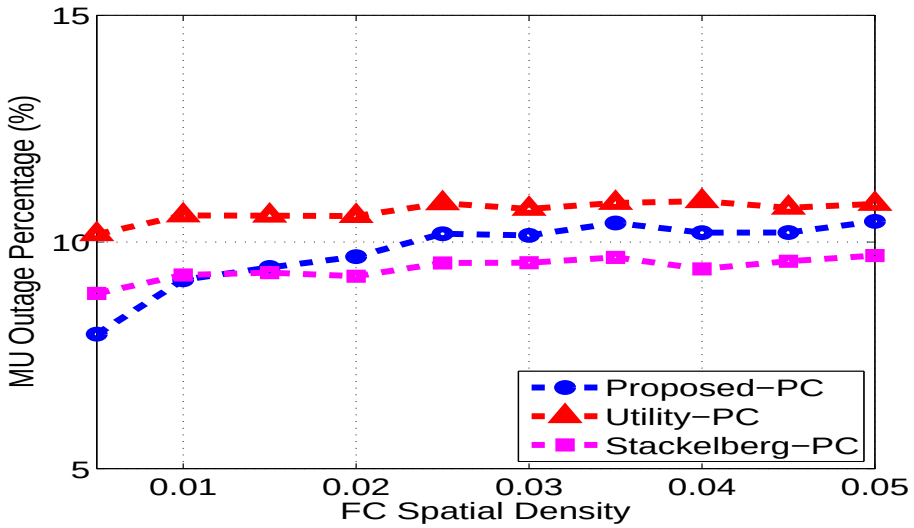

(b) MU Outage Percentage

Figure 4.4: Impact of FC Spatial density on the CU Outage Percentage

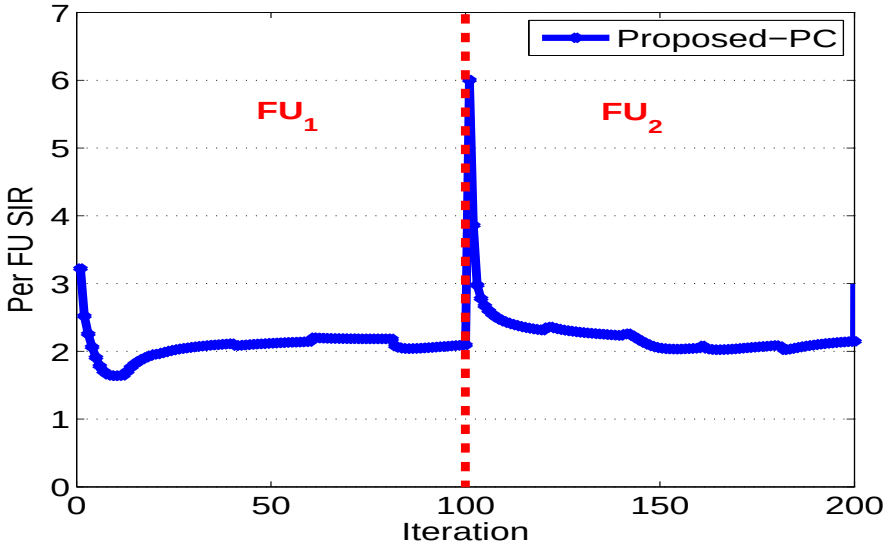

Figure 4.5: SIR Temporal Evolution for two randomly picked FUs

FUs. On the other hand, Fig. 4.4(b) shows that for a FC density less than 0.01, our scheme has the least MU outage percentage, and beyond that value, Stackelberg-PC has the least MU outage percentage, which is an expected result since Stackelberg-PC was designed with the objective of prioritizing the MU in terms of QoS guarantee. However, overall the three schemes present almost same MU outage percentage for different FC spatial densities.

In Fig. 4.5 and Fig. 4.6, we plot the SIR evolution of two randomly picked FUs and two randomly picked MUs (respectively) during its assigned contiguous time slots. We clearly see that the SIR level of these FUs smoothly converges to a steady state. On the other hand, that of MU_2 presents more fluctuation, observed every 20 TSs due to the impact of its mobility on its channel gain variation.

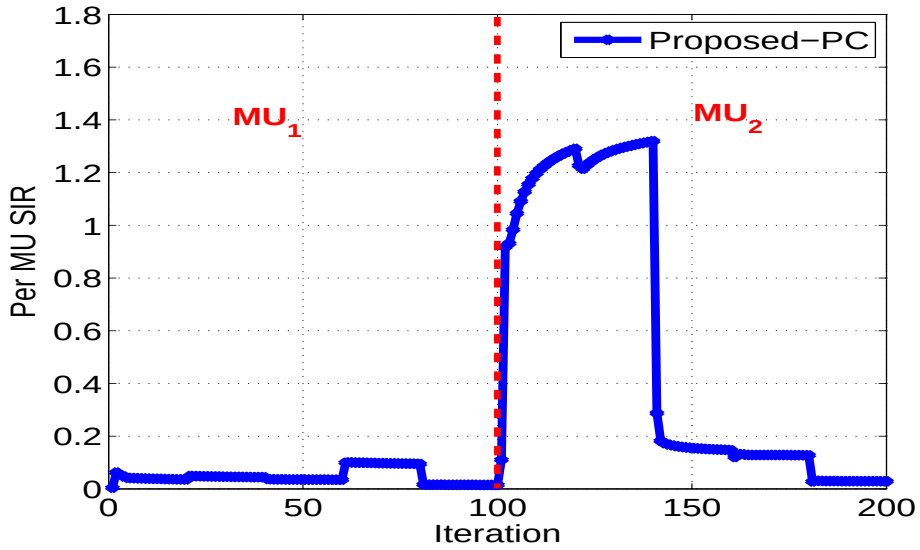

Figure 4.6: SIR Temporal Evolution for two randomly picked MUs

4.6 Summary

In this chapter, we designed a distributed, non-cooperative uplink PC algorithm that enables both the FUs and the MUs to autonomously meet their minimum required SIRs, whenever possible. We provide a theoretical analysis of the properties of our scheme, namely solution existence and stability. Moreover, through simulations, we show that our scheme outperforms some recently proposed schemes in terms of the number/rate of satisfied CUs. In addition to its distributiveness and simplicity/ease of computation, simulations show that our scheme is very stable and converges quite quickly to its steady state.

Chapter 5: Cross-Layer Performance Analysis of Uplink FC Networks

Uplink (UL) interference analysis in two tier femtocell (FC) networks has been the focus of many recent research works, due to its impact on the quality of service (QoS) offered by such networks. However, prior works studied such a parameter from a physical-layer viewpoint; i.e., they did not consider the mapping/interaction between the physical layer parameters and the upper layers, namely the data-link layer. In this chapter, we present an analytic study of the UL physical interference in FC networks and its impact on the delay and data loss rate experienced by constant-bit-rate (CBR) traffic, as well as on the maximum achievable femto-user (FU) throughput.

5.1 Introduction

Characterizing and analyzing interference is becoming more and more important in modern wireless communications mainly due to the emergence of new communication and networking paradigms, such as femtocell and cognitive radio networks, which necessitate and call for the sharing of the radio spectrum more than ever. Therefore, it has been the focus of many recent works, ranging from hardware-level design and optimization [4, 44, 62, 63, 68] to system-level analysis and characterization [7, 17, 18, 24, 33, 34, 42, 46, 50, 73]. In the following, we overview some of these works, highlight their limitations, and state how our work differs from them. Researchers at both

academia and industry have been studying and analyzing interference since the emergence of cellular networks. Similar to our work, in [7,17,18,24,42,50], the authors provide a system level analysis of the FC interference power and outage probability while taking into account the users' spatial distributions, the wireless propagation gain, etc. However, these works present some limitations. In fact, [17] only applies to single-tier networks. In addition, [7] and [42] analyze UL interference in two-tier networks while differentiating between two types of users: licensed primary users (PUs) and unlicensed secondary users (SUs) whose activity depends on the strength of the signal transmitted by the PUs. In our work, we consider a MC network overlaid with multiple FC networks where all considered active users (FUs and MUs) are licensed users sharing the same radio resource and their activity is independent of one another. On the other hand, [7,18,24,42,50] address two-tier wireless networks, but they did not consider the impact of using power control by the cellular users (CUs). In our work, however, we assume that both MUs and FUs use fractional power control. Moreover, we provide a statistical characterization of the SIR auto-correlation per FU for the case of mobile and stationary CUs, which represents a novel contribution that may be used in the design of more efficient retransmission schemes. Other prior works analyze the UL interference spectrum while taking into account physical layer issues that involve modulation and coding [44, 62, 63, 68]. These works may have applications in hardware radio design and optimization, but do not provide enough statistics for the analysis of the QoS experienced by the CU. For instance, in [68], the symbol and packet error probability are derived with respect to two different spread spectrum techniques: Direct Sequence and Frequency Hopping, while taking into account the channel fading and the interferers'

spatial distribution. The packet error probability models the block/bit error probability in a given packet at the receiver. That is, it characterizes the outage probability from a packet viewpoint. While such characterization could be useful/helpful for the study and design of error correcting schemes/codes, it doesn't allow us to assess the QoS experienced per user, namely the per-user transmission outage probability and delay. In fact, in our scheme, we are interested in the outage probability from a system level viewpoint rather than a link-level viewpoint. That is, we aim at characterizing the transmission outage probability (from a user viewpoint) in order to characterize the MAC performance metrics such as delay and data loss rate. In [62] and [63], the authors provide a system characterization that incorporates metrics such as error probability, channel capacity, power spectral density, and aggregate RF emission of the network for different linear modulation schemes (M-PSK and M-QAM). These characterizations could be helpful for hardware RF emission standardization to ensure proper functioning of different coexisting networks such as GPS, cellular networks, etc. In our analysis, however, we make abstraction of the modulation and coding part and analyze the interference power statistics rather than its temporal/spectral properties since we target the characterization of our FC system from a higher level, i.e. MAC layer level. Indeed, in our work, we propose a cross layer analysis, in which we study the impact of the PHY performance metrics on the MAC-related ones (delay, data loss rate, throughput), in power-controlled FC networks, thereby providing useful statistics/metrics and open new horizons for future applications design such as call admission control design [36, 37].

5.2 System Model

5.2.1 Network Model

We consider a single-carrier two-tier cellular system consisting of FCs (with average coverage radius R) overlaid on one MC (with coverage radius $R_M >> R$), all operating over an identical carrier frequency f. In our model, we assume that the FAPs are spatially distributed according to a homogeneous PPP with mean λ_{FAP}. We model the spatial distribution of the FUs and the MUs using two independent homogeneous PPPs, ϕ_1 and ϕ_2, in the two-dimensional plane, with intensities λ_1 and λ_2 respectively. For a PPP with intensity λ, the probability of n nodes being inside a region Z depends only on the total area A_Z of Z and is given by [51]:

$$\mathbb{P}(n \in Z) = \frac{(\lambda A_Z)^n}{n!} e^{-(\lambda A_Z)} \tag{5.1}$$

Here λ is the spatial density of interfering nodes (in our case λ_1 for FUs and λ_2 for MUs), in nodes per unit area. Once scattered over the geographic area, each FU is associated with the closest/nearest FAP in its neighborhood. This is just a graphical model that we use to mimic real deployments of FCs. In fact, in real deployment scenarios, it is not unlikely that FUs are not associated with their closest FAP; this might especially happen in areas with a high density of FCs. But we still assume that such minor variations/exceptions although not taken into account still do not hurt our system analysis, since we primarily aim to characterize cross-layer (physical and data link) performance parameters from a statistical viewpoint.

In this work, we consider the UL communication stream; i.e., communication from the MUs to the macrocell base station (MBS) and from the FUs to their corresponding FAPs. We assume that TDMA is used by the CUs (MUs and FUs) to access the wireless channel, and that the UL communications at the FCs are synchronized with those at the MC [57][1], and consequently are mutually synchronized. It is worth mentioning, that our statistical characterization is still valid under the assumption of asynchronous FU/MU operation. However, intra-FC synchronization needs to be maintained. We further assume that FUs residing in the same FC do not interfere with each other since they are scheduled in different time slots (TSs). Moreover, we assume that a MU that lies within the coverage area of a FC still communicates with the MBS, but it is scheduled on a TS that is orthogonal to the rest of the TSs used by the active FUs belonging to that FC. Hence, at any TS, there is at most one active user per FC. Although in our model, we consider TDMA as the MAC scheme, our system could be mapped into a TH-CDMA (Time-Hopping Code Division Multiple Access) system, where unlike [18], orthogonal codes are used by the users inside the same FC. In our model, each CU can only be in one of two states: On or Off; we use $\delta_i(t)$ to indicate CU i's activity/state:

$$\delta_i(t) = \begin{cases} 1 & \text{if user i is active (On) at time t} \\ 0 & \text{if user i is inactive (Off) at time t} \end{cases}$$

Also, we assume that all FUs and MUs have the same average activity rate, which is

[1]Once turned on and before initiating any communication, FCs get synchronized to the cellular core network using an asymmetric communication link such as xDSL thanks to an enhanced version of IEEE 1588 [57].

denoted by $\overline{\delta}$. According to our model, there is at most only one active FU (FU_i) in each femtocell FC_i at a given time slot t. Hence, we are interested in the interference caused by the neighboring active FUs and the neighboring active MUs at FAP_i. Given the users are located according to PPP, we model the interference's spatial distribution as follows: We consider that FAP_i is located at the center of a disk of radius R representing the area of FC_i covered by FAP_i. Since only FU_i is active at time slot t inside FC_i, then the interference at FAP_i is only caused by out-of-cell interference and it comes from the active FUs located in the annulus Z_1 (delimited by the radii R and R_1) and from the active MUs located in the annulus Z_2 (delimited by the radii R and R_2) as shown in Fig. 5.1. R_1 and R_2 are chosen such that the interference due to FUs beyond R_1 (respectively MUs beyond R_2) is negligible.

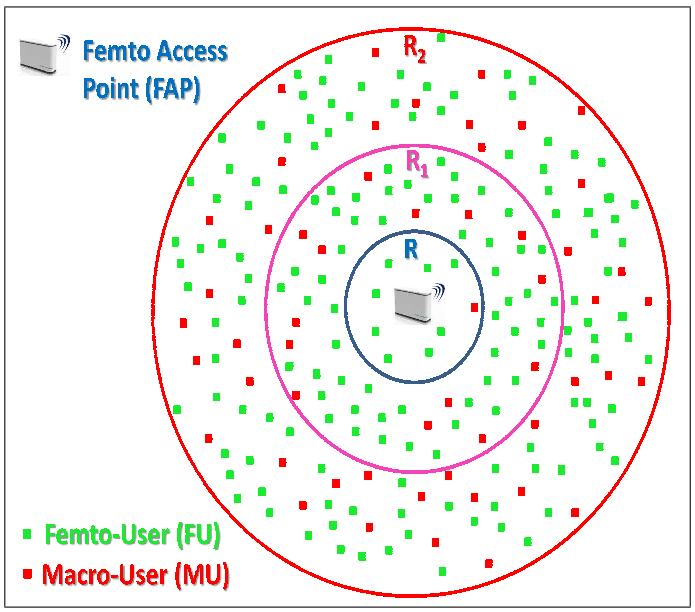

Figure 5.1: Graphical Network Pattern Model

Although in real world settings wireless signals emitted by cellular users are sub-

ject to shadowing (slow fading), fast fading, and pathloss, we here assume that cellular users are slowly-moving or fixed so that their transmitted signal degradation is mainly dominated by shadowing (slow fading) and pathloss effects in compliance with ITU specifications. In this chapter, we distinguish between three values of the pathloss exponent depending on the position of the cellular user (i.e. MU or FU). Let us denote α the pathloss exponent and r_j the distance between cellular user j and FAP_i. We have:

$$\alpha = \begin{cases} 2 & \text{if } r_j < R \\ \alpha_1 & \text{if } R \leq r_j < R_1 \\ \alpha_2 & \text{if } r_j \geq R_1 \end{cases}$$

with $\alpha_2 > \alpha_1 > 2$. This propagation model has been widely used to model the transmission in FC networks. We also adopt it in our work in order to gain some insights on the physical characteristics of FCs and their impact at the data link layer. Unfortunately, if we consider the combined action of shadowing and fast fading, the problem becomes analytically intractable and difficult to come up with some insightful/useful results. Therefore, we assume that the physical channel gain is represented by a combination of path-loss and log-normal shadowing in compliance with the ITU specification [2]. Hence, the amplitude of the signal received by FAP_i placed at a distance r_j from FU_j is:

$$A_{ji} = S_j r_j^{-\alpha_1} P_j$$

where α_1 denotes the path loss exponent associated with the interfering FUs in the zone Z_1, P_j the transmission power of FU_j, and S_j the log-normal shadowing coefficient for

the signal propagating from FU_j to FAP_i given as follows [74]:

$$S_j = 10^{-a(\xi_j/10)} 10^{-b(\xi_{ji}/10)} \tag{5.2}$$

where $a = b = \frac{1}{\sqrt{2}}$, ξ_j and ξ_{ji} are two independent realizations from a zero-mean normal random variable (RV) with standard deviation σ_{ξ_f}. ξ_j represents the propagation environment local to FU_j (the near field), while ξ_{ji} deals with the propagation environment of the path between FU_j and FAP_i (the far field). It is also important to mention that for two different FUs j and m, ξ_{ji} and ξ_{mi} are two independent identically distributed RVs. Likewise, the amplitude of the signal received by FAP_i placed at a distance r_k from MU_k:

$$A_{ki} = S_k r_k^{-\alpha} P_k$$

where α denotes the path loss exponent associated with the interfering MUs, P_k the transmission power of MU_k, and S_k the log-normal shadowing coefficient for the signal propagating from MU_k to FAP_i given as follows:

$$S_k = 10^{-a(\xi_k/10)} 10^{-b(\xi_{ki}/10)} \tag{5.3}$$

where ξ_k and ξ_{ki} are two independent realizations from a zero-mean normal RVs with standard deviation $\sigma_{\xi_m} > \sigma_{\xi_f}$. ξ_k represents the propagation environment local to MU_k (the near field), while ξ_{ki} deals with the propagation environment of the path between MU_k and FAP_i (the far field). Also in this case, for two different MUs, k and m, ξ_{ki} and ξ_{mi} are two independent identically distributed RVs.

5.2.2 Fractional Power Control

UL power control is considered as one of the fundamental approaches that helps mitigate the interference experienced by base stations in order to enhance the reliability and QoS of wireless networks. In this chapter, we assume that both FUs and MUs implement and use the recently proposed fractional power control approach [60], which is being investigated by some wireless operators such as Motorola [78] and Siemens [14]. In our work, we use the fractional power control scheme proposed in [60], tailored to the case where the wireless propagation environment is rather dominated with log-normal shadowing. Recall that in our analysis we assume that the amplitude of the signal received at FAP_i located at a distance r_i from its associated FU_i is:

$$A_{ii} = 10^{-a(\xi_i/10)} 10^{-b(\xi_{ii}/10)} r_i^{-2} P_i \tag{5.4}$$

Moreover, we assume that both ξ_i and ξ_{ii} are constant during the coherence interval (slow fading), and that its values could be obtained at FU_i from its associated FAP_i. Based on this assumption, our fractional power control scheme is designed in order to get rid of the near-field shadowing ξ_i and to reduce the impact of the far-field shadowing ξ_{ii} as follows:

$$P_i = \frac{10^{a(\xi_i/10)} 10^{s_1(\xi_{ii}/10)} P_{fu}}{\mathbb{E}\left[10^{a(\xi_i/10)} 10^{s_1(\xi_{ii}/10)}\right]} \tag{5.5}$$

In (5.5), s_1 is an exponent chosen from the interval $[0, 1]$ in order to compensate the effect of the far-field channel propagation loss ξ_{ii}, P_{fu} is the average FU transmission power satisfying $0 < P_{fu} \leq P_f^{max}$, with P_f^{max} being the maximum transmission power

allowed per FU. Moreover, observe that in the power control rule (5.5), we used the normalizing factor $\mathbb{E}\left[10^{a(\xi_i/10)}10^{s_1(\xi_{ii}/10)}\right]$ so that on average we have $\mathbb{E}\left[P_i\right] = P_{fu}$; that is the average transmission power per FU does not exceed the maximum power P_f^{max}. We also assume that the same power control policy is used by the MUs. Hence, the UL transmission power of MU_k is:

$$P_k = \frac{10^{a(\xi_k/10)}10^{s_2(\xi_{k0}/10)}P_{mu}}{\mathbb{E}\left[10^{a(\xi_k/10)}10^{s_2(\xi_{k0}/10)}\right]} \tag{5.6}$$

where ξ_k represents the propagation environment local to MU_k, ξ_{k0} deals with the propagation environment of the path between MU_k and its MBS, and P_m is the average MU transmission power satisfying $0 < P_{mu} \leq P_m^{max}$, with $P_m^{max} > P_f^{max}$ being the maximum transmission power allowed per MU.

5.3 Interference Analysis

In this section, we derive a statistical characterization of the UL interference in FC networks. We first derive its average and variance, and then derive its probability density function (PDF). In our FC network, we assume a TDMA operation where only one FU is active per FC per time slot. However, when the femto user FU_i is communicating with its associated FAP_i at time slot t, its signal may be affected by the transmissions of the neighboring active FUs and MUs. Hence the interference at FAP_i at time slot t

can be expressed as:

$$I(t) = \sum_{j \in Z_{F1}} \delta_j(t) r_j^{-\alpha_1} S_j(t) P_j(t) + \sum_{k \in Z_{M2}} \delta_k(t) r_k^{-\alpha} S_k(t) P_k(t) \tag{5.7}$$

The interference expression consists of two sums: the first one is over the set of neighboring active FUs, Z_{F1}, confined in the region Z_1, and the second one is over the set of neighboring active MUs, Z_{M2}, confined in the region Z_2. Let $X_j(t) = S_j(t)P_j(t), \forall j \in Z_{F1}$ and $X_k(t) = S_k(t)P_k(t), \forall k \in Z_{M2}$.

$$\begin{aligned} X_j(t) &= 10^{(-a\xi_j(t) - b\xi_{ji}(t)/10)} \left(\frac{10^{(a\xi_j(t) + s_1\xi_{jj}(t)/10)} P_{fu}}{\mathbb{E}\left[10^{(a\xi_j(t) + s_1\xi_{jj}(t)/10)}\right]} \right). \\ &= \frac{10^{((s_1\xi_{jj}(t) - b\xi_{ji}(t))/10)} P_{fu}}{\mathbb{E}\left[10^{((a\xi_j(t) + s_1\xi_{jj}(t))/10)}\right]} \end{aligned} \tag{5.8}$$

with ξ_{jj}, ξ_{ji}, are i.i.d (independent identically distributed) whose distribution is a Gaussian with zero mean and standard deviation $\sigma_{\xi_f} = 4dB$ for all $j \in Z_{F1}$. Hence, $X_j(t)$s are i.i.d log-normal RVs with mean μ_1 and variance σ_1^2 for all $j \in Z_{F1}$. Using some basic operations on independent normal variables as well as relationship between the statistics of a log-normal RV and its associated normal variable we can easily show that:

$$\mu_1 = \frac{\mathbb{E}\left[10^{((s_1\xi_{jj}(t) - b\xi_{ji}(t))/10)}\right] P_{fu}}{\mathbb{E}\left[10^{((a\xi_j(t) + s_1\xi_{jj}(t))/10)}\right]} = P_{fu} \tag{5.9}$$

$$\begin{aligned} \sigma_1^2 &= \frac{P_{fu}^2 \mathbb{V}\left[10^{((s_1\xi_{jj}(t) - b\xi_{ji}(t))/10)}\right]}{\left(\mathbb{E}\left[10^{((a\xi_j(t) + s_1\xi_{jj}(t))/10)}\right]\right)^2}. \\ \sigma_1^2 &= \left(\exp\left((s_1^2 + b^2) \left(\frac{\ln(10)}{10} \sigma_{\xi_f} \right)^2 \right) - 1 \right) P_{fu}^2 \end{aligned} \tag{5.10}$$

Likewise, as far as the MUs are concerned, we have:

$$\begin{aligned} X_k(t) &= 10^{(-a\xi_k(t)-b\xi_{ki}(t)/10)}\left(\frac{10^{(a\xi_k(t)+s_2\xi_{k0}(t)/10)}P_{mu}}{\mathbb{E}\left[10^{(a\xi_k(t)+s_2\xi_{k0}(t)/10)}\right]}\right) \\ &= \frac{10^{(-b\xi_{ki}(t)+s_2\xi_{k0}(t)/10)}P_{mu}}{\mathbb{E}\left[10^{(a\xi_k(t)+s_2\xi_{k0}(t)/10)}\right]} \end{aligned} \tag{5.11}$$

with ξ_{k0}, ξ_{ki}, are i.i.d RVs distributed according to a zero-mean Gaussian with standard deviation σ_{ξ_m} for all $k \in Z_{M2}$. Hence, $X_k(t)$s are i.i.d log-normal RVs with mean μ_2 and variance σ_2^2 for all $k \in Z_{M2}$.

$$\mu_2 = \frac{\mathbb{E}\left[10^{((s_2\xi_{k0}(t)-b\xi_{ki}(t))/10)}\right]P_{mu}}{\mathbb{E}\left[10^{((a\xi_k(t)+s_2\xi_{k0}(t))/10)}\right]} = P_{mu} \tag{5.12}$$

$$\begin{aligned} \sigma_2^2 &= \frac{P_{mu}^2\mathbb{V}\left[10^{((s_2\xi_{k0}(t)-b\xi_{ki}(t))/10)}\right]}{\left(\mathbb{E}\left[10^{((a\xi_k(t)+s_1\xi_{k0}(t))/10)}\right]\right)^2}. \\ \sigma_2^2 &= \left(\exp\left((s_2^2+b^2)\left(\frac{\ln(10)}{10}\sigma_{\xi_m}\right)^2\right)-1\right)P_{mu}^2 \end{aligned} \tag{5.13}$$

Thus, we have shown that the interference I(t) experienced at FAP_i is the sum of the independent log-normal RVs related to the FU interferers and the MU interferers: $X_j(t), j \in Z_{F1}$ with mean μ_1 and variance σ_1^2 and $X_k(t), k \in Z_{M2}$ with mean μ_2 and variance σ_2^2 respectively. In the rest of the chapter, we will use the interference expression given by (5.14) to carry out our statistical analysis.

$$I(t) = \sum_{j\in Z_{F1}} \delta_j(t) r_j^{-\alpha_1} X_j(t) + \sum_{k\in Z_{M2}} \delta_k(t) r_k^{-\alpha} X_k(t) \tag{5.14}$$

For ease of derivation, we use the following notation: $I(t) = I_1(t) + I_2(t)$, with $I_1(t) = \sum_{j \in Z_{F1}} \delta_j(t) r_j^{-\alpha_1} X_j(t)$ and $I_2(t) = \sum_{k \in Z_{M2}} \delta_k(t) r_k^{-\alpha} X_k(t)$.

Theorem 3. *The average μ_I and the variance σ_I^2 of the interference at FAP_i can be expressed as*

$$\begin{aligned} \sigma_I^2 &= \frac{\pi\overline{\delta}(\lambda_1(\sigma_1^2+\mu_1^2)+\lambda_2(\sigma_2^2+\mu_2^2))}{\alpha_1-1}\left(\frac{1}{R^{2(\alpha_1-1)}}-\frac{1}{R_1^{2(\alpha_1-1)}}\right) \\ &+ \frac{\pi\overline{\delta}\lambda_2(\sigma_2^2+\mu_2^2)}{\alpha_2-1}\left(\frac{1}{R_1^{2(\alpha_2-1)}}-\frac{1}{R_2^{2(\alpha_2-1)}}\right) \end{aligned} \tag{5.15}$$

$$\mu_I = \frac{2\pi\overline{\delta}(\lambda_1\mu_1+\lambda_2\mu_2)}{\alpha_1-2}\left(\frac{1}{R^{\alpha_1-2}}-\frac{1}{R_1^{\alpha_1-2}}\right)+\frac{2\pi\lambda_2}{\alpha_2-2}\overline{\delta}\mu_2\left(\frac{1}{R_1^{\alpha_2-2}}-\frac{1}{R_2^{\alpha_2-2}}\right) \tag{5.16}$$

Proof. The proof of this theorem uses the law of total expectation, the law of total variance and Campbell's theorem for PPP [69]. We have $\mu_I \triangleq \mathbb{E}[I(t)] = \mathbb{E}[I_1(t)] + \mathbb{E}[I_2(t)]$. Moreover the two sums $I_1(t)$ and $I_2(t)$ are independent since the two PPPs ϕ_1 and ϕ_2 are independent, the activity of MUs and FUs are independent, and the shadowing factors of the different interfering users are also mutually independent. Hence, $\sigma_I^2 \triangleq \mathbb{V}[I(t)] = \mathbb{V}[I_1(t)] + \mathbb{V}[I_2(t)]$. In the rest of this proof, we will only present the derivation of $\mathbb{E}[I_1(t)]$ and $\mathbb{V}[I_1(t)]$ (the derivation of $\mathbb{E}[I_2(t)]$ and $\mathbb{V}[I_2(t)]$ uses exactly the same techniques). Using the law of total expectation,

$$\mathbb{E}[I_1(t)] = \mathbb{E}_r[\mathbb{E}_\delta[\mathbb{E}_X[I_1(t)|r,\delta]]] = \mathbb{E}_r\left[\mu_1\overline{\delta}\sum_{j\in Z_{F1}} r_j^{-\alpha_1}\right]$$

By applying Campbell's Theorem, we get:

$$\mathbb{E}\left[I_1(t)\right] = \int_R^{R_1} \frac{\mu_1 \overline{\delta}}{r^{\alpha_1}} 2\pi\lambda_1 r\, dr = \frac{2\pi\lambda_1\mu_1\overline{\delta}}{\alpha_1 - 2}\left(\frac{1}{R^{\alpha_1-2}} - \frac{1}{R_1^{\alpha_1-2}}\right)$$

On the other hand, using the law of total variance we have $\mathbb{V}\left[I_1(t)\right] = \mathbb{E}\left[\mathbb{V}\left[I_1(t)|r,\delta\right]\right] + \mathbb{V}\left[\mathbb{E}\left[I_1(t)|r,\delta\right]\right]$ with:

$$\mathbb{E}\left[\mathbb{V}\left[I_1(t)|r,\delta\right]\right] = \sigma_1^2\overline{\delta}\mathbb{E}\left[\sum_{j\in Z_{F1}} (r_j^{-\alpha_1})^2\right]$$

$$\begin{aligned}
\mathbb{V}\left[\mathbb{E}\left[I_1(t)|r,\delta\right]\right] &= \mathbb{V}\left[\mu_1 \sum_{j\in Z_{F1}} \delta_j(t) r_j^{-\alpha_1}\right] \\
&= \mu_1^2(\overline{\delta} - \overline{\delta}^2)\mathbb{E}\left[\sum_{j\in Z_{F1}} (r_j^{-\alpha_1})^2\right] \\
&+ \mu_1^2\overline{\delta}^2\left(\mathbb{E}\left[(\sum_{j\in Z_{F1}} r_j^{-\alpha_1})^2\right] - \mathbb{E}\left[\sum_{j\in Z_{F1}} r_j^{-\alpha_1}\right]^2\right)
\end{aligned}$$

On the other hand, we have:

$$\begin{aligned}
\mathbb{E}\left[\left(\sum_{j\in Z_{F1}} r_j^{-\alpha_1}\right)^2\right] &= \mathbb{E}\left[\sum_{j\in Z_{F1}} (r_j^{-\alpha_1})^2\right] + \mathbb{E}\left[\sum_{i\neq j\in Z_{F1}} \frac{1}{r_i^{\alpha_1} r_j^{\alpha_1}}\right] \\
&= \mathbb{E}\left[\sum_{j\in Z_{F1}} (r_j^{-\alpha_1})^2\right] + \int\int_{Z_{F1}} r_1^{-\alpha_1} r_2^{-\alpha_1}\, \phi_1(dr_1)\, \phi_1(dr_2) \\
&= \mathbb{E}\left[\sum_{j\in Z_{F1}} (r_j^{-\alpha_1})^2\right] + \mathbb{E}\left[\sum_{j\in Z_{F1}} r_j^{-\alpha_1}\right]^2
\end{aligned}$$

Hence, $\mathbb{V}\left[\mathbb{E}\left[I_1(t)|r,\delta\right]\right] = \mu_1^2\overline{\delta}\mathbb{E}\left[\sum_{j\in Z_{F1}}(r_j^{-\alpha_1})^2\right]$. Thus:

$$\begin{aligned}\mathbb{V}\left[I_1(t)\right] &= \overline{\delta}(\sigma_1^2+\mu_1^2)\mathbb{E}\left[\sum_{j\in Z_{F1}}(r_j^{-\alpha_1})^2\right] \\ &= \overline{\delta}(\sigma_1^2+\mu_1^2)\frac{\pi\lambda_1}{\alpha_1-1}\left(\frac{1}{R^{2(\alpha_1-1)}}-\frac{1}{R_1^{2(\alpha_1-1)}}\right)\end{aligned}$$

□

Knowing the statistics of the UL interference is very useful especially to the design of FC networks and to the improvement of its PHY layer performance. For instance, it could be used to optimize the fractional power control exponent s_1 used by the FUs so that the average UL interference experienced at the FAP and/or its variance is minimized. On the other hand, deriving the interference's PDF can be very useful, too. It can be used, for example, in non-cooperative systems whose operations rely on the estimation of the interference [16]. Observe that the expression of the interference at FAP_i is nothing but the sum of independent log-normal RVs. Hence, using the Fenton-Wilkinson approximation [30] about the distribution of the sum of log-normal RVs, it follows that:

Corollary 2. *At any time slot t, $I(t)$ is a log-normal random variable whose PDF is*

$$f_I(x) = \frac{1}{\sqrt{2\pi}x\sigma_{eq}}\exp\left(\frac{-(\ln x-\mu_{eq})^2}{2\sigma_{eq}^2}\right) \tag{5.17}$$

where $\mu_{eq} = \ln\left(\frac{\mu_I^2}{\sqrt{\sigma_I^2+\mu_I^2}}\right)$ *and* $\sigma_{eq}^2 = \ln\left(\frac{\sigma_I^2+\mu_I^2}{\mu_I^2}\right)$.

Proof. Providing an accurate PDF of the UL interference $I(t)$ is mathematically intractable since it is expressed as the sum of log-normally distributed RVs and the number of summands follows a Poisson distribution. Therefore, we approximated it using the following approach. We have divided the problem of finding the PDF of $I(t)$ into two sub-problems:(i) Determining the nature of the probability distribution that statistically characterizes the aggregate interference at FAP_i (normal, lognormal, etc.) (ii) Characterizing the shape of this distribution via its associated mean and variance. In order to answer part(i), we have used the Fenton-Wilkinson approach which states that the sum of a finite number of independent log-normal distributions is a log-normal distribution. This approach is actually more accurate than the central limit theorem since it applies independently of the number of RVs in the sum (whether it is high or low), moreover it is more specific since it only applies to the log-normal distribution type of PDF. Part (ii) has already been computed in Theorem 1, in which we have taken into account that the interferer locations are described by homogeneous PPPs. □

5.4 Signal to Interference Ratio and Outage Probability

In this section, we first derive some statistical characteristics of the UL signal to interference ratio (SIR) that allowed us characterize the link outage probability. Then, we study the temporal auto-correlation of the SIR for the case of stationary CUs, as well as for the case of slowly-moving CUs using the uniform mobility model.

5.4.1 Statistical Characterization

Taking into account the wireless propagation model and the fractional power control described in Section 5.2, the signal transmitted by FU_i to its FAP_i placed at a distance r_i is:

$$A_{ii}(t) = \frac{10^{((s_1-b)\xi_{ii}(t)/10)} P_{fu} r_i^{-2}}{\mathbb{E}\left[10^{a(\xi_i/10)} 10^{s_1(\xi_{ii}/10)}\right]} \tag{5.18}$$

Hence, the SIR of FU_i transmitting at time slot t to its associated FAP_i can be written as:

$$\gamma(t) = \frac{10^{((s_1-b)\xi_{ii}(t)/10)} P_{fu} r_i^{-2}}{\mathbb{E}\left[10^{a(\xi_i/10)} 10^{s_1(\xi_{ii}/10)}\right] I(t)} \tag{5.19}$$

We notice from (5.19) that the SIR $\gamma(t)$ is equal to the ratio of two independent log-normal random variables. Hence, we conclude that $\gamma(t)$ is log-normally distributed as shown in Theorem 3 and its proof.

Theorem 4. *At any time slot t, the SIR $\gamma(t)$ corresponding to the transmission of FU_i in FC_i to FAP_i is a log-normal random variable whose PDF is*

$$f_\gamma(u) = \frac{1}{\sqrt{2\pi} u \sigma_{s-eq}} \exp\left(\frac{-(\ln u - \mu_{s-eq})^2}{2\sigma_{s-eq}^2}\right) \tag{5.20}$$

where $\mu_{s-eq} = \ln\left(\frac{\mu_s^2}{\sqrt{\sigma_s^2+\mu_s^2}}\right)$ *and* $\sigma_{s-eq}^2 = \ln\left(\frac{\sigma_s^2+\mu_s^2}{\mu_s^2}\right)$.

And μ_s and σ_s are the average and variance of the SIR:

$$\mu_s = P_{fu}(\overline{r})^{-2} e^{-\mu_{eq}+\frac{\sigma_{eq}^2}{2}} \tag{5.21}$$

$$\sigma_s^2 = \frac{P_{fu}^2}{\overline{r}^4}\left(e^{(s_1^2+b^2)\left(\frac{\ln(10)}{10}\sigma_{\zeta_f}\right)^2+\sigma_{eq}^2}-1\right)e^{\sigma_{eq}^2-2\mu_{eq}} \tag{5.22}$$

And $\overline{r}$ is the average distance between FU_i and its FAP_i

$$\overline{r} = \frac{1}{2\sqrt{2\pi}\lambda_{FAP}} \tag{5.23}$$

Proof. For analytical tractability, in this proof, we will replace r_i the distance separating FAP_i from FU_i in the SIR expression (5.19) by $\overline{r}$ defined as the average distance between a FU and its associated FAP. It has been shown that the distance between a point u and the nearest point from a point process $\mathbf{X}$ with intensity λ is Rayleigh-distributed with mean $m = \frac{1}{2\sqrt{2\pi\lambda}}$ [69]. By applying this to our network settings, we get the average distance between a FU_i and its associated FAP_i, which happens to be the nearest one among its neighboring FAPs, is $\overline{r} = \frac{1}{2\sqrt{2\pi}\lambda_{FAP}}$.

Let $Y = 10^{((s_1-b)\xi_{ii}(t)/10)} = e^{(s_1-b)\xi_{ii}(t)\ln(10)/10} = e^Z$, $Z \sim \mathcal{N}\left(0, (s_1^2+b^2)\left(\frac{\ln(10)}{10}\sigma_f\right)^2\right)$. Moreover, from the analysis made in the previous section, the interference $I(t)$ experienced at FAP_i is log-normally distributed. That is $I(t) = e^X$, with $X \sim \mathcal{N}(\mu_{eq}, \sigma_{eq}^2)$. Hence, we can write:

$$\gamma(t) = \frac{P_{fu}(\overline{r})^{-2} e^{Z-X}}{\mathbb{E}\left[10^{a(\xi_i/10)} 10^{s_1(\xi_{ii}/10)}\right]}$$

with Z and X being two independent normal variables. The independence property of these two variables can be easily deduced from the fact that the random variables

ξ_{ii}, ξ_{jj}, ξ_{ji}, ξ_{kk} and ξ_{k0} are mutually independent $\forall j \in Z_{F1}, j \neq i$ and $\forall k \in Z_{M2}$. Hence, $(Y - Z) \sim \mathcal{N}\left(-\mu_{eq}, \left((s_1^2 + b^2)\left(\frac{\ln(10)}{10}\sigma_f\right)^2 + \sigma_{eq}^2\right)\right)$. Consequently, $\gamma(t)$ is log-normally distributed, with mean

$$\mu_s \triangleq \mathbb{E}\left[\gamma(t)\right] = P_{fu}(\overline{r})^{-2} e^{-\mu_{eq} + \frac{\sigma_{eq}^2}{2}}$$

and variance

$$\sigma_s^2 \triangleq \mathbb{V}\left[\gamma(t)\right] = \frac{P_{fu}^2}{\overline{r}^4}\left(e^{(s_1^2+b^2)\left(\frac{\ln(10)}{10}\sigma_{\zeta_f}\right)^2 + \sigma_{eq}^2} - 1\right) e^{\sigma_{eq}^2 - 2\mu_{eq}}$$

□

In addition, we assume that the transmission from FU_i to FAP_i fails if its SIR (γ) is below a certain defined threshold γ^{th}. This is the case if the interference at FAP_i is high enough compared to the amplitude of the signal transmitted by FU_i, so that this FAP cannot detect it.

Corollary 3. *The outage probability $P_o \triangleq \mathbb{P}(\gamma < \gamma^{th})$ of FU_i's transmission to FAP_i is:*

$$P_o = \frac{1}{2} erfc\left(-\frac{\ln(\gamma^{th}) - \mu_{s-eq}}{\sqrt{2\sigma_{s-eq}^2}}\right) \tag{5.24}$$

5.4.2 The Temporal Auto-Correlation of the SIR

In many link outage analysis works, the realizations of the SIR are assumed independent across time. However, this is not always the case, especially when the interferers

positions are correlated across time. In our analysis, we assume that the nodes are fixed (stationary) or are (at most) moving slowly. Therefore, in the following we derive the temporal autocorrelation of the UL SIR γ corresponding to the transmission of FU_i to FAP_i at two different TSs t_1 and t_2 chosen from a given coherence interval during which the channel propagation gain as well as the transmission power used by FU_i remain essentially constant (i.e. maintained at the same level), so that the signal received at FAP_i from FU_i could be approximated by a constant K_i. In this autocorrelation analysis we distinguish between two cases:

Case(1)—Mobile interferers: We consider that the interferers, the MUs and the FUs, are moving with constant speeds $\overline{v_1}$ and $\overline{v_2}$ respectively, and their displacement direction is described by an angle θ uniformly distributed in $[0, 2\pi]$.

Case(2)—Stationary interferers: We consider $\overline{v_1} = \overline{v_2} = 0$.

Theorem 5. *The temporal autocorrelation of the SIR (γ) corresponding to the transmission of FU_i to FAP_i at the time slots t_1 and t_2 ($t_1 < t_2$) is:*

Under case(1)—Mobile interferers:

$$R_\gamma(\tau) = \frac{K_i^2 \mathbb{E}\left[\frac{1}{\overline{\delta}^2(\beta_1 X_j + \beta_2 X_k)(\beta_3 X_j + \beta_4 X_k)}\right] - \mu_s^2}{\sigma_s^2} \tag{5.25}$$

where $\tau = t_2 - t_1$, X_j and X_k denote the log-normal shadowing coefficients related to the FUs and MUs respectively (as defined in (5.14)), and

$$\beta_1 = \frac{2\pi\lambda_1}{\alpha_1 - 2}\left(\frac{1}{R^{\alpha_1 - 2}} - \frac{1}{R_1^{\alpha_1 - 2}}\right)$$

$$\beta_2 = \frac{2\pi\lambda_2}{\alpha_1 - 2}\left(\frac{1}{R^{\alpha_1-2}} - \frac{1}{R_1^{\alpha_1-2}}\right) + \frac{2\pi\lambda_2}{\alpha_2 - 2}\left(\frac{1}{R_1^{\alpha_2-2}} - \frac{1}{R_2^{\alpha_2-2}}\right)$$

$$\beta_3 = \int_R^{R_1}\int_0^{2\pi} \frac{\lambda_1 r}{(r^2 + (\overline{v_1}\tau)^2 + 2\overline{v_1}\tau r\cos(\theta))^{\frac{\alpha_1}{2}}}\, dr\, d\theta$$

$$\beta_4 = \int_R^{R_2}\int_0^{2\pi} \frac{\lambda_2 r}{(r^2 + (\overline{v_2}\tau)^2 + 2\overline{v_2}\tau r\cos(\theta))^{\frac{\alpha}{2}}}\, dr\, d\theta$$

Under case(2)—Stationary interferers:

$\beta_1 = \beta_3$ *and* $\beta_2 = \beta_4$*, thus:*

$$R_\gamma(\tau) = \frac{K_i^2\mathbb{E}\left[\frac{1}{\overline{\delta}^2(\beta_1 X_j + \beta_2 X_k)^2}\right] - \mu_s^2}{\sigma_s^2} \tag{5.26}$$

Proof. Given that the SIR realizations are identically distributed but not independent (i.e. correlated) across time, the temporal autocorrelation of the SIR at the time slots t_1 and t_2 ($t_1 < t_2$) is:

$$R_\gamma(\tau) = \frac{\mathbb{E}\left[\gamma(t_1)\gamma(t_2)\right] - \mu_s^2}{\sigma_s^2}$$

where

$$\begin{aligned}
\mathbb{E}\left[\gamma(t_1)\gamma(t_2)\right] &= K_i^2\mathbb{E}\left[\frac{1}{I(t_2)I(t_1)}\right] \\
&= K_i^2\mathbb{E}\left[\int_0^{+\infty}\int_0^{+\infty} e^{-(xI(t_1)+yI(t_2))}\, dx\, dy\right] \\
&= K_i^2\int_0^{+\infty}\int_0^{+\infty}\mathbb{E}\left[e^{-(xI(t_1)+yI(t_2))}\right] dx\, dy
\end{aligned}$$

By further decomposing the interference into two interference terms induced by the

neighboring FUs and MUs as in (5.14), it follows that

$$\mathbb{E}[\gamma(t_1)\gamma(t_2)] = K_i^2 \left(\int_0^{+\infty} \int_0^{+\infty} \mathbb{E}\left[e^{-(xI_1(t_1)+yI_1(t_2))}\right] \mathbb{E}\left[e^{-(xI_2(t_1)+yI_2(t_2))}\right] \, dx \, dy \right) \tag{5.27}$$

When considering mobile interferers, we have

$$r_j(t_2) = \sqrt{r_j(t_1)^2 + (\overline{v_1}\tau)^2 + 2\overline{v_1}\tau r_j(t_1)\cos(\theta)} \, \forall j \in Z_{F1} \tag{5.28}$$

$$r_k(t_2) = \sqrt{r_k(t_1)^2 + (\overline{v_2}\tau)^2 + 2\overline{v_2}\tau r_k(t_1)\cos(\theta)} \, \forall k \in Z_{M2} \tag{5.29}$$

On the other hand for any point process ϕ, its Laplace functional is defined as

$$\boldsymbol{L}_\phi(f) \triangleq \mathbb{E}\left[e^{-\int_Z f(x)\,\phi(dx)}\right] = \mathbb{E}\left[e^{-\sum_{x\in Z} f(x)}\right] \tag{5.30}$$

Using (5.28) and (5.29), and applying (5.30) yield

$$\mathbb{E}\left[e^{-(xI_1(s)+yI_1(t))}\right] = e^{-\overline{\delta} X_j(\beta_1 x + \beta_3 y)}$$

where

$$\beta_1 = \int_R^{R_1} r^{-\alpha_1} 2\pi\lambda_1 r \, dr = \frac{2\pi\lambda_1}{\alpha_1 - 2}\left(\frac{1}{R^{\alpha_1-2}} - \frac{1}{R_1^{\alpha_1-2}}\right)$$

$$\beta_3 = \int_R^{R_1} \int_0^{2\pi} \frac{\lambda_1 r}{(r^2 + (\overline{v_1}\tau)^2 + 2\overline{v_1}\tau r\cos(\theta))^{\frac{\alpha_1}{2}}} \, dr \, d\theta$$

Likewise,

$$\mathbb{E}\left[e^{-(xI_2(t_1)+yI_2(t_2))}\right] = e^{-\overline{\delta}X_k(\beta_2 x+\beta_4 y)}$$

where

$$\begin{aligned}\beta_2 &= \int_R^{R_2} r^{-\alpha} 2\pi\lambda_2 r\, dr \\ &= \frac{2\pi\lambda_2}{\alpha_1-2}\left(\frac{1}{R^{\alpha_1-2}}-\frac{1}{R_1^{\alpha_1-2}}\right)+\frac{2\pi\lambda_2}{\alpha_2-2}\left(\frac{1}{R_1^{\alpha_2-2}}-\frac{1}{R_2^{\alpha_2-2}}\right)\end{aligned}$$

$$\beta_4 = \int_R^{R_2}\int_0^{2\pi} \frac{\lambda_2 r}{(r^2+(\overline{v_2}\tau)^2+2\overline{v_2}\tau r\cos(\theta))^{\frac{\alpha}{2}}}\, dr\, d\theta$$

Hence, it follows that

$$\begin{aligned}\mathbb{E}\left[\gamma(t_1)\gamma(t_2)\right] &= K_i^2\mathbb{E}\left[\left(\int_0^{+\infty}\int_0^{+\infty} e^{-\overline{\delta}X_j(\beta_1 x+\beta_3 y)}e^{-\overline{\delta}X_k(\beta_2 x+\beta_4 y)}\, dx\, dy\right)\right] \\ &= K_i^2\mathbb{E}\left[\frac{1}{\overline{\delta}^2(\beta_1 X_j+\beta_2 X_k)(\beta_3 X_j+\beta_4 X_k)}\right]\end{aligned}$$

□

The characterization of the temporal auto-correlation of the SIR in FCs is important. In fact, it helps characterize the correlation of transmission failures over time. Thus, it provides useful information for the design of retransmission strategies, or power control schemes for efficient reliable FC networks.

5.5 System Capacity and Delay Performance

In this section, we characterize the asymptotic capacity (i.e. steady state capacity) of a FC network. We determine the delay characteristics for CBR (constant bit rate) traffic in FC networks, and derive an upper bound on the achievable asymptotic FC service/throughput while taking into account the interference analysis done in the previous sections. First, by assimilating a FC to a $D/G/1$ queuing system, we characterize the average delay per FU. Then, we derive the probability that it exceeds a certain delay threshold. We further explain the derived delay result through an example of CBR, delay constrained type of traffic: Voice over IP (VoIP). Finally, we study the asymptotic achievable throughput in FC networks.

5.5.1 Delay Characterization

Since time is fairly shared among the FUs in the same FC, and the interferers are assumed to be spatially distributed according to a homogeneous PPP, then we can safely assume that the average packet delay experienced by any active FU in a given FC is the same. Therefore, to characterize the delay performance of a FC, it suffices to characterize it for one of its active FUs. Moreover, from any active FAP's viewpoint, the spatial and temporal distribution of the interferers have the same statistical characterization. Therefore, the statistical delay characterization that we provide hereafter for FC_i applies for any active FC deployed inside our MC.

In this section, we characterize the per packet average delay at FU_i. Recall that in our system we assume that the FCs use TDMA as a channel access technique. That

is, we assume that time is slotted and at every time slot only one FU is active per FC. Moreover, we assume that each active FU generates ν packets of voice traffic in its assigned time slot. Hence, given that FC_i contains multiple active FUs (n_f active FUs), FAP_i experiences an arrival of traffic with a constant data rate equal to ν packets per time slot. Hence, FC_i could be assimilated to a $D/G/1$ queuing system with a constant packet arrival rate equal to ν packets per time slot, served by a wireless channel with a per-packet average service time $\overline{\chi} = \mathbb{E}[\chi]$, where χ is a random variable representing the packet service time. Our aim is to derive the packet's average waiting time (W) in the queue of FU_i as well as its average service time $\overline{\chi}$, in order to deduce the per-packet average total delay ($\overline{D} = W + \overline{\chi}$) at FU_i. In our analysis, we further assume that FCs are heavily loaded. That is, the active FUs always have traffic to send in their assigned time slots. Hence, using Kingman's heavy traffic approximation, the steady state average queuing delay in our system is:

$$W = \frac{\nu(\overline{\chi^2} - (\overline{\chi})^2)}{2(1 - \nu\overline{\chi})} \tag{5.31}$$

In fact, Kingman's heavy traffic approximation [12] states that for a heavy loaded $G/G/1$ system with an average packet arrival rate ν and average service time $\overline{\chi}$, the average waiting time is $W = \frac{\nu(\sigma_a^2+\sigma_s^2)}{2(1-\nu\overline{\chi})}$, with σ_a^2 being the variance of the packet inter-arrival times, and σ_s^2 the variance of their service times. Note that in our case the $D/G/1$ system is a particular case of the $G/G/1$ system with the difference that the packet inter-arrival times are deterministic in our case, that is $\sigma_a^2 = 0$, leading then to Eq. (5.31). Now, all what remains to approximate $\overline{D}$ is to derive the first and second order moments of the

service time $\overline{\chi}$ and $\overline{\chi^2}$. In our system, we define the average packet service time ($\overline{\chi}$) as the average delay between the instant it is initially transmitted by FU_i and the instant of its successful reception at FAP_i. Moreover, we assume that a transmission attempt failure is solely due to excessive interference; i.e., due to high transmission powers of neighboring interferers causing $\gamma < \gamma^{th}$. Hence:

$$\begin{aligned}
\overline{\chi} &\triangleq \sum_{k=0}^{+\infty} T(k)\mathbb{P}(success|k) \\
&= \sum_{k=0}^{+\infty} T(k)(1 - P_o(t_{k+1})) \prod_{j=1}^{k} \mathbb{P}(\gamma(t_j) < \gamma^{th}) \\
&= \sum_{k=0}^{+\infty} T(k)(1 - P_o)P_o^k
\end{aligned}$$

where $T(k)$ denotes the delay corresponding to k retransmissions, t_j corresponds to the time slot of the j^{th} transmission attempt of the packet, and the expression of the outage probability P_o is given by Eq. (5.24). In the above derivation, we assumed that $\gamma(t)$ (for any time slot t) are i.i.d. Hence, basic order statistics (with some algebraic manipulation) yield the last line of the above derivation. Given our system settings, it is easy to show that the average delay of k retransmissions is $T(k) = (1 + n_f k)$. Plugging this value in the last line of the above derivation, we get two sums that, using some known results in geometric series, lead to the following expression

$$\overline{\chi} = 1 + \frac{n_f P_o}{1 - P_o} \tag{5.32}$$

On the other hand, the second moment of the service time can be written as

$$\overline{\chi^2} \triangleq \sum_{k=0}^{+\infty} (T(k))^2 (1 - P_o) P_o^k$$

Using the same calculus techniques for the derivation of Eq. (5.32), we can write

$$\overline{\chi^2} = 1 + \frac{2n_f P_o}{1 - P_o} + \frac{n_f^2 (P_o + P_o^2)}{(1 - P_o)^2} \tag{5.33}$$

Thus, we conclude the following result:

Theorem 6. *The average packet delay in a TDMA heavy-loaded FC system in which FUs are scheduled in a round-robbin fashion is:*

$$\overline{D} = 1 + \frac{n_f P_o}{1 - P_o} + \frac{\nu(\overline{\chi^2} - (\overline{\chi})^2)}{2(1 - \nu\overline{\chi})} \tag{5.34}$$

where $\overline{\chi}$ is given by Eq. (5.32) and $\overline{\chi^2}$ is given by Eq. (5.33).

Now that we have derived the per-packet average delay, we further assume that our system is delay sensitive and has a delay constraint expressed as

$$\mathbb{P}(D > D_{max}) < \epsilon \tag{5.35}$$

where D_{max} is the maximum allowed per packet delay, and ϵ is a design parameter that will be explained later in this section through an example. It has been shown in [76] that given a system with a constant data arrival rate ν and a variable channel capacity $C(t)$,

the probability of $D(t)$ exceeding a delay bound D_{max} satisfies:

$$\sup_t \mathbb{P}(D(t) > D_{max}) \approx f(\nu)e^{-g(\nu)D_{max}}$$

where $D(t)$ denotes the delay experienced by the packet generated at time t, and $f(\nu), g(\nu)$ are two functions of the source data rate ν. Note that this implicitly assumes that the t^{th} packet delay $D(t)$ is exponentially distributed. Hence, we can easily show that $\frac{f(\nu)}{g(\nu)} = \mathbb{E}[D(t)]$ and $f(\nu) = \mathbb{P}(D(t) > 0)$. In our system, we are making discrete time analysis (time is slotted) where the delay is expressed in terms of number of time slots. Therefore, we will use the geometric distribution (with parameter $p = 1 - P_o$) as a discrete approximation of the exponential distribution to derive $f(\nu)$. This approximation is legitimate when the time slot duration is small enough, which is the case in cellular networks in general where a time slot is approximately equal to 1 to 2 milliseconds. Thus, knowing that by definition $D(t) \geq 0$, we have:

$$\begin{aligned} f(\nu) \triangleq \mathbb{P}(D(t) > 0) &= 1 - \mathbb{P}(D(t) = 0) \\ &= 1 - p = P_o \end{aligned}$$

and consequently

$$g(\nu) \triangleq \frac{f(\nu)}{\mathbb{E}[D(t)]} = \frac{P_o}{\overline{D}}$$

Theorem 7. *For CBR traffic, the probability of the packet delay exceeding a threshold*

D_{max} in FC networks satisfies

$$\sup_t \mathbb{P}(D(t) > D_{max}) \approx P_o e^{-P_o \frac{D_{max}}{\overline{D}}} \tag{5.36}$$

This result can be useful for many applications, such as call admission control, cross-layer QoS-aware network design, etc.

Illustrative example: Consider a FC network whose FUs are scheduled in a TDMA fashion, and where each FU sends ν voice packets at its assigned slot. We know that in order to have an acceptable QoS for voice, the per-packet delay should not exceed $D_{max} = 400ms$, and the packet loss rate should not exceed about 3% [54]. Therefore, if a packet delay exceeds D_{max}, it is considered lost. The maximum allowed packet loss rate is nothing but the parameter ϵ introduced in Eq. (5.35). From Eq. (5.36), it then follows that the delay constraint is

$$P_o e^{-P_o \frac{D_{max}}{\overline{D}}} \leq \epsilon \tag{5.37}$$

Using the expression of $\overline{D}$ given in (Eq. 5.34) and solving (Eq. 5.37) for P_o yield the maximum allowed physical outage probability tolerated per FU in order to satisfy (5.37).

5.5.2 Asymptotic Capacity

The instantaneous channel capacity (at time slot j) is defined via the Shannon formula as $C(j) = b\log(1 + \gamma(j))$, where b denotes the channel bandwidth. Hence, for FC networks, the service provided to FU_i by the wireless channel is defined as

$S(t) \triangleq \sum_{j=1}^{t} C(j)$. Inspired by the effective bandwidth, Wu and Negi proposed the effective capacity theory [76], which is the dual of the original effective bandwidth theory [20]. The effective capacity is defined as the maximum constant arrival rate that a given service process can support in order to guarantee a QoS requirement specified by the QoS exponent $g(\nu)$. In our case, the effective capacity is nothing but the maximal achievable throughput under the maximum delay constraint, specified by the QoS exponent $g(\nu) = \frac{P_o}{D}$.

Analytically, the effective capacity can be formally defined as follows. Let the sequence $C(j); j = 1, 2, ...$ ($C(j)$ is the channel capacity at time slot j) denote a discrete time stationary and ergodic stochastic service process and $S(t) \triangleq \sum_{j=1}^{t} C(j)$ be the partial sum of the service process. Assume that the $G\ddot{a}rtner - Ellis$ limit of $S(t)$, expressed as

$$\Lambda_c(u) = \lim_{t \to +\infty} \frac{1}{t} \log \left(\mathbb{E} \left[e^{uS(t)} \right] \right)$$

exists and is a convex function differentiable for all real u. Then the effective capacity of the service process, denoted by $E_c(u)$, where $u > 0$, is defined as [76]:

$$E_c(u) \triangleq -\frac{\Lambda_c(-u)}{u} = -\lim_{t \to +\infty} \frac{1}{ut} \log \left(\mathbb{E} \left[e^{-uS(t)} \right] \right) \tag{5.38}$$

Based on our physical-layer framework developed in Section 5.4, we now derive an upper bound on the network effective capacity, which is stated in the following theorem.

Theorem 8. *In the high-SIR regime, the effective capacity of a FC network is upper bounded as follows:*

$$E_c(u) < \mathbb{E} \left[\log(\gamma) \right] \tag{5.39}$$

Proof. Case 1: Assuming i.i.d. SIR realizations across time: At the high-SIR regime, for any time slot j, we have $\log(1+\gamma(j)) \sim \log(\gamma(j))$, with $\log(\gamma(j))$ is normally distributed with parameters: $\mu \triangleq \mathbb{E}[\log(\gamma(j))] = \mu_{s-eq}$ and $\sigma^2 \triangleq \mathbb{V}[\log(\gamma(j))] = \sigma^2_{s-eq}$. Let $Y_j = \log(\gamma(j))$ where the index j refers to the j^{th} time slot. Hence, $Y_j \sim \mathcal{N}(\mu, \sigma)$. Since the random variables $Y_j; j = 1, 2, ...$ are assumed i.i.d., the sum $Y = \sum_{j=1}^{N} Y_j$ is normally distributed with mean $\mu_Y = N\mu$ and variance $\sigma^2_Y = N\sigma^2$. It follows that $\mathbb{E}\left[e^{-uS(t)}\right] = \lim_{N\to+\infty} \mathbb{E}\left[e^{-u\sum_{j=1}^{N}(\frac{t}{N})\log(1+\gamma(j))}\right]$, with:

$$\begin{aligned}\mathbb{E}\left[e^{-u\sum_{j=1}^{N}(\frac{t}{N})\log(1+\gamma(j))}\right] &\approx \mathbb{E}\left[e^{-u\sum_{j=1}^{N}(\frac{t}{N})Y_j}\right] \\ &\leq \mathbb{E}\left[e^{-u(\frac{t}{N})Y}\right] \\ &\leq M_Y\left(-u\frac{t}{N}\right) = e^{-(tu\mu)+\frac{1}{2}(\frac{t^2}{N}u^2\sigma^2)}\end{aligned}$$

Here, M_Y denotes the moment generating function of the random variable $Y = \sum_{j=1}^{N}\log(\gamma(j))$. Calculating the limit of the obtained result as N the number of time slots/samples goes to infinity yields

$$\mathbb{E}\left[e^{-uS(t)}\right] \leq e^{-(tu\mu)} \tag{5.40}$$

Thus, the asymptotic network capacity, assuming time independent SIR realizations, is upper bounded as follows:

$$E_c(u) \triangleq -\lim_{t\to+\infty}\frac{1}{ut}\log\left(\mathbb{E}\left[e^{-uS(t)}\right]\right) \leq \mu \tag{5.41}$$

Case 2: Assuming dependent but identically distributed SIR realizations across time: Note that in the case of identically-distributed but time-correlated realizations of the

SIR, under the high-SIR regime, we can proceed the same way as in case 1 discussed above to characterize the asymptotic capacity of FC networks, with the only difference is the fact that $Y = \sum_{j=1}^{N} Y_j$ is no longer normally distributed (but we still have $Y_j \sim \mathcal{N}(\mu, \sigma) \forall j = 1..N$). Hence,

$$\mathbb{E}\left[e^{-u\sum_{j=1}^{N}(\frac{t}{N})y_j}\right] \leq \int e^{-u\sum_{j=1}^{N}(\frac{t}{N})y_j} f_{\mathbf{Y}}(\mathbf{y})\, d\mathbf{y} \tag{5.42}$$

where $f_{\mathbf{Y}}(\mathbf{y})$ is the multivariate normal joint distribution function of the RVs $(Y_j; j = 1, 2, .., N)$ defined as:

$$f_{\mathbf{Y}}(\mathbf{y}) = (2\Pi)^{-\frac{N}{2}} |\mathbf{R}_y|^{-\frac{1}{2}} \exp\left(-\frac{1}{2}(\mathbf{y}^{\mathrm{T}} - \mu^{\mathrm{T}})\mathbf{R}_y^{-1}(\mathbf{y} - \mu)\right)$$

where $\mathbf{R}_y$ denotes their covariance matrix. Thus, all we need is to find an "adequately" chosen upper bound for the integral in (5.42), in order to obtain a finite upper bound of the asymptotic network capacity. Below, we present our approach to bound this quantity. Let us define the random vector $\mathbf{z} = \mathbf{y} - \mu$. Substituting this random variable in the right hand side (RHS) of the integral of (5.42) yields

$$\int e^{-u\sum_{j=1}^{N}(\frac{t}{N})y_j} f_{\mathbf{Y}}(\mathbf{y})\, d\mathbf{y} = (2\Pi)^{-\frac{N}{2}} |\mathbf{R}_y|^{-\frac{1}{2}} e^{-Nu\frac{t}{N}\mu} \left(\int e^{-u\sum_{j=1}^{N}(\frac{t}{N})z_j} e^{-\frac{1}{2}\mathbf{z}^{\mathrm{T}}\mathbf{R}_y^{-1}\mathbf{z}} |\mathbf{J}|\, d\mathbf{z}\right) \tag{5.43}$$

where $|\mathbf{J}|$ is the determinant of the Jacobian matrix (defined by: $\mathbf{J}_{mn} = \frac{\partial y_m}{\partial z_n}$). Note that in this case, $\mathbf{J}$ is the identity matrix (therefore, $|\mathbf{J}| = 1$). Moreover, we assume that at the high SIR-regime, $Y_j > \mathbb{E}[Y_j]$, for any time slot j, and hence, $Z_j > 0; \forall j$, implying

that $\forall u > 0, e^{-u\sum_{j=1}^{N}(\frac{t}{N})z_j} < 1$. Injecting this inequality in (25) yields

$$\mathbb{E}\left[e^{-u\sum_{j=1}^{N}(\frac{t}{N})Y_j}\right] \leq e^{-Nu\frac{t}{N}\mu}(2\Pi)^{-\frac{n}{2}}|\mathbf{R}_y|^{-\frac{1}{2}}\int e^{-\frac{1}{2}\mathbf{z}^{\mathrm{T}}\mathbf{R}_y^{-1}\mathbf{z}}\,d\mathbf{z} \tag{5.44}$$

Moreover, we know that given $\mathbf{K}$ a symmetric positive definite matrix, the multidimensional Gaussian integral satisfies:

$$\int \exp\left(-\frac{1}{2}\mathbf{x}^{\mathrm{T}}\mathbf{K}^{-1}\mathbf{x}\right)\,d\mathbf{x} = (2\Pi)^{\frac{N}{2}}|\mathbf{K}|^{\frac{1}{2}} \tag{5.45}$$

Since $Y_j, j = 1, 2, .., N$ are identically distributed, the covariance matrix $\mathbf{R}_y$ is symmetric positive-definite. Hence, the integral obtained in the RHS of (5.44) is nothing but the multidimensional Gaussian integral. Thus, by using the result in (5.45) and applying it to the RHS of (5.44), we get the same upper bound as in (5.40): $\mathbb{E}\left[e^{-u\sum_{j=1}^{N}(\frac{t}{N})Y_j}\right] \leq e^{-Nu\frac{t}{N}\mu}$. Then, by taking the limit as $N \to +\infty$, we get the same upper bound as in the time uncorrelated case: $\mathbb{E}\left[e^{-uS(t)}\right] \leq e^{-(tu\mu)}$. Thus, for this case, we also have:

$$E_c(u) \triangleq -\lim_{t\to+\infty}\frac{1}{ut}\log\left(\mathbb{E}\left[e^{-uS(t)}\right]\right) \leq \mu$$

□

As far as the low-SIR regime is concerned, for any time slot j, $\log(1+\gamma(j)) \sim \gamma(j)$, with $\gamma(j)$ log-normally distributed. Due to some computational complexity related to log-normal distribution, and the non-existence of a moment generating function for this type of distribution, we were not able to find an upper bound on the FC network asymptotic capacity at the low-SIR regime.

Table 5.1: Summary of Simulation Parameters

Maximum FU Power P^f_{max}	0.125 Watt
Maximum MU Power P^m_{max}	1 Watt
Femto SINR Threshold γ^{th}	3.2. dB
FC Coverage Radius (R)	7 m
Interference Zone Z_1 radius (R_1)	50 m
Interference Zone Z_2 radius (R_2)	100 m
Indoor Pathloss Exponent	2
Pathloss Exponent α_1	3
Pathloss Exponent α_2	5
FU Shadowing Standard deviation σ_{ξ_f}	3 db
MU Shadowing Standard deviation σ_{ξ_m}	6 db
Average activity rate $\overline{\delta}$	$\frac{1}{3}$
FU Spatial density λ_1	0.15
MU Spatial density λ_2	0.02
Power Control exponents s_1 and s_2	$\frac{1}{\sqrt{2}}$

5.6 Numerical Results

Using the physical model discussed in Section 5.2, we apply Monte Carlo numerical techniques to simulate the co-channel interference observed at the FAP for 10^6 samples. At each sample instant, the locations of the active MU and FU interferers are generated as a realization of their corresponding PPPs, and their shadowing coefficients as realizations of their related log-normal distributions. In our simulation, we use the same PHY propagation parameters as in [25] and [2] and fix the PPP intensities, unless otherwise stated. The main simulation parameters are summarized in Table 5.1.

In Fig. 5.2, we plot the theoretic outage probability derived in Eq. (5.24) and compare it with that obtained via Monte Carlo simulations. Note that there is a slight mismatch between the analytical curve and the simulated one since we derived the inter-

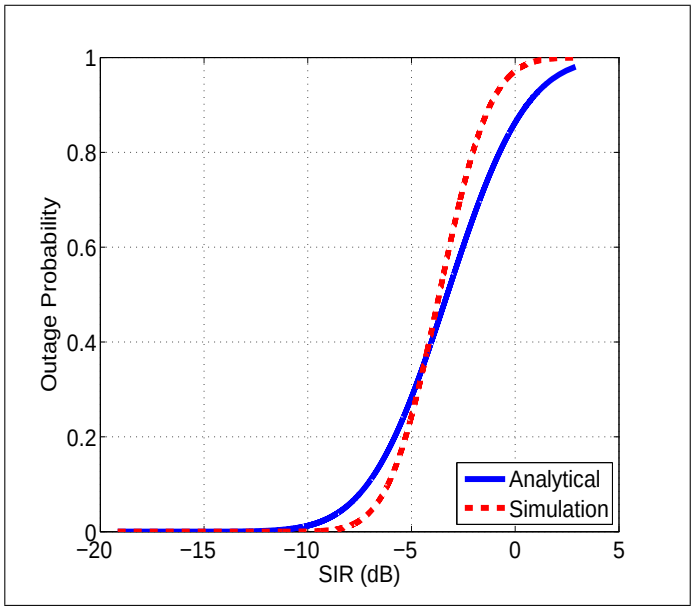

Figure 5.2: The Physical Outage Probability

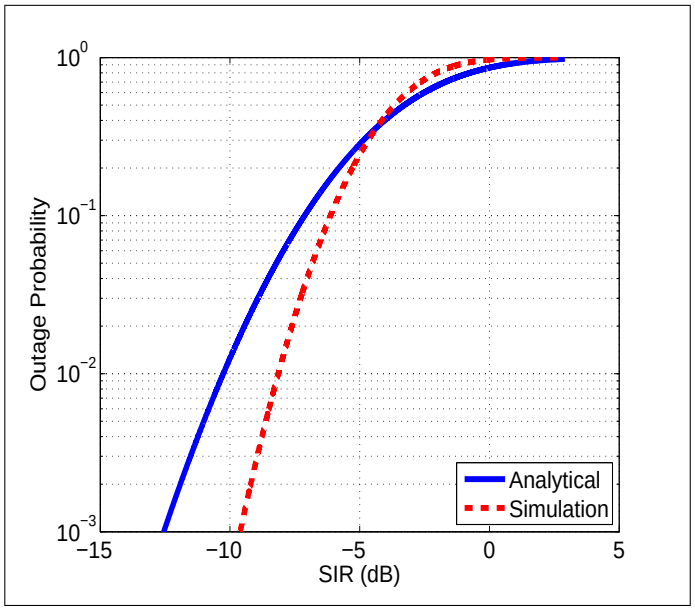

Figure 5.3: The Physical Outage Probability (Log-Scale)

ference PDF using an approximation rather than an exact derivation (due to analytical intractability, as mentioned in Section 5.3). The log-plot of this outage probability (see Fig. 5.3) shows that the analytical and the simulated outage probability coincide at high SIR regime, but they do not at low SIR regime (under -5 dB) and the gap between these two curves increases under -10 dB.

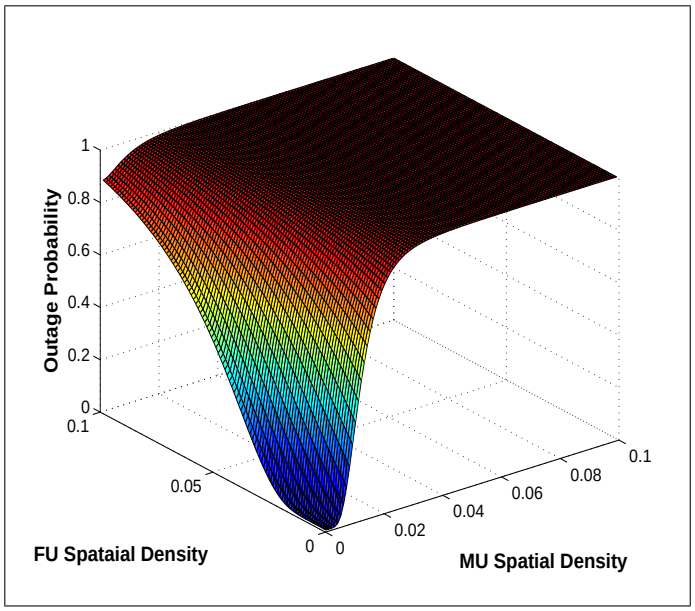

Figure 5.4: The Outage Probability as a function of the FU and MU density

On the other hand, in Fig. 5.4 and Fig. 5.5, we illustrate the evolution of the outage probability as a function of the FU density for different MC loads (i.e. load in MUs). These figures show that the MU spatial density has a much higher impact on the outage probability than the FU spatial density. The curves in Fig. 5.5 are of a paramount importance since they constrain the density and consequently the number of active FUs that could be accepted in the underlying MC to meet a desired value of the outage probability. Hence, it would be useful for the design of admission control mechanisms. For

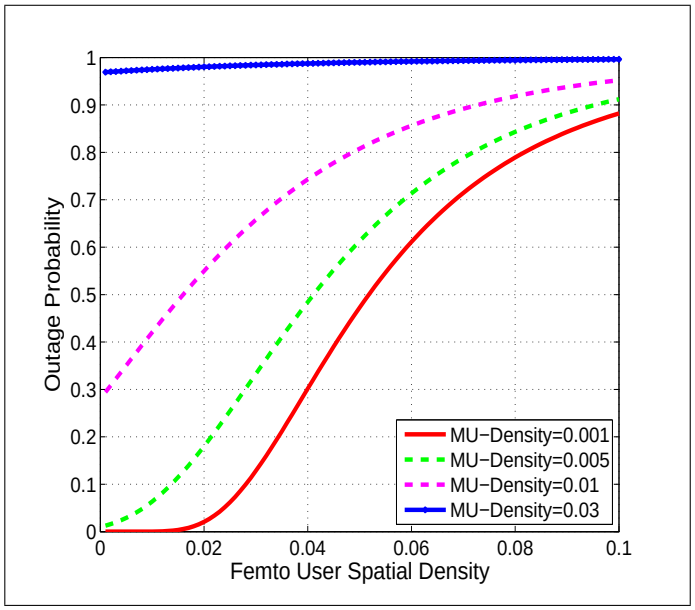

Figure 5.5: The Outage Probability as a function of the FU density

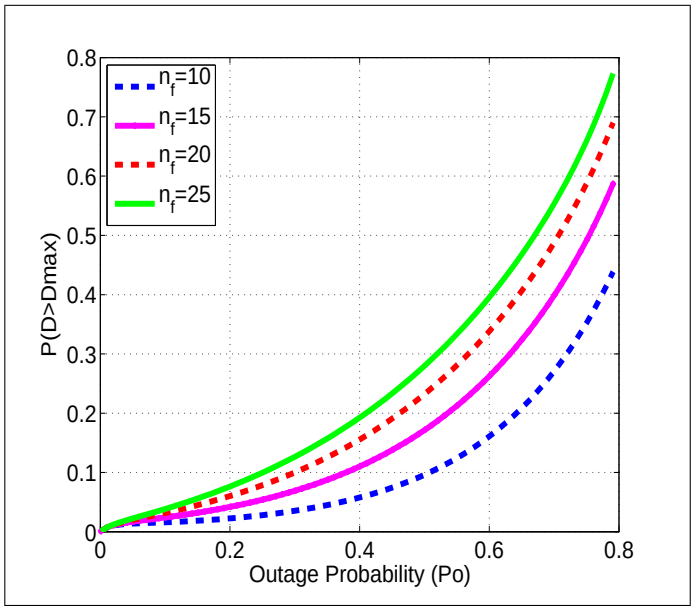

Figure 5.6: Delay Characterization for CBR traffic in FC network

instance, in order to maintain the outage probability at the FAP $P_o \leq 0.1$, the density of active FUs in the MC should not exceed 0.03 for a MU density $\lambda_2 \approx 0.001$. Finally, using the theoretical delay derivation in Eq. (5.36), we plot the delay constraint ($\mathbb{P}(D > D_{max})$) for a CBR traffic with constant rate equal to 64kbps whose tolerated packet loss rate is $\epsilon \leq 0.1$. Fig. 5.6 shows that the packet loss probability $\mathbb{P}(D > D_{max})$ increases slightly as the number of active FUs per FC (n_f) increases. However, it increases considerably as the physical outage probability P_o increases. Thus, a two tier FC/MC network with high density in FUs would have a low loss rate for CBR traffic only if its outage probability is maintained at a low level. One way to achieve this goal would be the design of interference-aware power control scheme.

5.7 Summary

In this chapter, we derived statistical characterizations of UL interference, SIR, and outage probability. Our analysis showed that UL interference and SIR in two-tier Poisson-distributed FC networks can be represented by a log-normal distribution. We verified this result using Monte-Carlo simulations. Moreover, we modeled and characterized link delay, data loss rate, and effective throughput of CBR delay-constrained traffic in two-tier FC networks. These derived results can be used to characterize many multimedia applications, such as interactive gaming, voice, and video applications. This work opens up several issues for future research on resource management in FC networks, including interference-aware fractional power control design, call admission control design, and the extension of the current results to multiple-tier heterogeneous networks.

Chapter 6: Conclusion

This chapter summarizes the main results and contributions of this dissertation and proposes some future research work directions.

6.1 Contributions Revisited

This dissertation makes four important contributions to the body of knowledge on resource allocation study and design for next generation wireless networks. In our work, we considered two types of architectures: next generation wireless backbone networks, namely wireless mesh networks (WMNs), and next generation wireless access networks, namely femtocells (FCs). Our contributions can be summarized in the following points:

- First, we design a new scheduling scheme for multi-radio multi-channel (MR-MC) WMNs. We provide two types of formulations: The first one is based on a graphical representation of the network topology as well as of the interference relationships, while the second one is based on a physical description of the system that takes into account channel fading. Our scheme improves the network throughput and the session satisfaction ratios by (i) eliminating interference among active links, (ii) taking into account the spatial traffic distribution during the channel assignment process, (iii) allowing the use of multiple channels per link, and (iv) privileging links with lower session satisfaction ratios.

- Second, we direct our attention to the problem of FC capacity improvement via adaptive power allocation to femto-users (FUs). To this end, we propose a new distributed non-cooperative uplink (UL) power allocation scheme for FC networks in which we try to fairly maximize the capacity of FUs while ensuring symbiosis between the FCs and the the underlying macrocell (MC), and inter-FCs. Our scheme is completely distributed and does not require any type of coordination, neither inter-tier (FC-MC) nor intra-tier (FC-FC) coordination. This property is made possible thanks to the use of exponential weighted moving average prediction technique. In fact, in our work, we propose an adaptive algorithm according to which each time slot, each FU decides its transmission power value based on the evolution of its signal to interference ratio (SIR), and the predicted value of the interference at its femto access point (FAP).

- Third, we develop a new distributed QoS-aware UL power control scheme for both FUs and macro-users (MUs), that aims at maintaining the minimum required SIR for a maximum number of cellular users (CUs). In addition to the fact that our scheme does not require any type of coordination, it is based on the use of ordinary differential equations (ODEs) to solve the power allocation problem, which is a new contribution in itself. In fact, in this work we adopt a reverse engineering approach: We first start by formulating the QoS constraint for the CUs, expressed in terms of a minimum SIR requirement that needs to be maintained. The differentiation of this system of constraints, yields a system of ODEs that describes the CUs' transmission power dynamics. On the other hand, we provide a theoretical analysis of our proposed scheme. Our analysis shows that our proposed set of

ODEs admits a unique solution. We also derive sufficient conditions for the stability of the solution at the equilibrium point. Analytical and simulation results encourage the implementation and potentially adoption of our scheme in existing deployed FC/MC systems.

- Finally, we derive a statistical characterization of the UL physical interference, SIR and outage probability in FC networks, and verify them using Monte-Carlo simulations. Then, we study the impact of these parameters on data link level performance metrics, namely the packet delay, data loss rate and the maximum achievable FU throughput for constant bit rate (CBR) type of traffic. In fact, in our work we provide a novel system modeling that allowed us to link the data-link layer performance metrics to those of the physical (PHY)-layer and characterize their interactions. Our analysis establishes key cross-layer relationships that can be useful for designing efficient resource utilization techniques for FC networks, such as interference-aware power control, QoS-aware call admission control, etc.

6.2 Future Work Directions

The performance enhancements achieved through this dissertation incite us to further investigate this research area. Our thesis work opens up new research horizons and directions.

For instance, a natural extension of our proposed work would be through the design of call admission control (CAC) mechanisms to help decide the acceptance of new traffic/users arrival based on the service level agreement (SLA) established between the

network and the users. The SLA basically defines the QoS that the FC network is committed to provide to the wireless users. CAC techniques perform better when jointly designed with resource allocation schemes. Indeed, due to the mobility of the cellular users, a FAP may need to predict the arrival of new FUs/MUs in order to optimize the resource allocation schemes, so that it can accept as many users as possible.

On the other hand, these schemes could be extended to more general network settings. In fact, we may consider more complicated scenarios, where we have multiple tier networks (rather than just two-tier), sharing a common wireless spectrum. An example of such scenario are the wireless networks operating over the unlicensed ISM band such as WiMax, WiRan, WiFi, RF networks, and the emerging near-field communication (NFC) networks. Indeed, the number of wireless networks operating over the ISM band is going crescendo with the emergence of new industrial, medical, scientific and entertaining wireless networking-based applications. Hence, the resource management in these types of networks is becoming more challenging than ever, and many issues still need to be addressed such as spectrum management and power allocation that take into account the dynamically changing heterogeneous wireless users spatial distribution. Another, closely related issue that could benefit from such resource allocation schemes is the design of CAC mechanisms to maintain the required QoS. The design of CAC techniques is challenging since it has to be performed in a distributed fashion and needs some ways to predict the introduction of new wireless users, their mobility pattern and its impact on the provided QoS.

Moreover, according to Cisco, in 2015 global mobile data traffic will increase 26-fold between 2010 and 2015. Mobile data traffic will grow at a compound annual growth

rate (CAGR) of 92 percent from 2010 to 2015, reaching 6.3 million tera bytes ($6.3\ 10^{18}$ bytes) per month by 2015[1]. Hence, the design of data offloading schemes from one tier to another would be of a paramount importance to alleviate such traffic burden from one single network and rather share this load among co-located networks for better QoS provisioning. Some results from the social networking paradigm may be used for this sake. Moreover, the deployment of data offloading schemes in such networks may lead to the derivation of new queuing models that would help characterize the capacity and QoS offered by such networks. In addition to traffic balancing, which helps preserve the network resources in order to have greater capacity in terms of number of accepted users, there is the problem of distributed service management to improve the mobile user's quality of experience (QoE) [6]. This problem is very challenging nowadays due to the proliferation of mobile multimedia applications, ranging from watching live TV via real-time streaming, online gaming, visio-conference, etc. In fact, the QoS/QoE related to these apps is highly degraded with mobility. In addition, this offered QoE gets even worse due to the increasing number of wireless mobile users which is made possible thanks to the widespread of new multimedia-capable hand-held mobile devices such as smartphones and PCs.

[1]Source: Cisco Visual Networking Index Global IP Traffic Forecast, 2010-2015

Bibliography

[1] In *http://www.olsr.org*.

[2] *ITU-R Rec, M.1225, Guidelines for evaluation of radio transmission technologies for IMT-2000*, Feb.

[3] *FCC, Spectrum Policy Task Force (SPTF), Report of the Spectrum Efficiency WG, November*, 2002.

[4] E. X. Alban, M. E. Magana, H. G. Skinner, and K. P. Slattery. Statistical modeling of the interference noise generated by computing platforms. *IEEE Transactions on Eletcromagnetic Compatibility*, Nov. 2011.

[5] H. M. Ali, A. Busson, and V. Veque. Channel assignment algorithms: A comparison of graph based heuristics. In *The 4th ACM workshop on Performance monitoring and measurement of heterogeneous wireless and wired networks*, 2009.

[6] O. Alsaleh, B. Hamdaoui, and A. Rayes. Improving quality of data user experience in 4g distributed telecommunication systems. In *Proc. IEEE International Conference on Collaboration Technologies and Systems (CTS)*, May 2012.

[7] A.Rabbachin, T. Q. S. Quek, H. Shin, and M. Z. Win. Cognitive network interference. *IEEE Journal on Selected Areas in Communications*, 29:480–493, Feb. 2011.

[8] S. Avallone and I.F. Akyildiz. A channel assignment algorithm for multi-radio wireless mesh networks. In *ICCCN*, pages 1034–1039, 2007.

[9] I. F. Aykilidz and X. Wang. A survey on wireless mesh networks. In *IEEE Communications Magazine*, 2005.

[10] V. Bahandri and N.H. Vaidya. Scheduling in multichannel wireless networks. *Distributed Computing and Networking*, 2010.

[11] P. Bahl, R. Chandra, and J. Dunagan. Ssch: Slotted seeded channel hopping for capacity improvement in ieee 802.11 ad-hoc wireless networks. In *ACM MobiCom*, 2004.

[12] D. Bertsekas and R. Gallager. *Data Networks*. Prentice Hall Inc., 1992.

[13] C. Bettstetter, G. Resta, and P. Santi. The node distribution of the random waypoint mobility model for wireless ad hoc networks. *IEEE Transactions on Wireless Communications*, 2, Sep. 2003.

[14] C. U. Castellanos, D. L. Villa, C. Rosa, K. I. Pedersen, F. D. Calabrese, P. H. Michaelsen, and J. Michel. Performance of uplink fractional power control in UTRAN LTE. In *Proc. IEEE Vehicular Technology Conference (VTC Spring)*, May 2008.

[15] N. Chakchouk and B. Hamdaoui. Distributed power control for two-tier co-channel femtocell networks with qos constraints. *submitted to IEEE Transactions on Wireless Commuications*.

[16] N. Chakchouk and B. Hamdaoui. Estimation-based non-cooperative power allocation in two-tier femtocell networks. In *Proc. IEEE Global Communications Conference (GLOBECOM)*, Dec. 2011.

[17] C. C. Chan and S. V. Hanly. Calculating the outage probability in a CDMA network with spatial poisson traffic. *IEEE Transactions on Vehicular Technology*, 50:183–204, Jan. 2001.

[18] V. Chandrasekhar and J. G. Andrews. Uplink capacity and interference avoidance for two-tier femtocell networks. *IEEE Transactions on Wireless Communications*, 8:3498–3509, Jul. 2009.

[19] V. Chandrasekhar, J.G. Andrews, T. Muharemovic, Z. Shen, and A. Gatherer. Power control in two-tier femtocell networks. *IEEE Transactions on Wireless Communications*, 8:4316–4328, Aug. 2009.

[20] C. S. Chang and J. A. Thomas. Effective bandwidth in high-speed digital networks. *IEEE Journal on Selected Areas in Communications*, 13:1091–1100, Aug. 1995.

[21] W. Cheng, X. Cheng, T. Znati, X. Lu, and Z. Lu. The complexity of channel scheduling in multi-radio multi-channel wireless networks. In *IEEE INFOCOM*, April 2009.

[22] F. M. Chiussi, D. Logothetis, I. Widjaja, and D. Kataria. Femtocells. *IEEE Communications Magazine*, Jan. 2010.

[23] D. Chizhik, J. Ling, P. W. Wolniansky, R. A. Valenzuela, N. Costa, and K. Huber. Multiple-input-multiple-output measurements and modeling in manhattan. *IEEE Journal on Selected Areas in Communications*, April 2003.

[24] X. Chu, J. Y. Wu, and H. Wang. Outage probability analysis for collocated spectrum-sharing macrocell and femtocells. In *Proc. IEEE International Conference on Communication(ICC)*, pages 1–5, June 2011.

[25] H. Claussen. Performance of macro and co-channel femtocells in a hierarchical cell structure. In *Proc. IEEE International Symposium on Personal, Indoor and Mobile Radio Communications (PIMRC)*, pages 1–5, Dec. 2007.

[26] H. Claussen. Co-channel operation of macro- and femtocells in a hierarchical cell structure. *Int'l. Journal Wireless Inform. Networks*, 15:137–147, 2008.

[27] D. S. J. De Couto, D. Aguayo, J. Bicket, and R. Morris. A high-throughput path metric for multi-hop wireless routing. In *Proceedings of ACM Mobicom*, 2003.

[28] V.G. Douros, G.C. Polyzos, and S. Toumpis. Negotiation-based distributed power control in wireless networks with autonomous nodes. In *Proc. IEEE 73rd Vehicular Technology Conference (VTC-Spring)*, May 2011.

[29] V.G. Douros, G.C. Polyzos, and S. Toumpis. Model predictive control for smooth distributed power adaptation. In *Proc. IEEE Wireless Communications and Networking Conference (WCNC)*, 2012.

[30] L. Fenton. The sum of log-normal probability distributions in scatter transmission systems. *IRE Transactions on Communications Systems*, 8:57–67, March 1960.

[31] G.J. Foschini and Z. Miljanic. A simple distributed autonomous power control algorithm and its convergence. *IEEE Transactions on Vehicular Technology*, 42:641–646, Nov 1993.

[32] L. Fu, S.C. Liew, and J. Huang. Effective carrier sensing in csma networks under cumulative interference. In *IEEE INFOCOM*, March 2010.

[33] A. Ganesh and G. Torrisi. Large deviations of the interference in a wireless communication model. *IEEE Transactions on Information Theory*, 54:3505–3517, Aug. 2008.

[34] K. Gulati, B. L. Evans, J. G. Andrews, and K. R. Tinsley. Statistics of co-channel interference in a field of Poisson and Poisson-Poisson clustered interferers. *IEEE Transactions on Signal Processing*, 58:6207–6222, Dec. 2010.

[35] P. Gupta and P. R. Kumar. The capacity of wireless networks. *IEEE Trans. on Information Theory*, March 2000.

[36] B. Hamdaoui and P. Ramanathan. A network-layer soft handoff approach for mobile wireless ip-based systems. *IEEE Journal on selected Areas in Communications*, 22:630–642, May 2004.

[37] B. Hamdaoui and P. Ramanathan. A cross-layer admission control framework for wireless ad-hoc networks using multiple antennas. *IEEE Transactions on Wireless Communications*, 6:4014–4024, Nov. 2007.

[38] A. Hertz and D. de Werra. Using tabu search techniques for graph coloring. *Computing*, (39), 1987.

[39] P. Hoeher, S. Kaiser, and P. Robertson. Two-dimensional pilot-symbolaided channel estimation by wiener filtering. In *Proc. IEEE Int. Conf. Acoustics, Speech, and Signal Processing*, page 18451848, 1997.

[40] T. Holliday, P. Glynn, and A. Goldsmith. On entropy and lyapunov exponents for finite-state channels. *IEEE Transactions on Information Theory*, . 2004.

[41] E.J. Hong, S.Y. Yun, and D. Cho. Decentralized power control scheme in femtocell networks : A game theoretic approach. In *Proc. IEEE 20th International Symposium on Personal, Indoor and Mobile Radio Communications (PIMRC)*, Sept. 2009.

[42] K. Huang, V. K. N. Lau, and Y. Chen. Spectrum sharing between cellular and mobile ad hoc networks: Transmission-capacity tradeoff. *IEEE Journal on selected Areas in Communications*, 27, Sep. 2009.

[43] Z. Huang, Z. Zeng, H. Xia, and J. Shi. Power control in two-tier ofdma femtocell networks with particle swarm optimization. In *Proc. IEEE 73rd Vehicular Technology Conference (VTC-Spring)*, May. 2011.

[44] J. Ilow and D. Hatzinakos. Analytic alpha-stable noise modeling in a poisson field of interferers or scatterers. *IEEE Transactions on Signal Processing*, 46:1601–1611, Jun. 1998.

[45] K. Jain, J. Padhye, V. Padmanabhan, and L. Qiu. The impact of interference on multi-hop wireless network performance. In *ACM Proceedings of MOBICOM*, 2003.

[46] G. Jeney. Practical limits of femtocells in a realistic environment. In *Proc. IEEE Vehicular Technology Conference (VTC Spring)*, July 2011.

[47] H.S. Jo, C. Mun, J. Moon, and J.G. Yook. Interference mitigation using uplink power control for two-tier femtocell networks. *IEEE Transactions on Wireless Communications*, 8:4906–4910, Oct. 2009.

[48] S. Kandukuri and S. Boyd. Optimal power control in interference-limited fading wireless channels with outage-probability specifications. *IEEE Transactions on Wireless Communications*, January 2002.

[49] X. Kang, Y.C. Liang, and H.K. Garg. Distributed power control for spectrum-sharing femtocell networks using stackelberg game. In *Proc. IEEE International Conference on Communications (ICC)*, June 2011.

[50] Y. Kim, S. Lee, and D. Hong. Performance analysis of two-tier femtocell networks with outage constraints. *IEEE Transactions on Wireless Communications*, 9:2695–2700, Sep. 2010.

[51] J. Kingman. *Poisson Processes*. Oxford Univ. Press, 1993.

[52] M. Kodialam and T. Nandagopal. Characterizing the capacity region in multi-radio multi-channel wireless mesh networks. In *ACM Proceedings of MOBICOM*, pages 73–87, 2005.

[53] K.R. Krishnan and H. Luss. Power selection for maximizing sir in femtocells for specified sir in macrocell. In *Proc. IEEE Wireless Communications and Networking Conference (WCNC)*, March. 2011.

[54] J. F. Kurose and K. W. Ross. *Computer Networking: A Top-Down Approach*. Addison-Wesley, 2009.

[55] P. Kyasanur and N. H. Vaidya. Capacity of multi-channel wireless networks: Impact of number of channels and interfaces. In *ACM MobiCom*, 2005.

[56] H.C. Lee, D.C. Oh, and Y.H. Lee. Mitigation of inter-femtocell interference with adaptive fractional frequency reuse. In *Proc. IEEE International Conference on Communications (ICC)*, May 2010.

[57] S. Lee. An enhanced IEEE 1588 time synchronization algorithm for asymmetric communication link using block burst transmission. *IEEE Communications Letters*, 12:687–689, Sep. 2008.

[58] F. Li, X. Tan, and L. Wang. A new game algorithm for power control in cognitive radio networks. *IEEE Transactions on Vehicular Technology*, 60, Nov. 2011.

[59] M.K. Marina and S.R. Das. A topology control approach for utilizing multiple channels in multi-radio wireless mesh networks. In *The 2nd International Conference on Broadband Networks*, pages 381–390, 2005.

[60] N N. Jindal, S. Weber, and J.G. Andrews. Fractional power control for decentralized wireless networks. *IEEE Transactions on Wireless Communications*, 7:5482–5492, Dec. 2008.

[61] D. Ngo, L.B. Le, T. Le-Ngoc, E. Hossain, and D.I. Kim. Distributed interference management in two-tier cdma femtocell networks. *IEEE Transactions on Wireless Communications*, 11:979–989, March 2012.

[62] P. C. Pinto and M. Z. Win. Communication in a Poisson field of interferers-part I: Interference distribution and error probability. *IEEE Transactions on Wireless Communications*, 9:2176–2186, Jul. 2010.

[63] P. C. Pinto and M. Z. Win. Communication in a Poisson field of interferers-part II: Channel capacity and interference spectrum. *IEEE Transactions on Wireless Communications*, 9:2187–2195, Jul. 2010.

[64] S.Y. Pyun and D.H. Cho. Resource allocation scheme for minimizing uplink interference in hierarchical cellular networks. In *Proc. IEEE 71st Vehicular Technology Conference (VTC 2010-Spring)*, May 2010.

[65] K.N. Ramachandran, E.M. Belding, K.C. Almeroth, and M.M. Buddhikot. Interference-aware channel assignment in multi-radio wireless mesh networks. In *IEEE INFOCOM*, 2006.

[66] R.Jain, D.M. Chiu, and W. Hawe. A quantitative measure of fairness and discrimination for resource allocation in shared conputer systems. *Technical Report TR-301*, DEC Research Report, Sep. 1984.

[67] Z. Shi, H. Wang, and M. Zhao M.C. Reed. An uplink analytical model for two-tiered 3g femtocell networks. In *Proc. of the 8th International Symposium on*

Modeling and Optimization in Mobile, Ad Hoc and Wireless Networks (WiOpt), July 2010.

[68] E. S. Sousa. Performance of a spread spectrum packet radio network link in a poisson field of interferers. *IEEE Transactions on Information Theory*, 38:1743–1754, Nov. 1992.

[69] D. Stoyan, W. Kendall, and J. Mecke. *Stochastic Geometry and its Applications*. John Wiley and Sons, 1995.

[70] R.A. Stubbs and S. Mehrotra. A branch and cut method for 0-1 mixed convex programming. *Mathematical Programming*, 1999.

[71] A.P. Subramanian, H. Gupta, S.R. Das, and J. Cao. Minimum interference channel assignment in multiradio wireless mesh networks. *IEEE Transactions on Mobile Computing*, 7(12), December 2008.

[72] K. Sundaresan and S. Rangarajan. Efficient resource management in ofdma femto cells. In *Proc. of the tenth ACM international symposium on Mobile ad hoc networking and computing MobiHoc*, May 2009.

[73] A. Valcarce and J. Zhang. Empirical indoor-to-outdoor propagation model for residential areas at 0.9 to 3.5 GHz. *IEEE Antennas and Wireless Propagation Letters*, 9:682–685, Jul. 2010.

[74] A. J. Viterbi. *CDMA: Principles of Spread Spectrum Communication.* MA: Addison-Wesley, 1995.

[75] R.0 Wang and D. Cox. Channel modeling for ad hoc mobile wireless networks. In *Proc. IEEE Vehicular Technology Conference (VTC)*, March 2002.

[76] D. Wu and R. Negi. Effective capacity: A wireless link model for support of quality of service. *IEEE Transactions on Wireless Communications*, 2:630–643, Jul. 2003.

[77] Y. Wu, T. Zhang, and D. H. K. Tsang. Joint pricing and power allocation for dynamic spectrum access networks with stackelberg game model. *IEEE Transactions on Wireless Communications*, 10, Jan. 2011.

[78] W. Xiao, R. Ratasuk, A. Ghosh, R. Love, Y. Sun, and R. Nory. Uplink power control, interference coordination and resource allocation for 3GPP E-UTRA. In *Proc. IEEE Vehicular Technology Conference (VTC Fall)*, Sep. 2006.

[79] Y. Xiao, G. Bi, and D. Niyato. A simple distributed power control algorithm for cognitive radio networks. *IEEE Transactions on Wireless Communications*, 10, Nov. 2011.

[80] W. Xie, Y.J. Zhang, M.L. Sichitu, L. Fu, and Y. Yao. Feasibility of optimally assigning channels by exhaustive search in commercial multi-radio wireless mesh networks. *Telecommunication Systems*, 2010.

[81] R. D. Yates. A framework for uplink power control in cellular radio systems. *IEEE Journal on Selected Areas in Communications*, 13:1341–1347, Sep. 1995.

[82] M. Yavuz, F. Meshkati, S. Nanda, A. Pokhariyal, N. Johnson, B. Raghothaman, and A. Richardson. Interference management and performance analysis of UMTS/HSPA+ femtocells. *IEEE Communications Magazine*, 47:102–109, Sep. 2009.